UNIVERZITA PALACKÉHO V OLOMOUCI

Přírodovědecká fakulta

Katedra biochemie

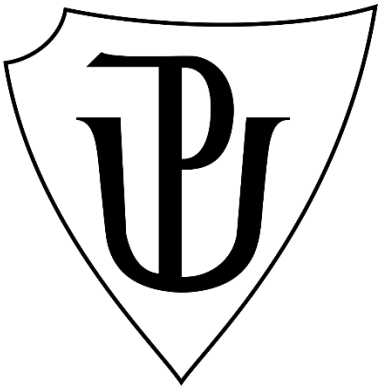

Role of PD-1 and tyrosine phosphatase-1 (SHP-2) activity on Lck activity in human T-lymphocytes

DIPLOMOVÁ PRÁCE

Autor:	**Bc. Helena Besta Smrčková**
Studijní program:	N1406 Biochemie
Studijní obor:	Biochemie
Forma studia:	Prezenční
Vedoucí práce:	**Juan Bautista De Sanctis, Ph.D.**
Rok:	2026

Prohlašuji, že jsem diplomovou práci vypracovala samostatně s vyznačením všech použitých pramenů a spoluautorství. Souhlasím se zveřejněním diplomové práce podle zákona č. 111/1998 Sb., o vysokých školách, ve znění pozdějších předpisů. Byla jsem seznámena s tím, že se na moji práci vztahují práva a povinnosti vyplývající ze zákona č. 121/2000 Sb., autorský zákon, ve znění pozdějších předpisů.

V Olomouci dne 21.4.2026 .....

Podpis studenta

Acknowledgments

First and foremost, I would like to express my deepest gratitude to my supervisor, Prof. Juan Bautista De Sanctis. I cannot thank him enough for his endless patience, genuine kindness, and unwavering support throughout this entire journey. He was always there to help, guide, and discuss my work, no matter the time or circumstance. Beyond his exceptional academic mentorship, he and his amazing wife, Jenny, welcomed me with open arms, truly becoming a second family to me during a time when I needed it most.

I am also incredibly grateful to my wonderful labmate and classmate, Hana Duchová. Thank you for being a constant source of light and positivity. Your ability to consistently cheer me up in the lab made the long hours and difficult days so much easier to bear.

Special thanks go to Dr. Ivo Frydrych for his invaluable assistance, expertise, and guidance during the flow-cytometry measurements. His technical support and willingness to help were instrumental to the progress of my research.

Financial support for this research was provided by Savage under grant number C.02.01.01/00/22_008/0004644, and by PerMed under grant number TN02000109.

Finally, I would like to thank myself. Throughout the course of this thesis, I faced severe illness and navigated ongoing health issues that tested me in every possible way. Despite the physical and mental toll, I did not give up on myself. I am incredibly proud of my resilience, my determination to keep going through the hardest days, and of finishing everything I set out to do.

Bibliografická identifikace

Jméno a příjmení autora	Bc. Helena Besta Smrčková
Název práce	Role PD1 a aktivity tyrosinové fosfatasy 2 (SHP-2) na aktivitu Lck lidských T-lymfocytů
Typ práce	Diplomová
Pracoviště	Ústav molekulární a translační medicíny
Vedoucí práce	Prof. Juan Bautista De Sanctis
Rok obhajoby práce	2026

Abstrakt

T buněčné vyčerpání je stav charakterizovaný zvýšenou expresí imunitních kontrolních bodů (immune checkpoints), jako je protein programované buněčné smrti 1 (PD-1) a jeho ligand PD-L1. T buněčné vyčerpání také výrazně omezuje účinnost adaptivní imunitní odpovědi při chronické expozici určitému antigenu. Aby došlo k jeho překonání a obnově efektorových funkcí T-lymfocytů, je nutná přesná farmakologická modulace nitrobuněčných signálních drah, specificky cílících na molekuly, jako je Lck kináza a SHP-2 fosfatáza. Tato práce si kladla za cíl zhodnotit *in vitro* účinky různých cílených farmakologických inhibitorů a látek, konkrétně Dasatinibu (inhibitor Lck), inhibitorů tyrosinových fosfatas (TPI-1, PTP1Bi) a CuET, podávaných samostatně i v multilékových kombinacích, na expresi PD-1 a PD-L1, jakož i na fosforylaci Lck v lidských T-lymfocytech a jejich cytotoxickou funkci.

Mononukleární buňky periferní krve (angl. PBMCs) byly izolovány z krve zdravých dárců pocházející z Transfúzního oddělení FN Olomouc, následně byly kultivovány a podrobeny buď farmakologické stimulaci (PMA/ionomycin), nebo stimulaci zprostředkované receptory (fytohemaglutinin, PHA). Modulace povrchové exprese PD-1 a PD-L1 byla kvantifikována pomocí průtokové cytometrie. Dále byla hodnocena cytotoxická aktivita ošetřených T-lymfocytů proti 2D kulturám nádorových buněk. Současně byl pomocí analýzy metodou Western blot hodnocen stav fosforylace Lck na specifických aminokyselinových zbytcích (Tyr394, Tyr192 a Tyr505). Analýza pomocí průtokové cytometrie odhalila, že intenzita buněčné odpovědi byla vysoce závislá na typu stimulace. Ve vzorcích stimulovaných PMA/ionomycinem vedlo ošetření Dasatinibem, TPI-1 a kombinací Dasatinib + TPI-1 + PTP1Bi ke statisticky významnému snížení exprese PD-L1, přičemž současně došlo ke zvýšení buněčné populace exprimující PD-1 i PD-L1.

Ve vzorcích stimulovaných PHA ošetřených kombinací CuET + TPI-1 došlo k významnému zvýšení exprese PD-1. Analýza Western blot prokázala, že buněčná stimulace úspěšně indukovala expresi PD-1 spolu s fosforylací Lck. Z kvalitativního hlediska Dasatinib konzistentně potlačoval fosforylaci Lck napříč testovanými podmínkami. Testy cytotoxicity odhalily odlišné odpovědi specifické pro jednotlivé buněčné linie. U linií A549 a K562 nebyly zaznamenány žádné statisticky významné změny napříč ošetřeními. Cytotoxicita se však plošně zvýšila u linií Jurkat (Dasatinib+TPI-1, CuET, TPI-1, CuET+TPI-1) a HCT116 (TPI-1, CuET+TPI-1, Dasatinib+TPI-1). Stojí za povšimnutí, že zatímco CuET a TPI-1 obecně zvyšovaly cytotoxicitu u buněk MOLT-4 a HCT116 p53-/-, ošetření Dasatinibem vedlo u těchto specifických linií ke snížení cytotoxicity. Tato zjištění zdůrazňují komplexní, na mnoha faktorech závislou dynamiku modulace imunitních kontrolních bodů pomocí cílených inhibitorů kináz a fosfatáz. Synergická aplikace více lékových terapií, jako jsou kombinace zahrnující CuET, Dasatinib, TPI-1 a PTP1Bi, má velký potenciál pro přesné ovlivnění signálních drah T-buněčného receptoru (TCR). Tyto kombinace mohou představovat slibnou translační strategii pro potlačení vyčerpání T-lymfocytů a zvýšení účinnosti imunoterapeutických intervencí.

Klíčová slova	T-buněčné vyčerpání, PD-1, PD-L1, Lck kináza, SHP-2, inhibitory kináz a fosfatáz, cytotoxicita T-buněk, Dasatinib, disulfiram, imunoterapie
Počet stran	72
Počet příloh	4
Jazyk	Anglický

Bibliographical identification

Autor's first name and surname	Bc. Helena Besta Smrčková
Title	Role of PD-1 and tyrosine phosphatase-2 (SHP-2) activity on Lck activity in human T-lymphocytes
Type of thesis	Diploma
Department	Institute of Molecular and Translational Medicine
Supervisor	Prof. Juan Bautista De Sanctis
The year of presentation	2026

Abstract

T-cell exhaustion, characterized by the upregulation of immune checkpoints such as Programmed cell death protein 1 (PD-1) and its ligand PD-L1, severely limits the efficacy of the adaptive immune response in settings of chronic antigen exposure. Overcoming this exhaustion and restoring T-cell effector function requires precise pharmacological modulation of intracellular signaling pathways, specifically targeting molecules like the Lck kinase and SHP-2 phosphatase. This study aimed to evaluate the *in vitro* effects of various targeted pharmacological inhibitors, specifically Dasatinib, tyrosine kinase inhibitors (TPI-1 and PTP1Bi) and CuET, administered individually and in multidrug combinations, on PD-1 and PD-L1 expression, as well as on Lck phosphorylation in human T-lymphocytes and their cytotoxic function. Peripheral blood mononuclear cells (PBMCs) were isolated from healthy human donors, and subsequently cultivated and subjected to either pharmacological stimulation (PMA/ionomycin) or receptor-mediated stimulation (Phytohemagglutinin, PHA). The modulation of PD-1 and PD-L1 surface expression was quantified using flow cytometry. Additionally, cytotoxic activity of treated T-lymphocytes against 2D cancer cell cultures was assessed. Concurrently, the phosphorylation status of Lck at specific residues (Tyr394, Tyr192, and Tyr505) were assessed via Western blot analysis. Flow cytometric analysis revealed highly stimulation-dependent responses. In the PMA/ionomycin cohort, treatments with Dasatinib, TPI-1, and the combination of Dasatinib + TPI-1 + PTP1Bi led to a statistically significant downregulation of single-positive PD-L1 expression, while simultaneously increasing the PD-1+/PD-L1+ double-positive cell population. In the PHA cohort, the combinatory treatment of CuET + TPI-1 significantly upregulated single-positive PD-1 expression. Western blot analysis demonstrated that cellular stimulation successfully induced PD-1

expression alongside Lck phosphorylation. Dasatinib consistently abrogated Lck phosphorylation across the tested conditions. Cytotoxicity assays revealed distinct cell-line-specific responses. A549 and K562 showed no significant changes across treatments. On the other hand, cytotoxicity broadly increased in Jurkat (Dasatinib+TPI-1, CuET, TPI-1, CuET+TPI-1) and HCT116 (TPI-1, CuET+TPI-1, Dasatinib+TPI-1) lines. Notably, while CuET and TPI-1 generally enhanced cytotoxicity in MOLT-4 and HCT116 p53-/- cells, Dasatinib treatment resulted in decreased cytotoxicity in these specific lines. The findings underscore the complex, context-dependent dynamics of immune checkpoint modulation by targeted kinase and phosphatase inhibitors. The synergistic application of multidrug therapies, such as combinations involving Dasatinib, TPI-1, and PTP1Bi, demonstrates significant potential in fine-tuning T-cell receptor (TCR) signaling pathways. These combinations may offer a promising translational strategy to counteract T-cell exhaustion and enhance the efficacy of immunotherapeutic interventions.

Keywords	T-cell exhaustion, PD-1, PD-L1, Lck, SHP-2, kinase and phosphatase inhibitors, T-cell cytotoxicity, Dasatinib, Disulphiram, immunotherapy
Number of pages	72
Number of appendices	4
Language	English

TABLE OF CONTENTS

Aims of the thesis

Theoretical part

- To undertake a thorough literature review that delineates the current status of research on T-cell exhaustion and its associated markers, with a primary focus on PD-1 and a secondary emphasis on PD-L1, as well as SHP phosphatases, particularly SHP-2, and Lck, while underscoring their clinical significance.

Experimental part

- To evaluate the effects of pharmacological modulation of Lck and SHP-2, as well as cellular activation, on the immune checkpoints PD-1 and PD-L1.

- To investigate the phosphorylation of the protein Lck at residues Tyr394, Tyr192, and Tyr505, and its correlation with PD-1 induction and SHP-2 inhibition.

- To assess lineage-specific and treatment-specific cytotoxic function of stimulated T-lymphocytes.

1 INTRODUCTION

The mammalian immune system relies on the adaptive immune response to provide highly specialized, pathogen-specific defenses and long-term immunological memory. The primary effectors of this cell-mediated immunity are T-cells, which recognize specific antigens presented by Antigen-Presenting Cells (APCs) on Major Histocompatibility Complex (MHC) molecules (Janeway et al., 2001; Malissen et al., 2014). The activation of naïve T-cells is a tightly regulated, multi-signal process requiring TCR-MHC engagement (Signal 1), co-stimulation via receptors such as CD28 (Signal 2), and microenvironmental cytokine signaling (Signal 3) (Bretscher & Cohn, 1970; Acuto & Michel, 2003; Goral, 2011).

The translation of these external antigenic cues into precise cellular responses relies on the structural assembly of the TCR-CD3 complex. Antigen recognition by the TCR must be efficiently coupled with the intracellular signaling motifs (ITAMs) of the invariant CD3 chains (Pennock et al., 2013; Shah et al., 2021). Effective signal transduction is intrinsically dependent on co-receptors such as CD4 and CD8, whose cytoplasmic tails interact with the non-receptor tyrosine kinase Lck (Artyomov et al., 2010). Upon TCR engagement, Lck plays a foundational role by phosphorylating the ITAMs on the CD3 complex, thereby initiating the downstream intracellular kinase cascade required for robust T-cell activation, clonal expansion, and differentiation (Arnaud, 1997; Carson et al., 1991).

However, to prevent uncontrolled systemic inflammation and autoimmunity, this potent activation is strictly counterbalanced by inhibitory immune checkpoints (Kumari et al., 2023). Following activation, T-cells upregulate Programmed cell death protein 1 (PD-1) (Buchbinder & Desai, 2015). When PD-1 binds to its primary ligands, PD-L1 and PD-L2, which are expressed on peripheral tissues or co-opted by tumor cells, it transmits a profound inhibitory signal that limits effector T-cell activity (Keir et al., 2008). The intracellular mechanism of PD-1-mediated suppression heavily relies on the recruitment of Src homology 2 domain-containing phosphatase 2 (SHP-2). Once recruited to the intracellular tail of PD-1, SHP-2 dephosphorylates proximal signaling molecules, crucially including Lck and CD28, effectively severing the TCR signal transduction cascade (Cammann et al., 2022). In environments characterized by chronic antigen exposure, sustained PD-1/PD-L1 signaling drives T-cells into a state of "exhaustion,"

characterized by a progressive loss of effector functions, diminished proliferative capacity, and altered transcriptional profiles (Marasco et al., 2020).

Overcoming T-cell exhaustion and restoring immune efficacy requires precise pharmacological intervention targeting these specific intracellular and extracellular macromolecules. Various targeted inhibitors have been developed to modulate these pathways. Dasatinib, a potent tyrosine kinase inhibitor, is known to target Lck, thereby allowing for the modulation of TCR signaling thresholds (Schade et al., 2008). Conversely, to counteract the immunosuppressive phosphatase activity driven by checkpoint engagement, specific inhibitors such as TPI-1 (which targets SHP-1 and less SHP-2) and inhibitors of Protein Tyrosine Phosphatase 1B (PTP1B) are utilized (Kundu et al., 2010; Baumgartner et al., 2023). By blocking SHP-2 and PTP1B, these agents prevent the premature dephosphorylation of Lck and other critical signaling nodes. Furthermore, agents like CuET (bis(diethyldithiocarbamate)copper) have emerged as highly relevant compounds in this context, modulating intracellular protein degradation pathways and influencing the broader microenvironmental factors that dictate T-cell viability and function (Wang et al., 2022; Dumut et al., 2025).

While targeting individual nodes has provided mechanistic insights, monotherapies often yield limited clinical efficacy, fail to completely reverse exhaustion, and can induce significant systemic toxicity (Wu et al., 2026). Consequently, there is a critical imperative to develop and evaluate multidrug therapies. It is particularly important to systematically try out different therapeutic combinations *in vitro* to fully understand their combined effects. Rigorous *in vitro* modeling allows researchers to observe how the simultaneous pharmacological manipulation of Lck, PD-1, and SHP-2 interacts at the cellular level, and critically, how these combined interventions influence the ultimate cytotoxic function of lymphocytes, as is addressed in this thesis. Identifying optimal synergistic combinations in these controlled settings is essential for overcoming T-cell exhaustion while simultaneously mitigating the deleterious effects and side effects experienced by patients undergoing immunotherapy.

2 LITERATURE REVIEW

2.1 T-cells

The mammalian immune system is a complex, integrated network of biological structures and processes that protects the organism against disease. It is broadly categorized into two subsystems: the innate immune system and the adaptive immune system. The innate system provides an immediate, non-specific defense, comprising physical barriers (e.g., skin), chemical mediators, and cellular components such as macrophages and neutrophils (Parkin & Cohen, 2001). In contrast, the adaptive immune system offers a specialized, pathogen-specific response and immunological memory. The primary effectors of the adaptive system are lymphocytes: B-cells, which govern humoral immunity through antibody production, and T-cells, which orchestrate cell-mediated immunity (Janeway et al., 2001).

T-cells, or T-lymphocytes, originate in the bone marrow and mature in the thymus, which is why they are called "T" cells. They are small, spherical cells with a large nucleus, minimal cytoplasm, and a surface rich in T-cell receptors (TCRs) and co-receptors that determine their function and specificity. (Smith-Garvin et al., 2009).

There are several distinct subsets of T-cells, distinguished primarily by their surface glycoproteins, such as CD3, CD4, and CD8 (see Table 1 on page 4). CD4+ Helper T-cells don't kill pathogens directly; they secrete cytokines that activate B-cells to produce antibodies and macrophages to destroy microbes. (Kan et al., 2024). CD8+ Cytotoxic T-cells are key effectors of cell-mediated immunity, inducing apoptosis in virus-infected or cancerous somatic cells. (Raskov et al., 2020). Regulatory T-cells are a CD4+ subset, often with CD25 and FoxP3 markers, that modulate the immune system and prevent autoimmune diseases. (Sakaguchi et al., 2008). Memory T-cells develop after exposure to a specific antigen and provide quick protection during future encounters due to their longevity and enhanced function. (Burleson et al., 2015)

Table 1. Overview of T-cell subsets and surface markers.

T-cell type	Primary Surface Markers	Main Function
Helper T-cell (Th)	CD3+, CD4+	Cytokine secretion, B-cell activation, Macrophage activation
Cytotoxic T-cell (Tc)	CD3+, CD8+	Direct killing of infected or cancerous cells via perforin/granzyme
Regulatory T-cell (Treg)	CD3+, CD4+, CD25+	Immune suppression, maintenance of tolerance
Memory T-cell	CD45RO+	Rapid response upon re-exposure to the antigen

2.1.1 T-cell involvement in the immune response

T-cells are crucial for the adaptive immune response. Unlike B-cells that recognize free-floating antigens, T-cells only identify antigens presented on the surface of host cells via Major Histocompatibility Complex (MHC) molecules. (Malissen et al., 2014).

When a pathogen enters the body, Antigen-Presenting Cells (APCs), like dendritic cells, process its proteins into peptides and present them on MHC molecules. Naïve CD4+ T-cells recognize antigens on MHC Class II, while naïve CD8+ T-cells recognize antigens on MHC Class I. (see Figure 1) (Vyas et al., 2008).

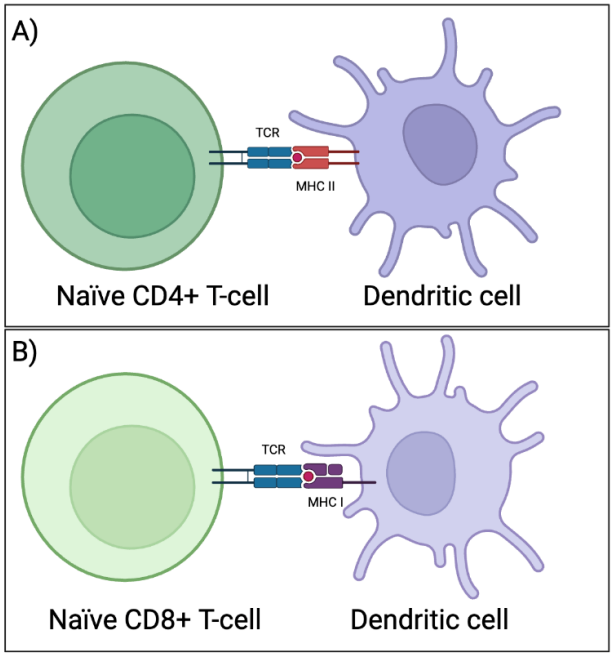

Figure 1. Antigen recognition of T-cells. *Section A) depicts a CD4+ T-cell interacting with an antigen (red sphere) presented on an MHC II molecule of a dendritic cell. Section B) depicts a CD8+ T-cell interacting with an antigen (red sphere) presented on an MHC I molecule of a dendritic cell. This figure was created using BioRender.*

Naïve T-cells, upon recognition, undergo clonal expansion and differentiation, migrating to the infection site to execute effector functions. This specificity enables the immune system to target infected cells while sparing healthy tissue.

2.1.1.1 T-cell activation

The activation of a naïve T-cell is a tightly regulated event that requires a specific sequence of signals. The "Two-Signal Hypothesis" posits that T-cell activation requires two concurrent events (Bretscher & Cohn, 1970), though modern immunology recognizes a crucial third signal (cytokines) for differentiation (Goral, 2011).

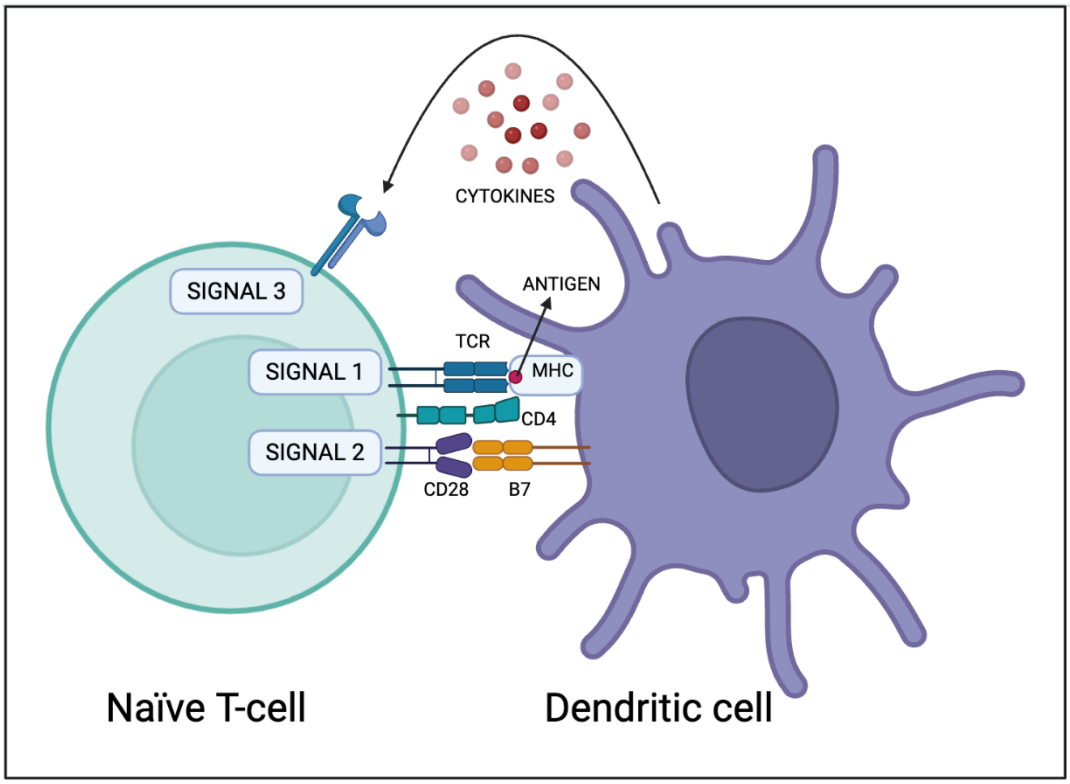

Figure 2. *The three-signal model of T-cell activation. This diagram illustrates the interaction between a naïve T-cell (left) and an antigen-presenting dendritic cell (right). Full activation requires three distinct signals: (1) antigen recognition via the TCR-MHC complex, (2) co-stimulation through CD28 and B7 molecules, and (3) cytokine signaling to direct differentiation. This figure was created using BioRender and inspired by Lee et al. (2020).*

During “Signal 1” (Antigen Recognition), the TCR interacts with the specific peptide-MHC complex on the APC. This interaction is stabilized by the co-receptors CD4 or CD8 (See Figure 2). This signal provides specificity but is insufficient on its own. Stimulation of the TCR without co-stimulation leads to anergy (unresponsiveness) (Bretscher, 1999).

The “Signal 2” (Co-stimulation) is a non-antigen-specific signal provided by the interaction between co-stimulatory molecules on the APC (such as CD80/B7-1 and CD86/B7-2 from the B7 family) and the CD28 receptor on the T-cell (See Figure 2 on

page 5). CD28 engagement lowers the threshold for T-cell activation and promotes survival and proliferation (Acuto & Michel, 2003).

During “Signal 3” (Cytokine Signaling), cytokines present in the microenvironment (e.g., IL-12, IL-4) direct the differentiation of the T-cell into specific effector subtypes (e.g., Th1, Th2, Th17) (Athie-Morales et al., 2004; Bao & Reinhardt, 2015; Powell et al., 2019).

To prevent autoimmunity and uncontrolled inflammation, T-cell activation is counterbalanced by inhibitory signals, often referred to as immune checkpoints (Kumari et al., 2023). Following activation, T-cells upregulate surface proteins such as Cytotoxic T-lymphocyte-associated protein 4 (CTLA-4) and Programmed cell death protein 1 (PD-1) (Buchbinder & Desai, 2015).

CTLA-4 competes with CD28 for binding to B7 molecules on APCs but with much higher affinity (Rowshanravan et al., 2017). Unlike CD28, CTLA-4 transmits an inhibitory signal that dampens T-cell proliferation (Walunas et al., 1994).

PD-1 binds to its ligands PD-L1 and PD-L2 on peripheral tissues. This interaction inhibits effector T-cell activity in tissues, thereby limiting collateral damage during chronic inflammation (Keir et al., 2008).

To induce robust T-cell activation and evaluate immune checkpoint regulation, two mitogenic protocols can be used: Phytohemagglutinin (PHA) and a combination of Phorbol 12-myristate 13-acetate (PMA) and Ionomycin. PHA, a lectin from Phaseolus vulgaris, activates T-cells by cross-linking surface glycoproteins, simulating antigen signaling for polyclonal T-cell proliferation (Movafagh et al., 2011). The PMA/Ionomycin cocktail bypasses surface receptors. PMA directly activates Protein Kinase C (PKC) as a diacylglycerol analogue, while Ionomycin acts as a calcium ionophore, enhancing calcium influx and activating calcineurin. (Gao et al., 2022). Both stimulation methods activate NFAT and NF-κB pathways, leading to rapid upregulation of activation markers, notably PD-1, which serves as a negative feedback regulator after strong mitogenic signaling. (Oestreich et al., 2008; Ahn et al., 2018).

2.1.1.2 T-cell receptor signal transduction

When TCRs engage with antigenic peptides presented by APCs such as dendritic cells, macrophages, or B cells, a complex molecular cascade is triggered (Pennock et al., 2013).

This cascade translates external environmental cues into internal signals, leading to T-cell activation, clonal expansion, and differentiation (Curtsinger et al., 2003).

The TCR complex, essential for signaling, is made of variable antigen-recognition chains and invariant signaling chains. The human genome contains four TCR genes—α, β, γ, and δ—forming two heterodimers. Most mature T-cells express the TCRαTCRβ heterodimer (αβ T-cells), while a smaller group expresses TCRγTCRδ (γδ T-cells). (Zhao et al., 2018; Born et al., 1987; Holtmeier & Kabelitz, 2005). Structurally, these TCR chains consist of an extracellular region, a transmembrane region, and a short cytoplasmic tail. The extracellular region is further divided into a variable immunoglobulin-like (V) domain, which serves as the antigen-recognition site, and a constant immunoglobulin-like (C) domain (see Figure 3). The C domain is crucial for the interaction with the CD3 signaling chains (Van Boxel et al., 2010; Shah et al., 2021).

For proper TCR function and localization on the cell surface, antigen-binding heterodimers must associate with six CD3 chains through non-covalent interactions. The CD3 chains form three dimers: δε, γε, and ζ ζ. In contrast to the short tails of TCRαTCRβ chains, CD3 chains contain signaling motifs (ITAMs) for intracellular signal propagation (Arnaud, 1997; Carson et al., 1991).

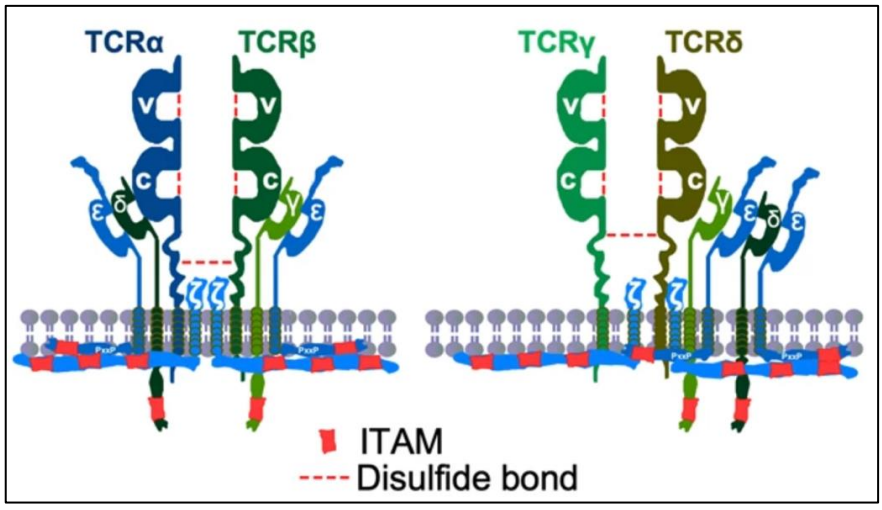

Figure 3. Structural assembly and signaling configuration of the TCR–CD3 complex. *The TCR complex comprises antigen-binding TCRαTCRβ or TCRγTCRδ heterodimers non-covalently associated with invariant CD3 signaling molecules. The CD3 component consists of δε, γε heterodimers alongside a ζ ζ homodimer. While the TCR heterodimers are stabilized by both intramolecular and intermolecular disulfide bonds, the variable (V) regions recognize pMHCs. The cytoplasmic domains of the CD3 chains collectively contain 10 immunoreceptor tyrosine-based activation motifs (ITAMs). In the resting state (absence of pMHC), the intracellular domains of the CD3 molecules adopt a closed conformation, rendering the ITAMs inaccessible to kinase-mediated phosphorylation. This figure was taken from Shah et al. (2021) and adjusted.*

Effective signaling involves co-receptors CD4 and CD8, which help the TCR differentiate MHC molecule classes and stabilize the TCR-pMHC interaction. CD4, a monomeric protein with four extracellular domains, recognizes MHC Class II molecules. (Ge et al., 2006). Its cytoplasmic tail interacts with the non-receptor tyrosine kinase Lck (Artyomov et al., 2010). Conversely, CD8 is typically a heterodimer (CD8αCD8β) that contains a single V domain per chain and recognizes MHC Class I molecules. These co-receptors ensure that CD4+ T-cells respond to antigens on APCs, while CD8+ T-cells can target any nucleated cell presenting antigens on MHC Class I (Srinivasan et al., 2024).

Signal transduction begins when ligand binding leads to receptor aggregation or conformational changes, allowing protein tyrosine kinases (PTKs) like Lck to phosphorylate tyrosine residues on the receptor complex's cytoplasmic tails. (Straus, 1992; Bozso et al., 2020). These phosphorylated sites act as docking platforms for molecules with specific domains, such as SRC homology 2 (SH2) and phosphotyrosine-binding (PTB) domains. A critical molecule recruited to these sites is the Zeta-chain-associated protein kinase 70 (ZAP-70), which binds via its SH2 domains (see Figure 4) (Chan et al., 1991). Once activated, ZAP-70 phosphorylates the transmembrane adaptor protein LAT (Linker for Activation of T-cells) (Aguado et al., 2006). These adaptors, which generally lack intrinsic enzymatic activity, function as scaffolds. They possess multiple binding domains (for phosphotyrosine, proline-rich regions, and lipids) that facilitate protein-protein interactions. By forming multiprotein complexes, adaptors integrate proximal biochemical signals (mediated by kinases, phosphatases, and phospholipases) with distal signaling pathways, ultimately activating the transcription factors required for gene expression and full T-cell activation (Shah et al., 2021). Upon phosphorylation, LAT recruits additional signaling molecules (see Figure 4), including the cytosolic adaptor SLP-76 (via Gads) and phospholipase Cγ1 (PLCγ1) (Malissen et al., 2005). This formation of a signalosome (see Figure 4 on page 9) allows PLCγ1 to hydrolyze membrane lipids, generating second messengers that trigger calcium flux and Ras/MAPK pathway activation (Fernández-Aguilar et al., 2023).

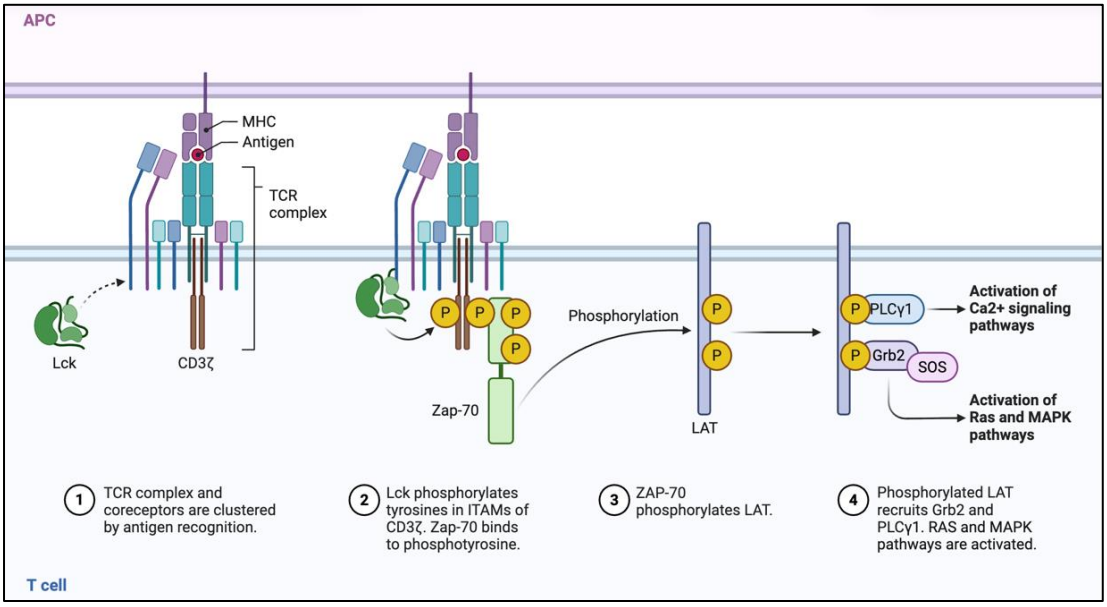

Figure 4. TCR signaling cascade. *This figure was created by adjusting the "TCR Downstream Signaling" template using BioRender.*

2.1.1.3 T-cell exhaustion

T-cell exhaustion is a dysfunction that occurs during chronic infections and cancer, characterized by a loss of effector functions, persistent expression of inhibitory receptors, and unique transcriptional and metabolic profiles. (Wherry, 2011).

The main cause of exhaustion is ongoing antigen exposure. In acute infections, antigens are cleared, and the effector T-cells become memory T-cells. However, in chronic conditions like HIV, Hepatitis C, or solid tumors, the immune system cannot eliminate the antigen. (Vigano et al., 2020). Continuous TCR stimulation leads to the overexpression of inhibitory receptors such as PD-1, TIM-3, and LAG-3. This chronic signaling alters the cell's epigenetic landscape, rendering it unable to respond effectively to stimulation (Pauken & Wherry, 2015).

Phenotypically, exhausted T-cells exhibit reduced proliferation and impaired production of IL-2, TNF-α, and IFN-γ, and increased expression of PD-1 and PD-1ligand. For the host, this results in the inability to control the viral load or tumor growth (Zeng et al., 2020).

Conditions strongly linked to T-cell exhaustion include chronic viral infections such as Human Immunodeficiency Virus (HIV), Hepatitis B (HBV), and Hepatitis C (HCV) (Ye et al., 2015; Cortés et al., 2023). Additionally, various solid tumors (melanoma, lung cancer) and hematologic malignancies create an immunosuppressive microenvironment that induces T-cell exhaustion to evade immune destruction (Kim & Cho, 2022).

Overcoming T-cell exhaustion has become a cornerstone of modern immunotherapy. The discovery that blocking inhibitory pathways can reinvigorate exhausted T-cells led to the development of Immune Checkpoint Inhibitors (ICIs). For example, the Anti-CTLA-4 Antibody Ipilimumab (Yervoy) blocks CTLA-4 (CTLA-4 function is described in section 2.1.1.1. T-CELL ACTIVATION), enhancing the priming of T-cells in lymph nodes (Lipson & Drake, 2011).

While these therapies have revolutionized cancer treatment, they are not effective in all patients, and reversing "terminally exhausted" T-cells remains a significant challenge in current immunological research.

2.2 Programmed cell death 1 (PD-1) receptor

As described in section 2.1 T-CELLS, T-cell activation is contingent upon the initial antigen-specific signal relayed to TCRs through the antigen-loaded MHC (pMHC). Costimulatory molecules are essential in modulating T-cell responses, affecting their intensity, characteristics, and duration. Some interactions enhance naive T-cell activation and proliferation, while others inhibit activation and promote regulatory mechanisms. (Francisco et al., 2010; Li et al., 2009). One significant receptor-ligand network involved in this process is the PD-1 receptor pathway, which primarily provides a co-inhibitory signal. Interactions between PD-1 and its ligands (PD-L1 and PD-L2) help sustain peripheral tolerance and can be exploited by tumors and viruses that induce chronic infections to evade immune surveillance (Riella et al., 2012).

2.2.1 Structure and function of PD-1

The inhibitory receptor programmed death 1 (PD-1, also CD279) is a cell surface molecule characterized by a single immunoglobulin (Ig) superfamily domain and a cytoplasmic domain that contains two tyrosine-based signaling motifs (see Figure 5 on page 11): an inhibitory motif (ITIM) and an immunoreceptor tyrosine-based switch motif (ITSM) (Dong et al., 1999). PD-1 interacts with two ligands, PD-L1 (B7-H1; CD274) and PD-L2 (B7-DC; CD273)(Latchman et al., 2001; Tseng et al., 2001; Agata et al., 1996), both of which feature extracellular domains resembling IgV-like and IgC-like structures (see Figure 5 on page 11), along with a short intracellular domain (Riella et al., 2012).

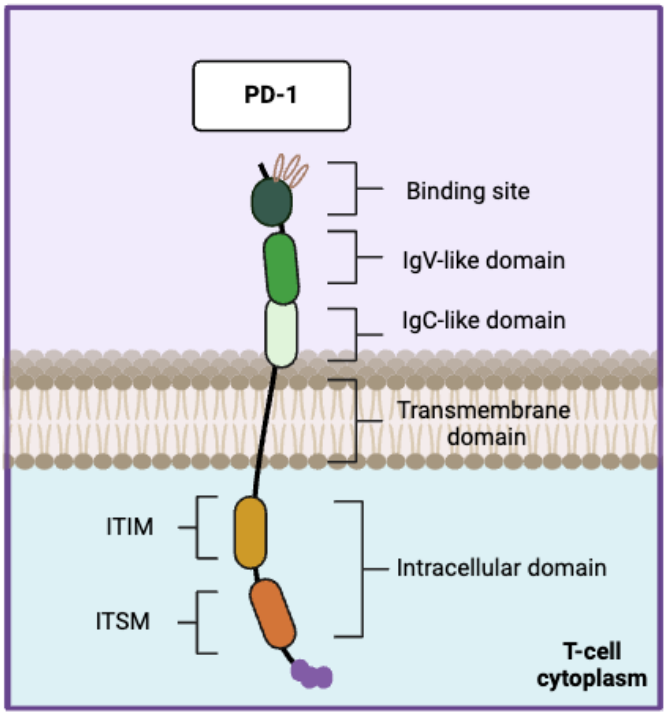

Figure 5. Schematic representation of the PD-1 receptor structure. *The diagram illustrates the transmembrane protein Programmed cell death protein 1 (PD-1) embedded within the T-cell membrane. The extracellular region consists of an N-terminal binding site, an IgV-like domain, and an IgC-like domain. The protein traverses the lipid bilayer via a transmembrane domain. The intracellular cytoplasmic tail contains two key tyrosine-based signaling motifs: the immunoreceptor tyrosine-based inhibitory motif (ITIM) and the immunoreceptor tyrosine-based switch motif (ITSM), which are critical for mediating inhibitory signaling. This figure was created using BioRender.*

PD-1 expression is inducibly upregulated in T-cells and B-cells following activation (Agata et al., 1996), as well as in natural killer T (NKT) cells, natural killer (NK) cells, activated monocytes, and specific subsets of dendritic cells (Keir et al., 2008). Notably, PD-1 expression is enhanced after engagement of the T-cell receptor (TCR) or B-cell receptor (BCR) in naive lymphocytes, with sustained antigen stimulation leading to elevated PD-1 levels (Freeman et al., 2006). Additionally, common γ-chain cytokines (such as IL-2, IL-7, IL-15, and IL-21), Toll-like receptors (TLRs), and interferons have been shown to augment PD-1 expression on T-cells (Kinter et al., 2008). The expression of PD-1 is partially regulated by the translocation of the nuclear factor of activated T-cells c1 (NFATc1) into the nucleus (Oestreich et al., 2008). NFATc1, in conjunction with AP-1 and NF-κB, represents a critical set of transcription factors activated upon antigen recognition by T-cells. While PD-1 upregulation in naive T-cells peaks approximately 48 hours after stimulation with anti-CD3 or anti-CD3/anti-CD28 in vitro (Yamazaki et al., 2002), PD-1 levels in allogeneic CD4+ T-cells progressively increase over time following skin transplantation *in vivo*, reaching their zenith on day 10 post-transplantation (Sandner

et al., 2005). The assessment of PD-1 expression across various immune cell subsets at different time points during transplantation warrants further investigation. Moreover, certain subsets of T-cells, including $CD4^{+}Foxp3^{+}$ regulatory T-cells (Tregs)(Baecher-Allan et al., 2003), T follicular helper cells (T_{FH}) (Haynes et al., 2007), memory T-cells (Duraiswamy et al., 2011), and "exhausted" CD8+ T-cells exhibit elevated levels of PD-1 expression (Wherry et al., 2007). The PD-1 promoter remains demethylated in exhausted T-cells even in the absence of antigenic stimulation (Youngblood et al., 2013; Youngblood et al., 2011).

2.2.1.1 PD-1 pathway

Upon ligand binding and recruitment to the immunological synapse (see Figure 6 on page 13), the tyrosines in ITIM and ITSM undergo phosphorylation (Freeman et al., 2000; Schildberg et al., 2016), facilitating the recruitment of SHP2 [Src homology 2 (SH2) domain-containing tyrosine phosphatase 2], which subsequently dephosphorylates multiple mediators of T-cell activation (Yokosuka et al., 2012). Hui et. al. (2017) have demonstrated that SHP-2, associated with PD-1, dephosphorylates CD28 more efficiently than TCRs and other downstream components such as CD3-ζ, ZAP70, and LAT/SLP76. This differential effect is attributed to the higher rephosphorylation rate of CD3-ζ by Lck. Enhanced net dephosphorylation of CD28 by PD-1 has been validated through in vitro cellular assays. Even in the absence of CD28/B7 interactions at the immunological synapse, PD-1 attenuates T-cell activation by targeting TCRs and downstream molecules, as observed in cytotoxic CD8+ T-cell interactions with B7-negative target cells (Hui et. al., 2017; Yokosuka et al., 2012). PD-1 interacts with two ligands from the B7 family: PD-L1 (B7-H1, CD274) and PD-L2 (B7-DC, CD273) (Schildberg et al., 2016). PD-L1 is constitutively expressed across various cell types and can be induced by cytokines, such as IFN-γ, as part of an adaptive resistance mechanism (Tumeh et al., 2014). PD-L1 expression within the tumor microenvironment, closely associated with CD8+ T-cell infiltration, is correlated with favorable clinical responses to PD-1-targeted immunotherapy (Taube et al., 2014). In contrast, PD-L2 expression is inducible and more restricted, occurring under specific conditions such as exposure to IL-4 and GM-CSF (Schildberg et al., 2016). The PD-1 pathway significantly influences T-cell metabolism by inhibiting Akt activation, thereby reducing mTOR activity and shifting metabolism from glycolysis to fatty acid oxidation (Chang et al., 2015; Staron et al., 2014; Patsoukis et al., 2015).

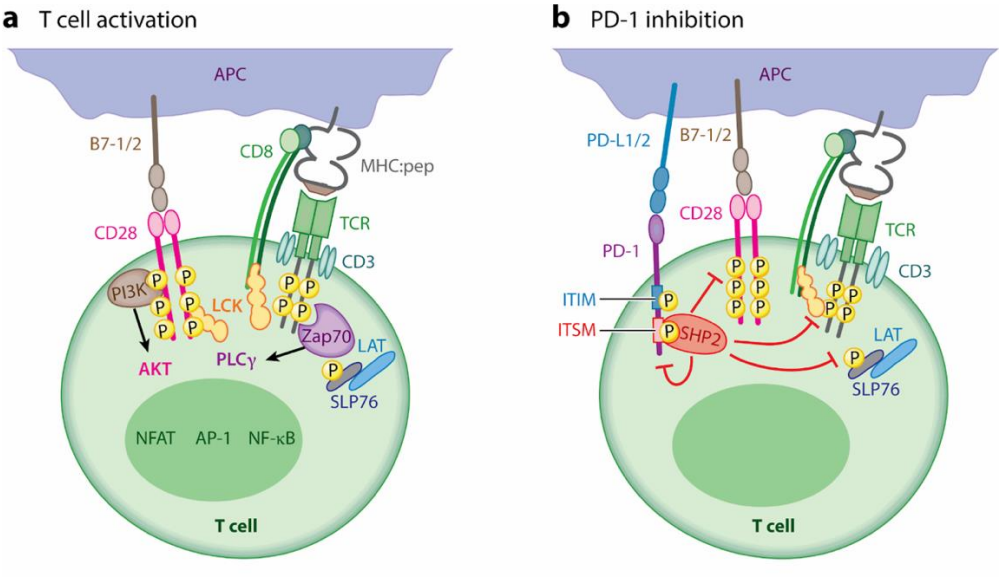

Figure 6. PD-1-driven inhibition of TCR signaling*. In a normal activation state (a), the engagement of the TCR and co-stimulatory molecule CD28 initiates a phosphorylation cascade involving PI3K, AKT, and ZAP70, which drives the activation of essential transcription factors like NFAT and NF-κB. However, during PD-1 inhibition (b), PD-1 binding to its ligands PD-L1/2 recruits the phosphatase SHP-2 to the receptor's intracellular tail. SHP-2 subsequently dephosphorylates proximal signaling molecules, effectively severing the downstream pathways and preventing T cell activation. This figure was taken from Hashimoto et al. (2018) and adjusted.*

2.2.2 Role of PD-1 in T-cell exhaustion

As stated in chapter 2.1.1.3, T-cell exhaustion represents a state of dysfunction in T-cells that occurs during numerous chronic infections and cancer. It is characterized by diminished effector function, persistent expression of inhibitory receptors, and a transcriptional profile distinct from that of functional effector or memory T-cells. This exhaustion impedes optimal control of infections and tumors. Immunoregulation plays a central role in T-cell exhaustion, with these negative pathways classified into three primary categories: cell surface inhibitory receptors (e.g., PD-1), soluble factors (e.g., IL-10), and immunoregulatory cell types (e.g., regulatory T-cells (Treg cells) and other similar cells (Wherry, 2011).

Exhausted CD8+ T-cells exhibit metabolic deficiencies, with PD-1 regulating early glycolytic and mitochondrial changes and repressing PGC-1α (peroxisome proliferator-activated receptor γ coactivator 1α). Overexpression of PGC-1α has been shown to enhance metabolic function and performance in these cells during chronic viral infection (Bengsch et al., 2016). Decreased mTOR activation in PD-1-expressing CD8+ T-cells increases FoxO1 (forkhead box O1) activity, maintaining PD-1 expression and cell survival (Staron et al., 2014).

Furthermore, these processes result in stable epigenetic "scars" that lock T-cells into a dysfunctional state that is often resistant to full reversal (Pauken et al., 2016), while simultaneously coordinating with other inhibitory receptors like LAG-3 and altering T-cell motility to impede effective target interaction (Blackburn et al., 2009; Zinselmeyer et al., 2013).

2.2.3 Clinical relevance and therapeutic applications

The clinical translation of PD-1 biology began with the landmark approval of the monoclonal antibodies pembrolizumab (Poole, 2014) and nivolumab (Motzer et al., 2014), which fundamentally altered the oncology landscape by targeting the interaction between the PD-1 receptor on T-cells and its ligands (PD-L1/PD-L2) on tumor cells. Initially validated in ipilimumab-refractory melanoma and subsequently in non-small cell lung cancer (NSCLC), these first-generation inhibitors demonstrated that releasing the "brakes" on the immune system could yield durable, long-term remission in patients with previously incurable metastatic disease (Hamid et al., 2013; Topalian et al., 2012). These early pivotal trials established the proof-of-concept for checkpoint blockade, shifting the focus of cancer treatment from targeting the tumor directly to empowering the host immune system, and set the stage for the rapid expansion of indications across diverse solid and hematologic malignancies.

Building on this foundation, the therapeutic landscape has evolved significantly between 2020 and 2026, shifting toward perioperative applications and novel combinatorial strategies to overcome resistance. A major paradigm shift occurred with the validation of neoadjuvant and adjuvant checkpoint blockade in early-stage solid tumors; notably, the CheckMate 816 and KEYNOTE-671 trials established that integrating PD-1 inhibitors with chemotherapy in resectable NSCLC significantly improves event-free survival and pathological complete response rates compared to chemotherapy alone (Forde et al., 2022; Wakelee et al., 2023). This strategy capitalizes on the presence of a larger antigen load and intact lymphatic drainage prior to surgery, theoretically priming a more robust systemic T-cell response against micrometastatic disease than adjuvant therapy alone (Topalian et al., 2015).

Furthermore, the management of resistance mechanisms has driven the development of bispecific antibodies and dual-checkpoint inhibition. The RELATIVITY-047 trial demonstrated that combined LAG-3 and PD-1 inhibition (relatlimab and nivolumab) offers superior progression-free survival in metastatic melanoma compared to PD-1

inhibition alone, validating LAG-3 as the third distinct checkpoint target in the clinic (Tawbi et al., 2022). Concurrently, next-generation bispecific molecules targeting PD-1/CTLA-4 (such as cadonilimab) and PD-1/VEGF (such as ivonescimab) have shown promising efficacy in gastric and lung cancers, respectively, by localizing immune activation within the tumor microenvironment while potentially mitigating some systemic immune-related adverse events associated with separate antibody infusions (Keam, 2022; Zhou et al., 2021).

These advancements collectively signal a move toward precision immuno-oncology, where PD-1 blockade serves as a backbone for increasingly personalized, multimodal treatment regimens.

2.3 Src homology 2-domain containing phosphatases (SHPs)

The protein tyrosine phosphatase (PTP) superfamily represents a diverse group of enzymes critical for maintaining cellular homeostasis by counteracting the activity of protein tyrosine kinases (PTKs). Within the Class I cysteine-based PTPs, the Src homology 2 (SH2) domain-containing phosphatases (SHPs) constitute a unique subfamily of non-receptor PTPs characterized by their specific modular architecture and regulation (Tonks, 2016).

2.3.1 Overview of SHPs

In the mammalian genome, this family is primarily represented by two highly conserved enzymes: SHP-1 (encoded by *PTPN6*) and SHP-2 (encoded by *PTPN11*) (Tamir et al., 2000).

SHP-1 expression is largely restricted to hematopoietic lineages, where it acts as a canonical negative regulator of signaling (Matthews et al., 1992). The physiological importance of SHP-1 is exemplified by the "motheaten" mouse model, in which loss-of-function mutations in PTPTN6 (encoding SHP-1) lead to severe autoimmunity and systemic inflammation due to hyperactive immune cells (Hendriks et al., 2023; Kiratikanon et al., 2022).

SHP-1 and SHP-2 share 55% sequence identity in their catalytic domains and similar structures, but they differ in physiological functions and tissue distribution. (Ran et al., 2016). Germline mutations in *PTPN11* (gene encoding SHP-2) are the cause of approximately 50% of Noonan syndrome (a common genetic disorder causing developmental disruptions, distinct facial features, heart defects and many other health

issues) cases, while somatic gain-of-function mutations are frequent drivers in juvenile myelomonocytic leukemia (JMML) and various solid tumors, solidifying SHP-2 as a proto-oncogene (Tartaglia et al., 2011).

2.3.2 Structure and function of SHP-2

The structural biology of SHP-2 is defined by a "molecular switch" mechanism. The enzyme comprises two tandem SH2 domains at the N-terminus (N-SH2 and C-SH2), a catalytic PTP domain, and a C-terminal tail containing two critical tyrosyl phosphorylation sites (Tyr542 and Tyr580) (see Figure 7 on page 17)(W. Li et al., 1994; Bennett et al., 1994). The catalytic activity is centered on the P-loop signature motif (HC(X)5R), containing the essential nucleophilic cysteine (Cys459) required for phosphate hydrolysis (LaRochelle et al., 2018).

In the basal, unstimulated state, SHP-2 exists in a "closed," auto-inhibited conformation. Crystallographic studies reveal that the N-SH2 domain wedges into the catalytic cleft of the PTP domain. Specifically, the D'E loop of the N-SH2 domain interacts directly with the catalytic site, blocking substrate entry. A critical interaction involves Asp61 in the N-SH2 domain, which forms hydrogen bonds near the catalytic Cys459, effectively locking the enzyme in an inactive state (Darian et al., 2011).

Activation is triggered when the SH2 domains engage with specific phosphotyrosine (pTyr) motifs—typically bis-phosphorylated immune receptor tyrosine-based inhibitory motifs (ITIMs) or docking sites on scaffolding proteins like GAB1, GAB2, or IRS-1. The binding of pTyr peptides to the N-SH2 domain induces a steric clash that disrupts the N-SH2/PTP interface. This allosteric shift releases the N-SH2 domain, exposing the catalytic pocket ("open" conformation) (see Figure 7 on page 17) and increasing phosphatase activity (Neel et al., 2003; Pierotti & Köhn, 2026).

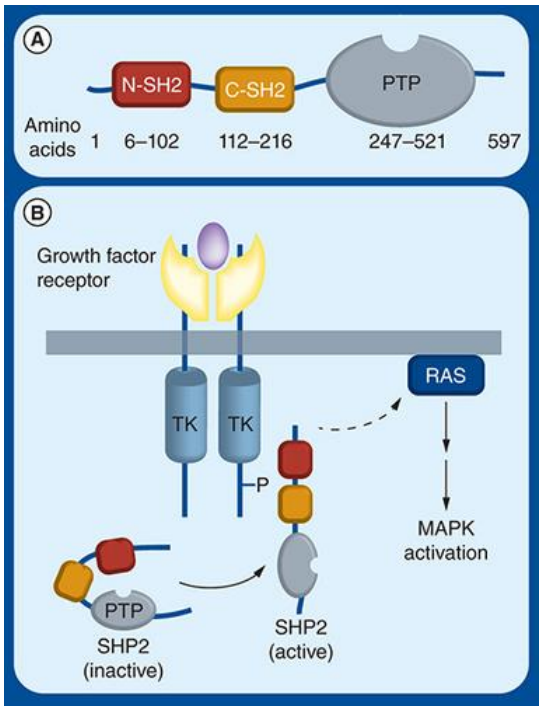

Figure 7. Structure and activation mechanism of SHP-2. *(A) Schematic representation of the domain structure of the SHP-2 protein, highlighting the N-terminal SH2 domain, the C-terminal SH2 domain, and the protein tyrosine phosphatase catalytic domain (PTP). (B) In its basal state, SHP-2 is autoinhibited (inactive) by an intramolecular interaction between the N-SH2 and PTP domains. Upon receptor stimulation, the receptor tyrosine kinase (TK) domains phosphorylate specific residues, creating binding sites. The SH2 domains of SHP-2 bind to these phosphotyrosine residues (P), releasing the autoinhibition and activating the phosphatase. This active SHP2 promotes downstream signaling, specifically the activation of the RAS-MAPK pathway. This figure was taken from Butterworth et al.(2014) and adjusted.*

2.3.2.1 Role of SHP-2 in signaling pathways

SHP-2 serves as a pleiotropic node in cellular signaling, integrating inputs from the cell surface to nuclear transcriptional machinery.

The most well-characterized function of SHP-2 is the positive regulation of the RAS/ERK MAPK pathway. Upon growth factor stimulation (e.g., EGF, PDGF), SHP-2 is recruited to the receptor complex via GAB1/2 adapters (M. Arnaud et al., 2004; Maroun et al., 2000; Yang et al., 2006). Once activated, SHP-2 dephosphorylates specific pTyr sites on GAB1 that act as docking sites for p120RasGAP (a negative regulator that hydrolyzes RAS-GTP to RAS-GDP). By removing these binding sites, SHP-2 prevents RAS inactivation, thereby prolonging RAS-GTP accumulation and sustaining ERK1/2 activation (Dance et al., 2007). Additionally, SHP-2 dephosphorylates Sprouty (Spry) proteins, which are intrinsic inhibitors of the RAS pathway, further amplifying the signal (Jarvis et al., 2006).

In the context of tumor immunology, SHP-2 functions as a metabolic brake on T-cells. As described in chapter 2.2.1.1. PD-1 PATHWAY, the ligation of PD-1 by PD-L1 results in the phosphorylation of the ITIM and ITSM motifs on the PD-1 cytoplasmic tail. SHP-2 binds predominantly to the ITSM motif (Patsoukis et al., 2020). Once recruited, SHP-2 dephosphorylates the co-stimulatory receptor CD28 and the TCR-associated kinase Lck (Cammann et al., 2022). This dephosphorylation creates a "short-circuit" in T-cell activation, leading to decreased cytokine production and T-cell exhaustion (Marasco et al., 2020).

2.3.3 Inhibitors of SHPs and their clinical relevance

Targeting phosphatases has historically been termed "undruggable" due to the highly polar, conserved, and positively charged nature of the PTP active site. Early "Type I" competitive inhibitors (e.g., sodium stibogluconate, NSC-87877) targeted the catalytic pocket but failed due to poor cellular permeability, lack of selectivity (inhibiting other phosphatases), and rapid oxidation (Zhang, 2016).

2.3.3.1 The allosteric revolution

The discovery of "Type II" allosteric inhibitors marked a paradigm shift. Instead of competing with the substrate at the active site, these small molecules bind to a hydrophobic tunnel formed at the interface of the N-SH2, C-SH2, and PTP domains. This binding stabilizes the auto-inhibited "closed" conformation, effectively gluing the N-SH2 domain over the catalytic pocket. The prototype allosteric inhibitor, SHP099, demonstrated that stabilizing the inactive conformation could potently suppress RAS/ERK signaling in cancer cells. While not suitable for human trials due to pharmacokinetic properties, it established the structural basis for subsequent drugs (Chen et al., 2016; Luo et al., 2022; Fedele et al., 2018).

TNO155 (developed by Novartis) is a highly potent, selective, and orally bioavailable allosteric inhibitor. It is currently in Phase I/II clinical trials (e.g., NCT03114319). TNO155 has shown efficacy in KRAS-mutant cancers by disrupting the SOS1-mediated feedback loop that reactivates RAS (LaMarche et al., 2020). RMC-4630 is another clinical-stage allosteric inhibitor targeting the SHP-2/RAS interface. The compound is being investigated in combination with direct KRAS-G12C inhibitors (e.g., sotorasib) to prevent adaptive resistance mechanisms where tumor cells upregulate RTK signaling to bypass KRAS blockade (Johnson et al., 2022).

In the context of T-cell modulating molecules affecting SHP-2 in preclinical research, TPI-1 functions as a potent immune enhancer by blocking the inhibitory activity of SHP-1 and, to a lesser extent, SHP-2, which normally serve as negative regulators of T-cell receptor (TCR) signaling. By preventing the dephosphorylation of proximal signaling kinases such as Lck and ZAP-70, TPI-1 effectively lowers the activation threshold of CD8+ T-cells, allowing them to recognize and respond to suboptimal tumor antigens (Kundu et al., 2010). This molecular intervention not only increases the production of effector cytokines like interferon-gamma (IFN-γ) but also rejuvenates exhausted T-cells within the immunosuppressive tumor microenvironment, thereby restoring their cytotoxic potential (Watson et al., 2016).

The PTP1B inhibitors (PTP1Bi) enhance T-cell effector functions primarily by modulating the JAK/STAT signaling axis rather than directly altering TCR sensitivity. By inhibiting PTP1B and PTPN2, these molecules enhance JAK1 and STAT1 activity, boosting transcriptional responses to inflammation and improving T-cell infiltration into "cold" tumors. (Baumgartner et al., 2023). Crucially, while these inhibitors target the catalytic domains of PTP1B/PTPN2, they maintain high selectivity against SHP-2, thereby avoiding direct interference with the Ras/ERK pathways that SHP-2 typically mediates (Qu et al., 2023). Hyperactivation of STAT1-dependent transcription increases the expression of cytolytic molecules like granzyme B and perforin, enhancing T-lymphocyte cytotoxicity. This reprogramming makes T-cells more resistant to tumor-suppressive signals, suggesting that PTP1B may synergize with conventional checkpoint inhibitors to overcome adaptive immune resistance. (Baumgartner et al., 2023; Qu et al., 2023).

While promising, SHP-2 inhibition faces challenges. On-target toxicity is a concern given SHP-2's role in normal hematopoiesis and cardiac development. Furthermore, adaptive kinome reprogramming, where cancer cells bypass SHP-2 inhibition by activating parallel signaling kinases (e.g., FGFR or MET), suggests that SHP-2 inhibitors will likely serve best as backbones of combination therapies rather than monotherapies (Fedele et al., 2018).

2.4 Lymphocyte-specific protein tyrosine kinase (Lck)

The lymphocyte-specific protein tyrosine kinase (Lck) is a 56-kDa non-receptor tyrosine kinase belonging to the Src family of kinases (SFKs) (Elkamhawy et al., 2021). It functions as an obligate proximal signaling mediator within the hematopoietic lineage,

specifically localized to T-lymphocytes and natural killer (NK) cells (Palacios & Weiss, 2004; De Sanctis et al., 2024). Lck serves as the primary enzymatic trigger for the T-cell receptor (TCR) signaling apparatus, whereby it transduces extracellular antigen-recognition events into intracellular biochemical cascades. Beyond its role in peripheral immune responses, Lck activity is a fundamental requirement for thymic selection, dictating the maturation and lineage commitment of developing thymocytes (Palacios & Weiss, 2004; Van Laethem et al., 2013).

2.4.1 Structure and function of Lck

The structural architecture of Lck is defined by a modular arrangement of domains that facilitate its precise spatial and temporal regulation. The N-terminal SH4 domain (see Figure 8 on page 21) undergoes dual acylation, specifically myristoylation and palmitoylation, which dictates its sequestration into specialized, cholesterol-rich microdomains of the plasma membrane known as lipid rafts (L. Li et al., 2017). This is followed by the Unique Domain (UD), which contains a specialized zinc-clasp motif that mediates the non-covalent association of Lck with the cytoplasmic tails of CD4 or CD8 co-receptors (P. W. Kim et al., 2003). The regulatory core comprises the SH3 and SH2 domains, which facilitate protein-protein interactions via proline-rich motifs and phosphotyrosine residues, respectively, while the SH1 (kinase) domain executes phosphotransferase activity (Panchamoorthy et al., 1994; Kurochkina & Guha, 2012; De Sanctis et al., 2024).

The catalytic efficacy of Lck is meticulously governed by the phosphorylation status of three critical tyrosine (Tyr) residues, which act as allosteric and enzymatic switches (see Figure 8 on page 21).

Tyr505 (The Inhibitory Residue) is located at the C-terminal tail. Tyr505 is the primary site of negative regulation. Upon phosphorylation by the C-terminal Src kinase (Csk), pTyr505 engages in an intramolecular interaction with Lck's own SH2 domain. This interaction stabilizes the protein in a quiescent, closed conformation (see Figure 8 on page 21), thereby occluding the catalytic cleft and preventing substrate phosphorylation (Rossy et al., 2012; De Sanctis et al., 2024).

Tyr394 (The Autocatalytic Residue) is positioned within the activation loop of the kinase domain and is the primary site of trans-autophosphorylation. Phosphorylation of Tyr394 induces a conformational shift that reorients the catalytic residues, significantly enhancing the enzymatic activity (see Figure 9 on page 22). This state is widely

considered an open and active kinase. Double phosphorylation of Tyr394 and Tyr505 is possible, yielding an active enzyme distinct from the closed state. However, Lck activity is not regulated through the phosphorylation of its kinase domain (Fernández-Aguilar et al., 2023; Inderberg et al., 2017; De Sanctis et al., 2024). Instead, it is allosterically activated when its SH2 domain interacts with SFK-phosphorylated motifs (De Sanctis et al., 2024).

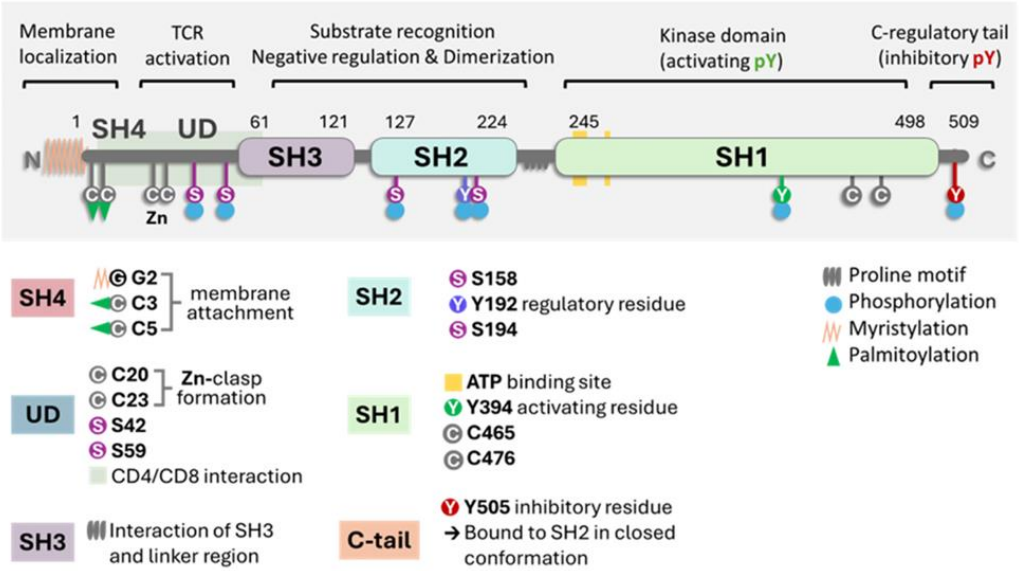

Figure 8. Schematic representation of the domain structure of the Lck protein. *This scheme highlights the N-terminal SH4 and Unique (UD) domains, the central SH3 and SH2 domains, the catalytic SH1 kinase domain, and the C-regulatory tail. In its basal state, Lck is autoinhibited (inactive) by an intramolecular interaction where the phosphorylated C-terminal inhibitory residue (Y505) binds to the SH2 domain, maintaining a closed conformation. Upon TCR stimulation, the SH4 domain anchors the kinase to the membrane via myristoylation and palmitoylation, while the UD domain facilitates interaction with CD4/CD8 co-receptors through a zinc-clasp formation. Full catalytic activity is achieved via phosphorylation of the activating tyrosine residue (Y394) within the SH1 domain, which releases autoinhibition and activates the kinase. This active Lck promotes downstream signaling, specifically driving TCR activation pathways. This figure was taken from De Sanctis et al. (2024) and adjusted.*

Tyr192 (The Regulatory Modulator) is located within the SH2 domain and serves as a critical node in feedback regulation. Phosphorylation of this residue, typically mediated by the kinase Itk, alters the binding specificity of the SH2 domain and sterically hinders the association between Lck and the phosphatase CD45. Because CD45 is required to dephosphorylate the inhibitory pTyr505, pTyr192 effectively preserves the inactive state of Lck, serving as a biological "brake" to attenuate TCR signaling sensitivity (Kästle et al., 2020; Courtney et al., 2017; De Sanctis et al., 2024).

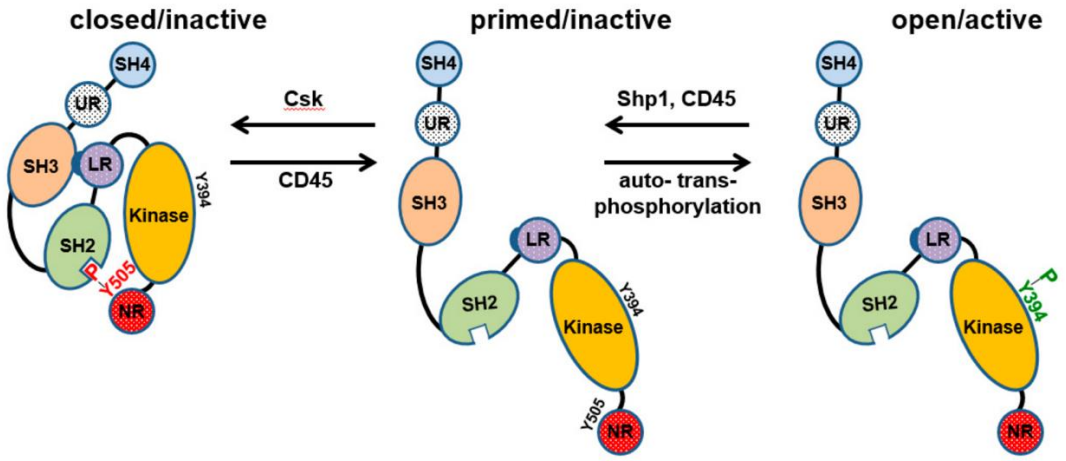

Figure 9. Dynamic structural shifts governing Lck enzymatic function. *This diagram outlines the activation cycle of the Lck kinase, which transitions through three distinct structural phases dictated by specific phosphorylation events. Initially, the enzyme is held in a tightly folded, dormant state when the Csk kinase adds a phosphate group to the Y505 residue. To prepare for cellular signaling, the CD45 phosphatase removes this inhibitory phosphate, causing the molecule to unfurl into an intermediate, "primed" configuration. Full catalytic activity is subsequently achieved when the Y394 residue undergoes auto-phosphorylation, locking the protein into a fully open and functional shape. This signaling phase is eventually turned off when phosphatases, specifically Shp1 or CD45, dephosphorylate Y394, returning the Lck molecule to its resting, primed state. This figure was taken from Bommhardt et al. (2019) and adjusted.*

2.4.2 Lck involvement in T-cell activation

As discussed in sections 2.1.1.1 and 2.1.1.2, the initiation of T-cell activation is predicated upon the formation of the immunological synapse, where TCR engagement with a pMHC complex triggers the recruitment of Lck-bound co-receptors. According to the kinetic segregation model, the narrow intermembrane space at the synapse excludes large ectodomain phosphatases such as CD45, creating a protected environment for Lck activity (F. Li et al., 2024; Davis & Van Der Merwe, 2006). Once localized, Lck executes the phosphorylation of immunoreceptor tyrosine-based activation motifs (ITAMs) within the CD3 and -chain subunits. These phosphorylated ITAMs serve as docking sites for the ZAP-70 kinase, which Lck subsequently activates via phosphorylation of Tyr319 and Tyr493, thereby unleashing the downstream LAT/SLP-76 signalosome (Fernández-Aguilar et al., 2023).

2.4.3 Inhibitors and modulators of Lck and their clinical relevance

Lck plays a key role in T-cell-mediated immunity, making it an important therapeutic target. Using small-molecule inhibitors like A-770041 can effectively suppress T-cell activation, offering a potential strategy for treating autoimmune disorders and preventing organ transplant rejection. (Stachlewitz et al., 2005; Burchat et al., 2005). Conversely, in

lymphoid malignancies like T-cell acute lymphoblastic leukemia (T-ALL), multikinase inhibitors such as Dasatinib are employed to target the constitutive Lck activity that drives malignant proliferation (Schade et al., 2008).

Recent insights show that CuET (bis-diethyldithiocarbamate-copper complex), the active metabolite of disulfiram (an anti-alcoholism drug), has a strong immunomodulatory role beyond classical inhibition. (Antabuse) (Dosset & Zanetti, 2022). Emerging research indicates that CuET—and its parent compound—directly modulates Lck activity by covalently binding to the Cys20 and Cys23 residues located in the N-terminal region of the kinase (Wang et al., 2022). This covalent ligation facilitates a conformational transition that promotes Tyr394 phosphorylation, thereby significantly enhancing Lck catalytic activity (S. Zhang et al., 2023). In the context of oncology, this mechanism is of profound clinical relevance; while CuET exerts direct anti-cancer effects by inducing proteotoxic stress through NPL4/p97 inhibition, its ability to simultaneously activate Lck bolsters CD8+ T-cell-mediated anti-tumor immunity. Consequently, CuET acts as a unique bifunctional agent capable of "turning cold tumors hot" by stimulating T-cell infiltration and cytotoxic effector function (Wang et al., 2022; Dumut et al., 2025). It has been suggested, but never proven, that CuET could rescue exhausted cells.

3 MATERIALS AND METHODS

3.1 Materials

3.1.1 Laboratory equipment

Product	Supplier
Analytical balance KERN ABT 220-5DM	KERN & SOHN GmbH
Automatic / Mechanical pipettes	Eppendorf (Research® plus)
ChemiDoc™ MP Imaging System	Bio-Rad Laboratories, Inc.
Dry block thermostat Bio TDB-100	Biosan, Latvia
EnSpire Multimode Plate Reader	PerkinElmer, Inc., USA
Gel Electrophoresis Mini-PROTEAN Tetra	Bio-Rad Laboratories, Inc.
Heracell™ 150i CO2 Incubator	Thermo Scientific™, USA
Herasafe KS, Class II Biological Safety Cabinet	Thermo Scientific™, USA
Hettich Universal 32R Refrigeration Centrifuge	Andreas Hettich GmbH & Co. KG
Hybridisation oven Techne Hybridizer HB-1D	Bibby Scientific Ld., UK
IKA® VORTEX 3	Sigma-Aldrich, USA

Inverted microscope	Zeiss, Germany
MilliQ® Ultrapure Water Systems	Merck KGaA, Germany
Revvity EnVision Nexus Multimode plate reader	Revvity, Inc., USA
Rotina 420 R Centrifuge	Andreas Hettich GmbH & Co. KG
Trans-Blot Turbo Transfer / Blotting System	Bio-Rad Laboratories, Inc.
Ultrasonic cleaner Sonorex Digitec DT	BANDELIN electronic GmbH
Vi-CELL™ XR cell viability analyzer	Beckman Coulter, Inc., USA

3.1.2 Chemicals

Product / Chemical	**Supplier**
1-butanol	Penta s.r.o., Czech Republic
Bovine serum albumin (BSA)	Sigma-Aldrich, USA
Complete Tablets, Mini EDTA-free, EASYpack	Roche Diagnostics Deutschland GmbH
CuET	Sigma-Aldrich, USA
Dasatinib	Sigma-Aldrich, USA
Dimethyl sulfoxide (DMSO)	Sigma-Aldrich, USA
eBioscience™ Cell Stimulation Cocktail (500X)	Thermo Scientific™, USA
Ethanol, 96%	Penta s.r.o., Czech Republic
Hystopaque 1077 Ficoll-Paque density gradient	Sigma-Aldrich, USA
Lectin from Phaseolus vulgaris	Sigma-Aldrich, USA
Penicillin-Streptomycin solution 100x	Gibco™, USA
Ponceau Stain	Sigma-Aldrich, USA
Propidium iodide	Sigma-Aldrich, USA
Protease Inhibitor Cocktail Tablets complete Tablets EASYpack	Roche Diagnostics Deutschland GmbH
Restore™ PLUS Western Blot Stripping Buffer	Thermo Scientific™, USA
RIPA Lysis and Extraction Buffer	Thermo Scientific™, USA
Sodium Dodecyl Sulfate (SDS)	Sigma-Aldrich, USA
SuperSignal™ West Pico PLUS Chemiluminescent Substrate	Thermo Scientific™, USA
Trans-Blot Turbo 5x Transfer Buffer	Bio-Rad Laboratories, Inc., USA
Tris/Glycine/SDS 10x	Bio-Rad Laboratories, Inc., USA
TrypLE™ Express Enzyme (1X), no phenol red	Gibco™, USA

3.1.3 Diagnostic kits, markers, and accessories

- Spectra™ Multicolor Broad Range Protein Ladder (Thermo Scientific™, USA, #26623)
- Pierce™ BCA protein assay kit (Thermo Fisher Scientific, UK/USA) (Includes Reagent A #23223 and Reagent B #23224)
- Pierce™ Bovine Serum Albumin Standard Pre-Diluted Set (Thermo Scientific™, USA, #23208)
- TGX Stain-Free™ FastCast™ Acrylamide Kit, 12% (Bio-Rad Laboratories, Inc., USA, #1610185)
- Trans-Blot Turbo RTA Mini 0.2 µm Nitrocellulose Transfer Kit (Bio-Rad Laboratories, Inc., USA, #1704270)

3.1.4 Buffers and solutions

- **Stock Phosphate-buffered saline (PBS) buffer (10x)** (pH 6.8 – 7.2): A ready-to-use 10x solution was prepared by the lab manager.
- **Working solution of PBS (1x)**: 100 ml of 10x PBS + 900 ml MiliQ water
- **Radioimmunoprecipitation assay (RIPA) buffer with inhibitors**: RIPA Lysis and Extraction Buffer + 1x complete protease inhibitor cocktail + 1x phosphatase inhibitor.
- **Sample loading Laemmli buffer (5x)**: ready-to-use 5x solution prepared by the lab manager (Tris, SDS, glycerol, beta-mercaptoethanol, bromphenol blue)
- **Working solution of Tris-Glycine-SDS (TGS) Running Buffer (1x)**: 100 ml of stock 10x TGS + 900 ml MiliQ water
- **Tris-buffered saline (TBS) buffer (10x) (pH 7.6)**: 24,2 g Tris base; 80 g NaCl, in 1 L of MiliQ water
- **Washing buffer Tris-buffered saline with Tween 20 (TBST)**: 1x TBS with 0,1% of Tween-20.
- **Blocking buffer / 5% Bovine Serum Albumin solution**: 5% BSA in TBST buffer
- **Transfer buffer**: 600 ml MilliQ water; 200 ml 5x Trans Blot Turbo Buffer; 200 ml 96% ethanol
- **Cell culture media preparation**: 500 ml chosen culture media + 50 ml FBS (10%) + 5 ml Penicillin-Streptomycin solution (100 U·ml-1), filtered (0.22 micron filter).

3.1.5 Antibodies

Antibody	Catalog number/ Supplier
anti GAPDH	Monoclonal Antibody (MA5-15738); Thermo Scientific™, USA
anti PD-1 (WB)	Monoclonal Antibody (53-9969-42) ; Thermo Scientific™, USA
anti PD-1 (FC)	PE anti-human CD279 (PD-1) Antibody; BioLegend, USA
anti PD-L1 (FC)	Monoclonal Antibody (53-5983-42) ; Thermo Scientific™, USA
anti pTyr192 LCK	Polyclonal Antibody (44-844G) ; Thermo Scientific™, USA
anti pTyr394 LCK	Polyclonal Antibody (PA5-78038) ; Thermo Scientific™, USA
anti pTyr505 LCK	Polyclonal Antibody (PA5-99353) ; Thermo Scientific™, USA
anti total LCK	Monoclonal Antibody (MA1-19197) ; Thermo Scientific™, USA
Secondary anti-mouse	HRP Goat anti-mouse IgG (minimal x-reactivity); BioLegend, USA
secondary anti rabbit	HRP Cojugated Polyclonal Antibody (32460), ; Thermo Scientific™, USA

3.1.6 Cell lines and cell culture consumables

Product / Item	Supplier / Details
Cell Lines	
A549	human epithelial cells, lung carcinoma
HCT-116	human epithelial cells, colorectal carcinoma
HCT-116 p53~/~	P53 double knock-out from ATCC #CCL-247, Horizon Discovery Ltd., UK
Jurkat	human T-lymphocyte cells, acute T-cell leukemia
K562	human bone marrow cells, chronic myelogenous leukemia
MOLT-4	human T lymphoblast cells, acute lymphoblastic leukemia
Other Items	
BioWhittaker® Dulbecco's Modified Eagle Medium (DMEM)	Lonza Walkersville, Inc, USA
BioWhittaker® RPMI-1640 medium with L-glutamine	Lonza Walkersville, Inc, USA
Cell Scraper	TPP Techno Plastic Products AG
Centrifuge tubes conical (15 ml & 50 ml)	TPP Techno Plastic Products AG
DURAN® sterile glass bottle 500mL	Schott AG, Germany

Fetal Bovine Serum (FBS)	Gibco™, USA
McCoy's 5A w/ L-Glutamine culture media	BIOSERA, France
OptiPlate 96-well	PerkinElmer, Inc., USA
Penicillin-Streptomycin solution 100x	Gibco™, USA
Syringe filters (0.2 µm & 0.22 µm)	Sarstedt AG & TPP
Tissue Culture Flask 75 cm2	TPP Techno Plastic Products AG
TrypLE™ Express Enzyme (1X), no phenol red	Gibco™, USA
Two-part disposable syringes	Chirana T. Injecta, Česká republika

3.1.7 Biological material

- Buffy Coat from healthy donors was retrieved at the Transfusion Department of the Faculty Hospital, Olomouc.

3.1.8 Software

- BioRender (Toronto, Canada; https://biorender.com/)
- Excel 365 (Microsoft Corporation, Washington, USA)
- Grammarly (California, USA; https://app.grammarly.com/)
- GraphPad Prism 9 (GraphPad Software, California, USA)
- Image Lab Software (Bio-Rad Laboratories, USA)
- Microsoft Word (Microsoft Corporation, Washington, USA)
- PowerPoint 365 (Microsoft Corporation, Washington, USA)

3.2 Methods

3.2.1 Isolation of lymphocytes from donors

Peripheral blood mononuclear cells (PBMCs) were isolated from the peripheral blood of healthy human donors, kindly provided by the Transfusion Department (with the approval from the Ethical Committee), using standard Ficoll-Hypaque density gradient centrifugation. Briefly, donor blood was transferred to sterile 50 mL conical tubes and diluted to a final volume of 20 mL with 1x sterile phosphate-buffered saline (PBS). For the density gradient, 10 mL of the diluted blood was carefully layered over 5 mL of sterile Ficoll-Hypaque solution in 15 mL conical tubes, ensuring the interface remained undisturbed. The samples were centrifuged at ~760 × g (2000 RPM) for 30 minutes at room temperature with the centrifuge brake disabled to preserve the gradient. Following centrifugation, the PBMC-containing buffy coat layer was harvested using a sterile Pasteur pipette, transferred to a fresh 15 mL tube, and washed three times with sterile 1x PBS. Each wash consisted of centrifugation at ~345 × g (1200 RPM) for 10 minutes, followed by decantation and resuspension.

3.2.2 T-cell cultivation and stimulation

To evaluate T-cell activation and the induction of exhaustion markers (e.g., PD-1), two stimulation methods were used: a pharmacological approach with a Phorbol 12-myristate 13-acetate (PMA) and ionomycin cocktail, and a receptor-mediated approach with Phytohemagglutinin (PHA). PMA/ionomycin acts intracellularly by activating Protein Kinase C and elevating cytoplasmic calcium, thereby bypassing surface receptor engagement to induce rapid and robust cytokine production. Conversely, PHA stimulates cells by cross-linking glycosylated surface proteins, including the T-cell receptor (TCR) and CD3 complex, mimicking physiological antigen-presenting cell (APC) interactions. While PHA is optimal for multi-day proliferation assays, PMA/ionomycin was prioritized for shorter-term assays (cytotoxicity and Western blotting) due to its rapid efficacy and tendency to induce activation-induced cell death (AICD) over extended periods.

Following isolation, washed PBMCs were resuspended in 6 mL of DMEM (Dulbecco's Modified Eagle Medium with fetal bovine serum and antibiotics). Cell viability and concentration were determined using a Vi-CELL™ Cell Viability Analyzer (Beckman Coulter) with a 20-fold dilution factor (50 µL cell suspension in 950 µL 1x PBS). Cells were subsequently diluted in DMEM to a total volume of 50 mL per condition and seeded into T175 flasks. Flasks were incubated horizontally at 37°C in a humidified

5% CO2 atmosphere for 48 hours to allow monocyte adherence, thereby enriching the non-adherent lymphocyte population.

For stimulation, the PMA/ionomycin cocktail was added at a ratio of 1 µL per 1 × 10^6 cells immediately following isolation, with a secondary restimulation performed at 24 hours. For PHA stimulation, cells were treated once at the onset of incubation with 1 µg/mL (1 µL per 1 × 10^6 cells). An unstimulated flask served as the negative control.

3.2.3 Preparation of treatment conditions

After the 48-hour incubation period, non-adherent cells were harvested into sterile 50 mL tubes, centrifuged at ~345 × g (1200 RPM) for 5 minutes, and washed twice with 20 mL of 1x PBS. Cells were recounted to ensure accurate seeding densities for downstream assays.

Stock solutions of the experimental compounds were prepared in dimethyl sulfoxide (DMSO) at the following concentrations: CuET (2 mM), Dasatinib (1 mM), TPI-1 (2 mg/mL), and PTP1Bi (10 mM).

3.2.3.1 Treatment of T-cells prior to flow cytometry

Flow cytometry was used to assess the expression of exhaustion markers PD-1 and PD-L1 across 10 distinct treatment conditions. Treatment solutions were prepared in DMEM. For each sample, 2 × 10^5 cells were suspended in 1 mL of the respective treatment media. The conditions included:

- **Control:** DMEM media only
- **CuET:** 1 µM final concentration (10 µL stock per 10 mL DMEM media)
- **Dasatinib**: (10 µL stock per 10 mL DMEM media)
- **TPI-1**: (2 µL stock per 10 mL DMEM media)
- **PTP1Bi**: (10 µL stock per 10 mL DMEM media)
- **Combinations:** T+P, C+T, C+D, C+P, and D+T+P, prepared using the respective stock volumes described above

Each treatment condition was applied to cells from the three stimulation groups (unstimulated, PMA/ionomycin, and PHA), totaling 30 samples per donor. Cells were incubated with the treatments for 3 hours at 37°C. Following incubation, cells were washed with 1x PBS, and the supernatant was decanted to a minimal residual volume. Cells were stained with anti-PD-1 (diluted 46 µL stock in 414 µL 1x PBS) and anti-PD-

L1 (diluted 1:10 to 0.1 mg/µL in PBS) antibodies. A volume of 10 µL of the antibody working solution was added to each tube that contained 20,000 cells, and the samples were incubated for 20 minutes at room temperature in the dark. Cells were subsequently washed three times with 1x PBS, resuspended in a minimal volume, and analyzed via flow cytometry.

3.2.3.2 Treatment of T-cells prior to Western blot analysis

For protein expression and phosphorylation pattern analysis, 8 × 10^6 cells per condition were aliquoted into 15 mL tubes containing 2 mL DMEM. A working solution of CuET was prepared by diluting 40 µL of stock in 40 mL of DMEM. Inhibitor stocks (1 µL each of Dasatinib, TPI-1, and/or PTP1Bi, depending on the assigned combination) were added directly to the 2 mL cell suspensions. The tubes were incubated for 30 minutes at 37°C. Subsequently, 2 mL of the prepared CuET working solution (or 2 mL of plain DMEM for non-CuET conditions) was added to the respective tubes, followed by an additional 15-minute incubation. Cells were then pelleted (~345 × g for 5 minutes), washed three times with 1x PBS, transferred to 1.5 mL microcentrifuge tubes, and pelleted once more. The supernatant was completely removed, and the dry cell pellets were flash-frozen and stored at -80°C until lysis.

3.2.3.3 Treatment of T-cells prior to cytotoxicity assay

Cytotoxicity assays were conducted using a protocol similar to that for Western blot preparation, with 8 × 10^6 cells in 2 mL of DMEM per condition. Inhibitor stocks (1 µL each of Dasatinib and/or TPI-1) were added to the appropriate tubes. PTP1Bi was not included in this specific assay because it was not available at the time (cytotoxicity was performed first out of all experiments). Cells were incubated for 30 minutes at 37°C. Then, 2 mL of the CuET working solution (prepared as described in Section 3.2.3.2) or plain DMEM was added to the relevant conditions, and the samples were incubated for an additional 15 minutes. Finally, cells were centrifuged (~345 × g for 5 minutes) and the treatment media was discarded prior to downstream viability analyses.

3.2.4 Flow cytometry of stimulated T-cells and data analysis

Following the staining protocol, flow cytometric analysis of the treated T-cells was performed using a BD FACSAria™ II cell sorter (BD Biosciences) with the kind help of Dr. Ivo Frydrych.

For quantitative and statistical evaluation, the mean fluorescence intensity (MFI) was extracted for each sample to assess the expression levels of the target surface markers. To ensure statistical robustness, each experimental condition was evaluated using biological replicates derived from four independent healthy donors (n = 4).

3.2.5 Cytotoxicity assessment of treated T-Cells and data analysis

To evaluate the cytotoxic efficacy of the treated lymphocytes against various cancer models, two-dimensional (2D) cancer cell cultures were prepared 48 hours prior to co-incubation. The target cell lines included HCT 116 (colorectal carcinoma, partially resistant to killing), HCT 116 p53-/- (p53 knockout colorectal carcinoma, partially resistant to killing), Jurkat (T-cell leukemia, susceptible to killing), K562 (myeloid leukemia, susceptible to killing), A549 (lung carcinoma, most resistant cell line tested), and MOLT-4 (T-lymphoblastoma, susceptible to killing). Target cells were harvested (adherent cells were trypsinized), washed with 1x PBS, and seeded into fluorimetry-compatible 96-well plates at a density of 2 × 10^4 cells/well (effector to target ratio 5:1). The plates were incubated at 37°C in a humidified 5% CO2 atmosphere for 48 hours in RPMI, McCoy's, or DMEM, depending on the cell line.

Following the 48-hour adherence/acclimation period, 100 µL of the pre-treated lymphocyte suspensions (prepared in Section 3.2.3.3) were added to the respective wells. The first row of each plate was maintained without lymphocytes to serve as a negative control. The co-cultures were then incubated for 24 hours. The experiments were performed in triplicate.

Cell death was quantified using a propidium iodide (PI) exclusion assay. A PI working solution was prepared by dissolving 2 mg of PI in 50 mL of 1x PBS. A volume of 20 µL of this solution was added to each well, and the plates were incubated in the dark at room temperature for 30 minutes. Fluorescence was subsequently measured at an emission wavelength of 618 nm using a microplate spectrofluorometer. To establish a 100% cell death reference for cytotoxicity calculations, control wells were treated with hydrogen peroxide prior to PI staining. Sample fluorescence was considered directly proportional to the number of dead cells.

$$\%\, cytotoxicity = \frac{sample\ fluorescence - neg.control\ fluorescence}{pos.control\ fluorescence - neg.control\ fluorescence}$$

Statistical analysis of the cytotoxicity data was performed using GraphPad Prism 9, with the Bonferroni multiple-comparison test for significance. Notably, basal viability

assessments confirmed that the low concentrations of compounds used did not significantly affect the intrinsic viability of either isolated lymphocytes (>95%) or target cancer cell lines (>90%) when administered alone.

3.2.6 Cell lysis prior to Western blot analysis

Cell pellets previously stored at -80°C (from Section 3.2.3.2) were thawed on ice. All subsequent protein extraction steps were performed on ice or at 4°C to prevent protein degradation. The pellets were then resuspended in 30–40 µL (depending on pellet size) of Radioimmunoprecipitation Assay (RIPA) buffer supplemented with protease and phosphatase inhibitors and vortexed for at least 5 seconds. To facilitate cell membrane disruption, samples were incubated in RIPA buffer on ice for 20 minutes, then sonicated in a water bath for 2 minutes at a temperature not exceeding 10°C. Finally, the lysates were centrifuged at ~13 700 × g (12,000 RPM) for 25 minutes at 4°C, and the protein-rich supernatants were transferred to clean, pre-chilled microcentrifuge tubes for downstream analysis.

3.2.7 Total protein concentration assessment by the BCA method

Total protein concentration was determined using the Bicinchoninic Acid (BCA) assay in a 96-well microplate format. A standard curve was generated using a pre-diluted Bovine Serum Albumin (BSA) standard set with concentrations ranging from 125 to 2000 µg/mL. RIPA buffer supplemented with inhibitors served as the blank. Sample lysates were diluted prior to measurement (2.5 µL of lysate mixed with 7.5 µL of Milli-Q water). BCA Reagents A and B were mixed at a 50:1 ratio, and 200 µL of the resulting working reagent was added to each well. The plate was incubated at 37°C for 30 minutes, after which absorbance was measured at 562 nm using a microplate spectrophotometer.

3.2.8 Protein separation by SDS-PAGE

Protein samples were normalized to load 10 µg of total protein per well. Samples were prepared by mixing the calculated volume of lysate with Milli-Q water and 5x Laemmli sample buffer, then denaturing in a heating block at 95°C for 5 minutes. Proteins were resolved using 12% polyacrylamide gels (1.5 mm thickness), which were cast according to the manufacturer's specifications (Bio-Rad), and 1-butanol was used for surface smoothing of the resolving gel. The gels were placed in an electrophoretic chamber filled with 1x Tris-Glycine SDS (TGS) running buffer. Electrophoresis was conducted at 80 V for 30 minutes to allow proteins to pass through the stacking gel, then increased to 120 V until the dye front reached the bottom of the resolving gel.

3.2.9 Semi-dry WESTERN BLOT

Proteins were transferred from the polyacrylamide gels to nitrocellulose membranes using a semi-dry transfer method via the Trans-Blot® Turbo™ Transfer System (Bio-Rad). Filter papers were pre-soaked in 1x transfer buffer (200 ml of 5x Trans-Blot Turbo 5x Transfer Buffer, 600 ml Milli-Q water, 200 ml of ethanol), and the transfer sandwich was assembled according to the manufacturer's guidelines. The assembled cassettes were inserted into the transfer system, and blotting was performed using the pre-programmed protocol for 1.5 mm gels (10-minute transfer time). Following the transfer, membranes were reversibly stained with Ponceau S to verify uniform protein transfer and equal loading.

3.2.9.1 Immunodetection and band intensity quantification

Following transfer verification, membranes were de-stained with 1x Tris-Buffered Saline containing 0.1% Tween-20 (TBS-T) until the Ponceau S was completely removed. Membranes were blocked in 5% BSA in TBS-T to prevent non-specific binding. Blocking conditions were optimized for specific targets: membranes probed for PD-1 were blocked for 1 hour at room temperature, whereas membranes probed for phosphorylated targets (pTyr394, pTyr192, pTyr505), total Lck, and GAPDH were blocked overnight at 4°C on a gentle shaker to prevent signal oversaturation and background noise.

Membranes were incubated with the following primary antibodies: anti-PD-1 (mouse, 1:500, overnight), anti-pTyr394 (rabbit, 1:1000, 2 hours at room temperature), anti-pTyr192 (rabbit, 1:1000, 2 hours at room temperature), anti-pTyr505 (rabbit, 1:1000, 2 hours at room temperature), anti-total Lck (mouse, 1:3000, 2 hours at room temperature), and anti-GAPDH (mouse, 1:2000, 1 hour at room temperature). Following primary antibody incubation, membranes were washed three times for 5 minutes each in 1x TBS-T at room temperature. Membranes were then incubated with horseradish peroxidase (HRP)-conjugated secondary antibodies (goat anti-mouse or goat anti-rabbit, 1:5000 in 5% BSA) for 1 hour at room temperature. This was followed by three additional 5-minute washes in 1x TBS-T.

Signal detection was achieved using the SuperSignal™ West Pico PLUS Chemiluminescent Substrate. Membranes were incubated with the substrate for 3 minutes in the dark (except for GAPDH, which was imaged immediately upon substrate application to prevent signal blowout). Chemiluminescence was captured using the Bio-Rad ChemiDoc™ MP Imaging System and processed with ImageLab® software. When

necessary, membranes were stripped for re-probing by washing twice for 5 minutes in 1x TBS-T, incubating in Restore™ PLUS Western Blot Stripping Buffer for 10 minutes, washing three times in 1x TBS-T, and repeating the blocking and immunodetection cycle.

Densitometric quantification of protein bands was performed using ImageLab® software, utilizing maximum background subtraction. Target band intensities were first normalized to their respective GAPDH loading controls, and subsequently normalized to the untreated control samples within each membrane to determine relative fold changes (values > 1 indicating an increase, and values < 1 indicating a decrease relative to the control). Statistical significance of the fold changes across the biological replicates (n=9 independent donors) was determined using GraphPad Prism 9.

4 RESULTS

4.1 Modulation of PD-1 and PD-L1 expression in T-lymphocytes

To evaluate the impact of various pharmacological interventions on immune checkpoint expression, flow cytometry was utilized to quantify the percentage of cells expressing PD-1 and/or PD-L1. Primary cells from eight donors were divided into two main experimental cohorts: a PMA/ionomycin-stimulated group (Donors 1–4) and a PHA-stimulated group (Donors 5–8), both compared alongside their respective unstimulated controls.

4.1.1 PMA/ionomycin cohort (donors 1–4)

In unstimulated cells, PD-L1 expression was significantly upregulated following treatment with CuET, Dasatinib, TPI-1, PTP1Bi, as well as the combinatory treatments of CuET + TPI-1 and Dasatinib + TPI-1 + PTP1Bi (see Figure 10 on page 36). However, upon stimulation with PMA/ionomycin for 48h, a statistically significant downregulation of PD-L1 was observed in cells treated with Dasatinib, TPI-1, and the Dasatinib + TPI-1 + PTP1Bi combination (see Figure 11 on page 36).

Regarding PD-1 expression, no statistically significant changes were observed in either the unstimulated or PMA/ionomycin-stimulated groups across any of the treatments (see Figure 12 and Figure 13 on page 37).

When evaluating PD-1 and PD-L1 co-expression, unstimulated cells showed no significant alterations (see Figure 14 on page 38). Conversely, PMA/ionomycin stimulation resulted in a statistically significant increase in the double-positive (PD-1+/PD-L1+) cell population following treatment with Dasatinib, TPI-1, PTP1Bi, CuET + Dasatinib, and Dasatinib + TPI-1 + PTP1Bi (see Figure 15 on page 38).

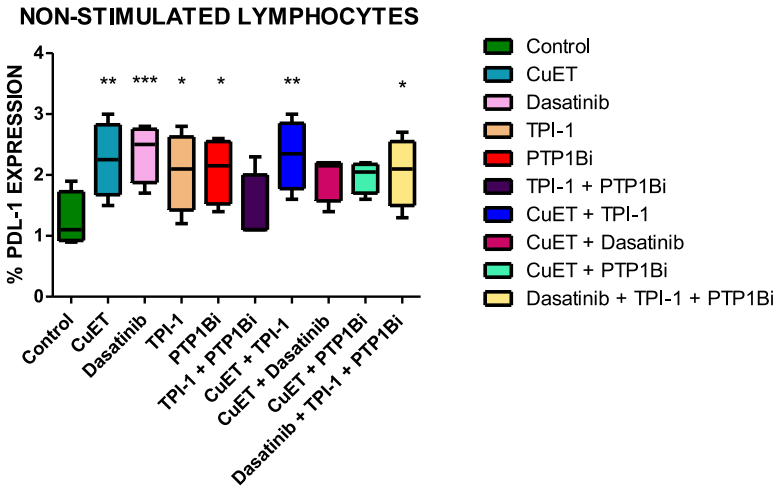

Figure 10. PD-L1 expression in non-stimulated lymphocytes across various treatment groups. *The y-axis represents the percentage of cells expressing PD-L1out of all detected cells. The x-axis lists the ten experimental groups. Each group is represented by a distinct color, as detailed in the legend on the right side of the graph. Statistical significance compared to the control group is indicated by asterisks above specific boxes (* represents p<0,05, ** represents p<0,001, *** represents p<0,000; number of assays was 4). This figure was made using GraphPad Prism 9. Please note the Y-axis scale compared to the next figure.*

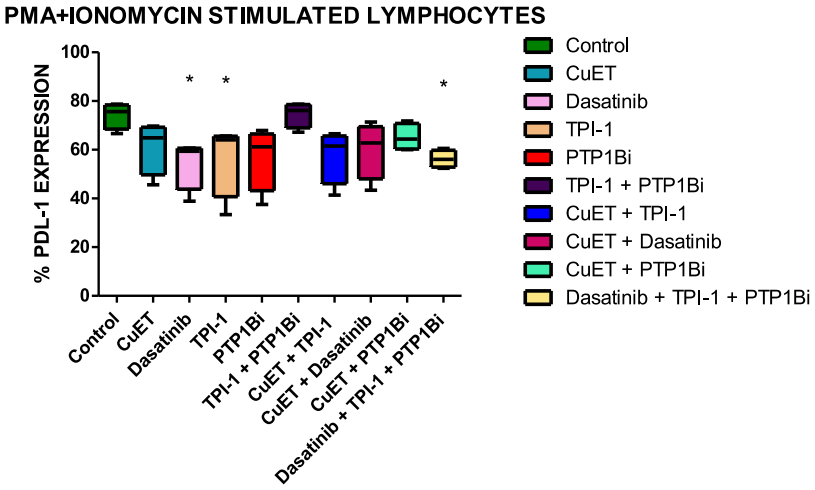

Figure 11. PD-L1 expression in PMA/ionomycin-stimulated lymphocytes across various treatment groups. *The y-axis represents the percentage of cells expressing PD-L1 out of all detected cells. The x-axis lists the ten experimental groups. Each group is represented by a distinct color, as detailed in the legend on the right side of the graph. Statistical significance compared to the control group is indicated by asterisks above specific boxes (* represents p<0,05; number of assays was 4). This figure was made using GraphPad Prism 9. Please note the Y-axis scale compared to the previous figure.*

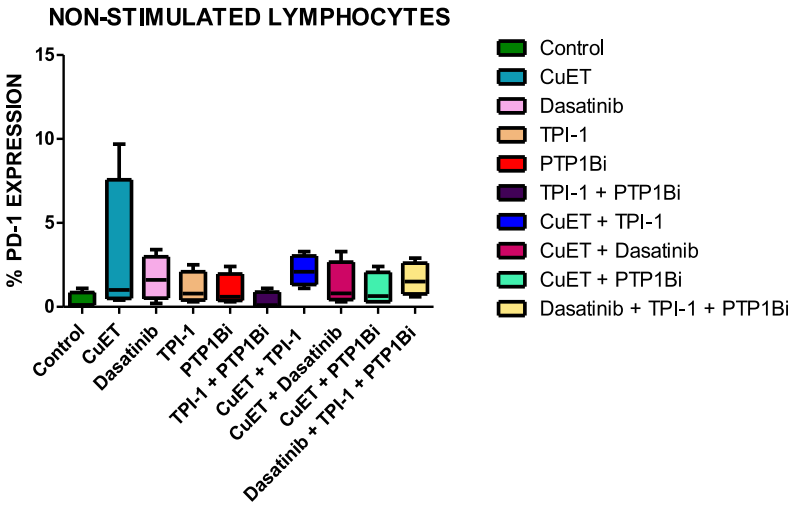

Figure 12. PD-1 expression in non-stimulated lymphocytes across various treatment groups. *The y-axis represents the percentage of cells expressing PD-1out of all detected cells. The x-axis lists the ten experimental groups. Each group is represented by a distinct color, as detailed in the legend on the right side of the graph. No statistical significance was observed; the number of assays was 4. This figure was made using GraphPad Prism 9. Please note the Y-axis scale compared to the next figure.*

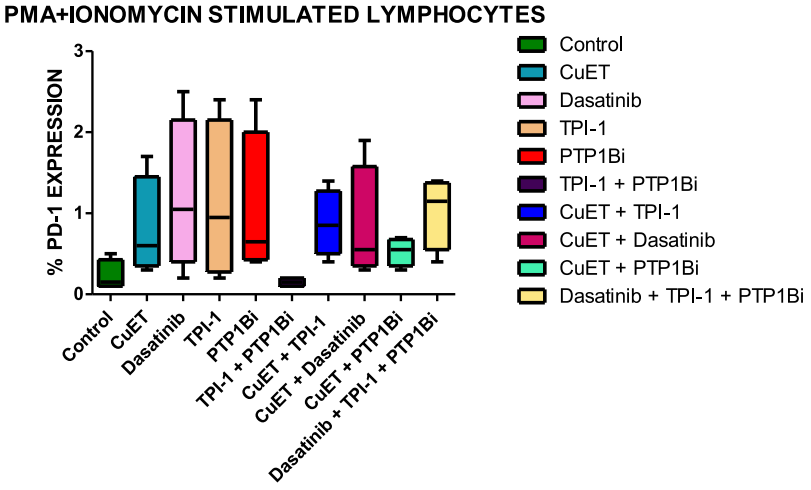

Figure 13. PD-1 expression in PMA/ionomycin-stimulated lymphocytes across various treatment groups. *The y-axis represents the percentage of cells expressing PD-1 out of all detected cells. The x-axis lists the ten experimental groups. Each group is represented by a distinct color, as detailed in the legend on the right side of the graph. No statistical significance was observed; 4 assays were performed. This figure was made using GraphPad Prism 9. Please note the Y-axis scale compared to the previous figure.*

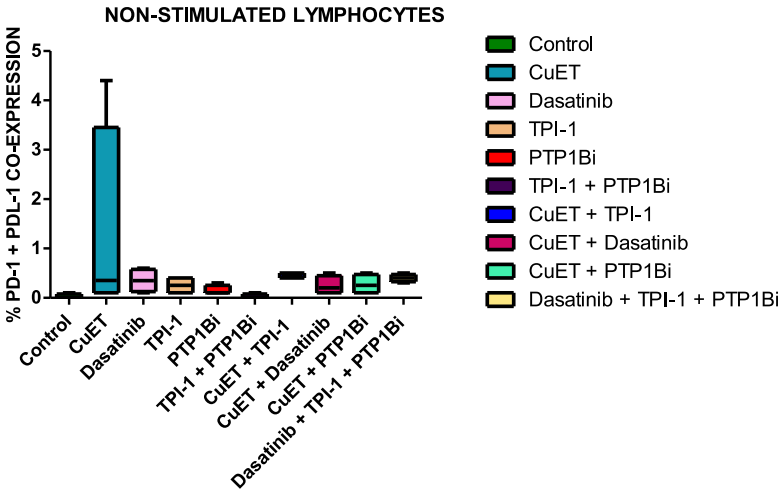

Figure 14. PD-1 and PD-L1 co-expression in non-stimulated lymphocytes across various treatment groups. *The y-axis represents the percentage of cells co-expressing PD-1 and PD-L1 out of all detected cells. The x-axis lists the ten experimental groups. Each group is represented by a distinct color, as detailed in the legend on the right side of the graph. No statistical significance was observed, and 4 assays were performed. This figure was made using GraphPad Prism 9. Please note the Y-axis scale compared to the next figure.*

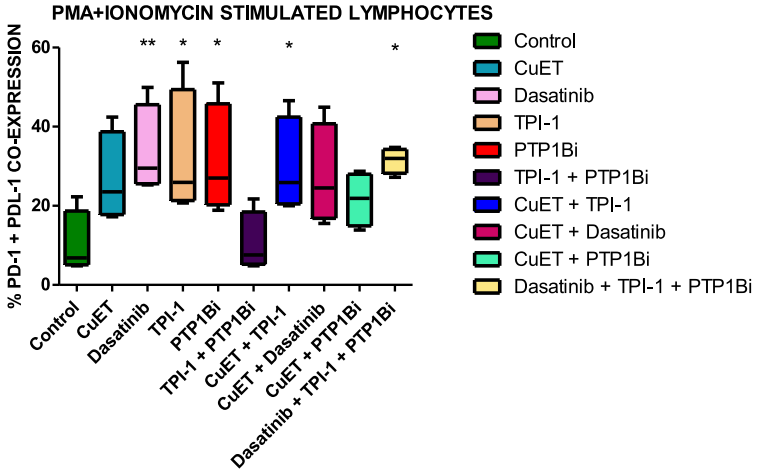

Figure 15. PD-1 and PD-L1 co-expression in PMA/ionomycin-stimulated lymphocytes across various treatment groups. *The y-axis represents the percentage of cells co-expressing PD-1 and PD-L1 out of all detected cells. The x-axis lists the ten experimental groups. Each group is represented by a distinct color, as detailed in the legend on the right side of the graph. Statistical significance compared to the control group is indicated by asterisks above specific boxes (* represents p<0,05, ** represents p<0,001; number of assays was 4). This figure was made using GraphPad Prism 9. Please note the Y-axis scale compared to the previous figure.*

4.1.2 PHA cohort (donors 5–8)

In the PHA cohort, single-positive PD-L1 expression remained unaltered, with no statistically significant changes observed in either the unstimulated or PHA-stimulated (48h) conditions (see Figure 16 on page 39 and Figure 17 on page 40).

In contrast, single-positive PD-1 expression was significantly upregulated by the CuET + TPI-1 combination in both unstimulated and PHA-stimulated cells for 48h (see Figure 18 on page 40 and Figure 19 on page 41).

Analysis of PD-1/PD-L1 co-expression revealed no significant changes in the unstimulated group (see Figure 20 on page 41). However, following PHA stimulation, the combinatory treatment of Dasatinib + TPI-1 + PTP1Bi induced a statistically significant upregulation in the double-positive cell population (see Figure 21 on page 42).

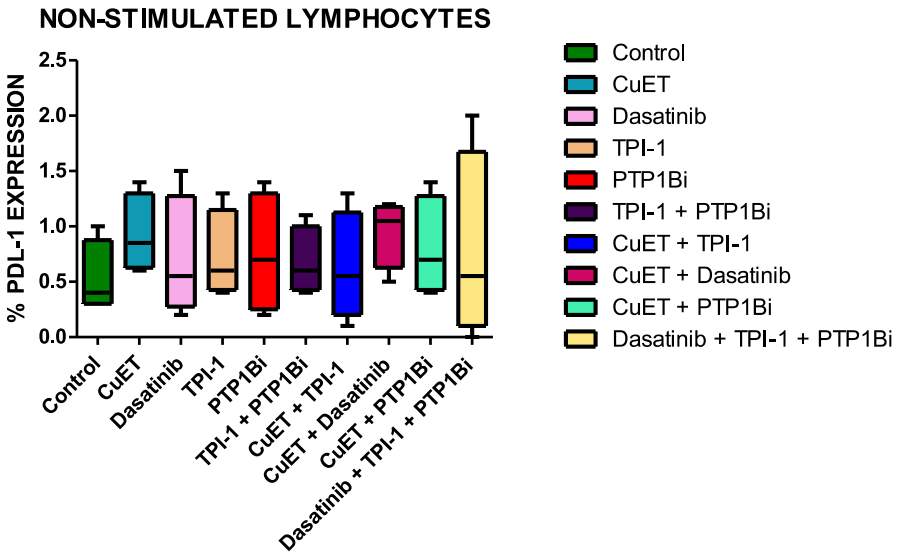

Figure 16. PD-L1 expression in non-stimulated lymphocytes (donors 5-8) across various treatment groups. *The y-axis represents the percentage of cells expressing PD-L1out of all detected cells. The x-axis lists the ten experimental groups. Each group is represented by a distinct color, as detailed in the legend on the right side of the graph. No statistical significance was observed, and 4 assays were performed. This figure was made using GraphPad Prism 9. Please note the Y-axis scale compared to the next figure.*

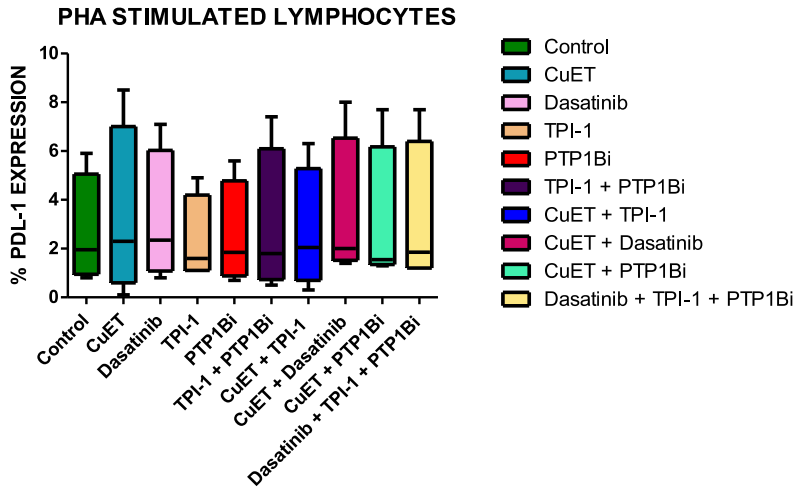

Figure 17. PD-L1 expression in PHA -stimulated lymphocytes across various treatment groups. *The y-axis represents the percentage of cells expressing PD-L1 out of all detected cells. The x-axis lists the ten experimental groups. Each group is represented by a distinct color, as detailed in the legend on the right side of the graph. No statistical significance was observed, and 4 assays were performed. This figure was made using GraphPad Prism 9. Please note the Y-axis scale compared to the previous figure.*

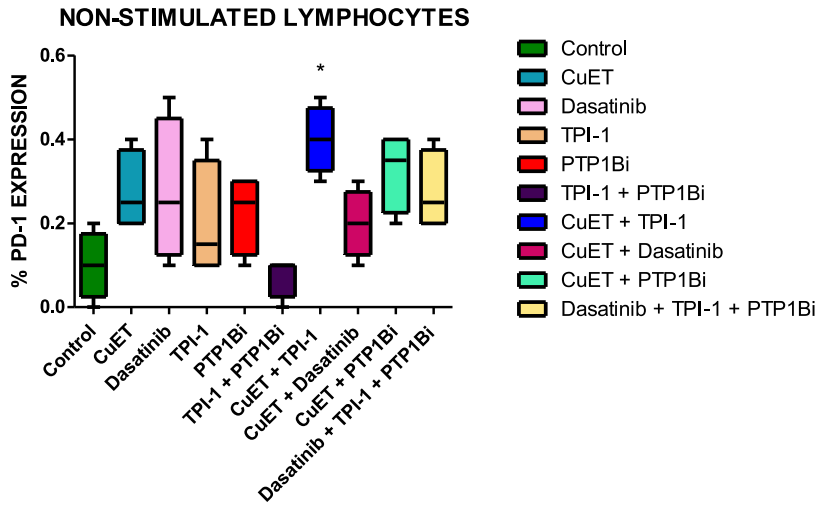

Figure 18. PD-1 expression in non-stimulated lymphocytes (donors 5-8) across various treatment groups. *The y-axis represents the percentage of cells expressing PD-1out of all detected cells. The x-axis lists the ten experimental groups. Each group is represented by a distinct color, as detailed in the legend on the right side of the graph. Statistical significance compared to the control group is indicated by asterisks above specific boxes (* represents p<0,05; number of assays was 4). This figure was made using GraphPad Prism 9.*

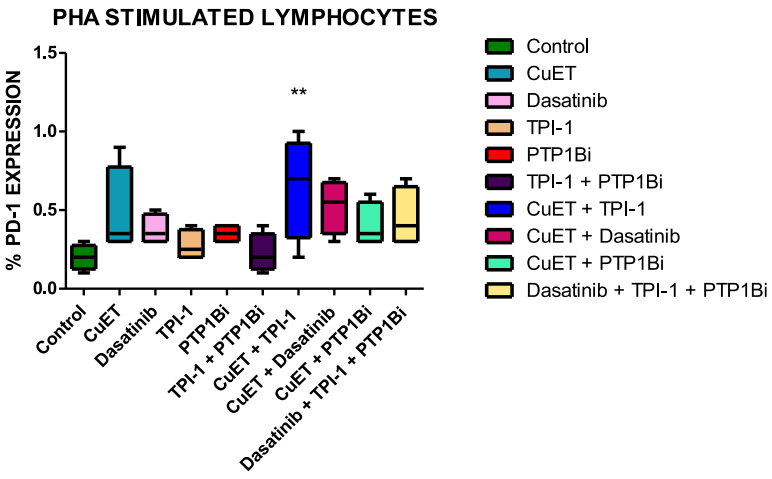

Figure 19. PD-1 expression in PHA -stimulated lymphocytes across various treatment groups. *The y-axis represents the percentage of cells expressing PD-1 out of all detected cells. The x-axis lists the ten experimental groups. Each group is represented by a distinct color, as detailed in the legend on the right side of the graph. Statistical significance compared to the control group is indicated by asterisks above specific boxes (** represents p<0,001; the number of assays was 4). This figure was made using GraphPad Prism 9.*

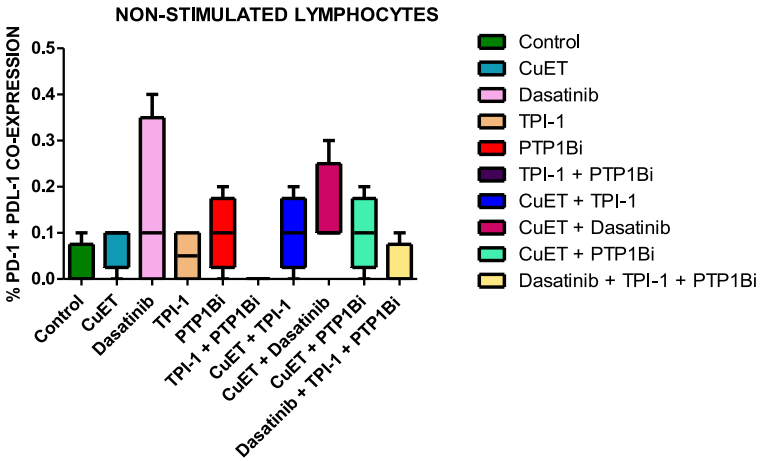

Figure 20. PD-1 and PD-L1 co-expression in non-stimulated lymphocytes (donors 5-8) across various treatment groups. *The y-axis represents the percentage of cells co-expressing PD-1 and PD-L1 out of all detected cells. The x-axis lists the ten experimental groups. Each group is represented by a distinct color, as detailed in the legend on the right side of the graph. No statistical significance was observed, and 4 assays were performed. This figure was made using GraphPad Prism 9.*

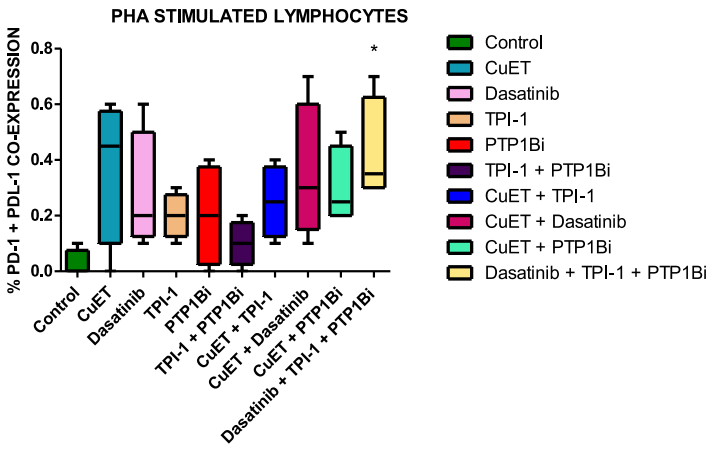

Figure 21. PD-1 and PD-L1 co-expression in PHA-stimulated lymphocytes across various treatment groups. *The y-axis represents the percentage of cells co-expressing PD-1 and PD-L1 out of all detected cells. The x-axis lists the ten experimental groups. Each group is represented by a distinct color, as detailed in the legend on the right side of the graph. Statistical significance compared to the control group is indicated by asterisks above specific boxes (* represents p<0,05; number of assays was 4). This figure was made using GraphPad Prism 9.*

4.2 Effects on Lck phosphorylation and protein expression

Western blot analysis was performed to assess protein expression and phosphorylation status. Overall, semi-quantitative analysis did not yield statistically significant differences across the treatment groups (see Figures 23 and 24 on page 44). However, qualitative observation indicated that Dasatinib treatment consistently abrogated phosphorylation, though this effect did not reach statistical significance. Notably, as depicted in Figure 22 on page 43, cellular stimulation successfully induced PD-1 expression concurrently with Lck phosphorylation at residues Tyr394, Tyr192, and Tyr505.

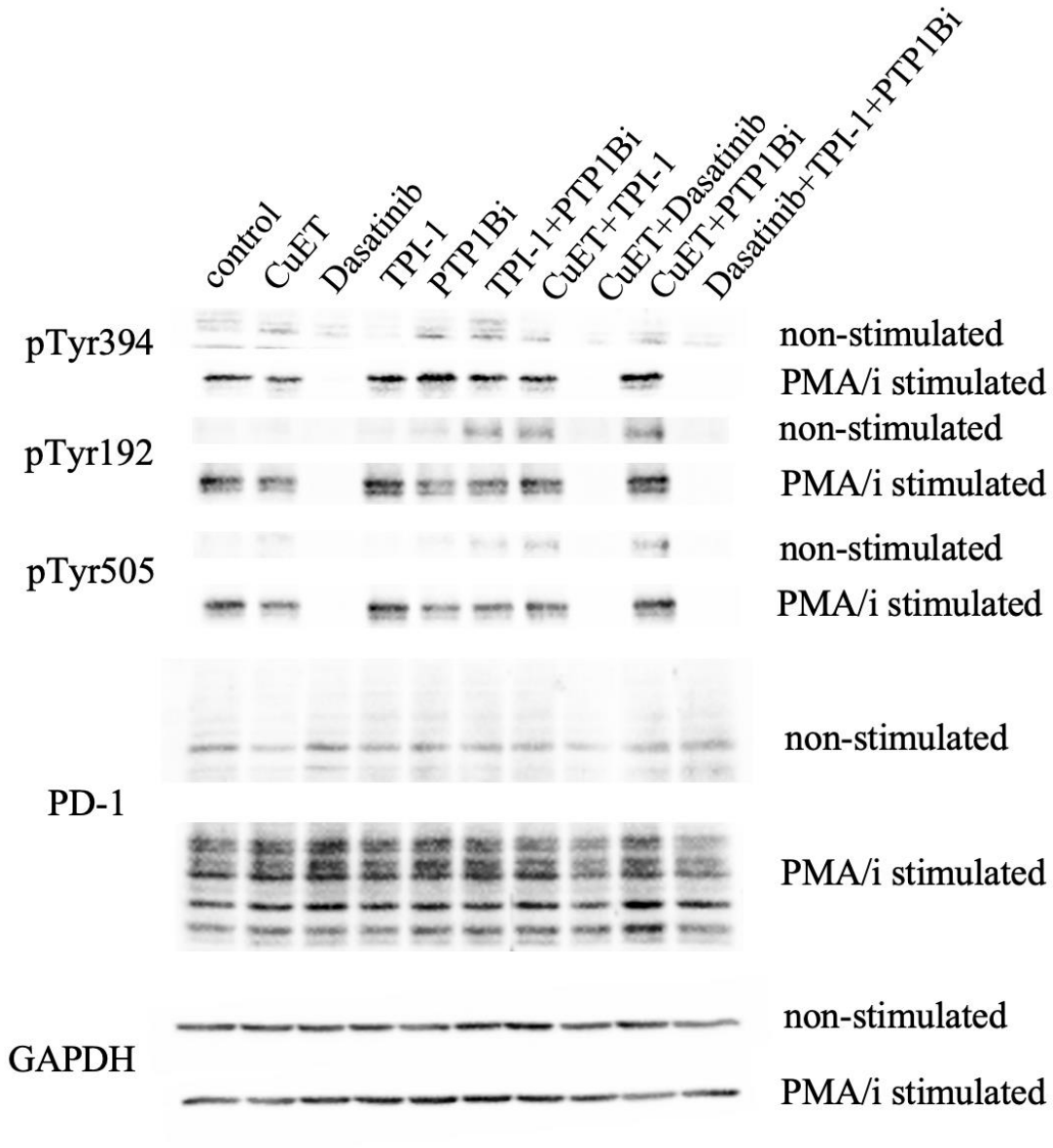

Figure 22. Effect of various targeted treatments on Lck phosphorylation and PD-1 expression in resting and activated cells. *A representative Western blot analysis evaluating the phosphorylation status of specific Lck tyrosine residues (pTyr394, pTyr192, and pTyr505) and the expression of PD-1. The last two strips with bands correspond to the housekeeping protein GAPDH used for normalization. Cells were either left untreated (non-stimulated) or activated with PMA/ionomycin (PMA/i stimulated). Both experimental cell groups were then treated with a vehicle control, CuET, Dasatinib, TPI-1, PTP1Bi, or combinations of these inhibitors. PD-1 undergoes glycosylation after T-cell activation, which can be visible as additional, more dense bands in the PMA/ionomycin-stimulated cohort.*

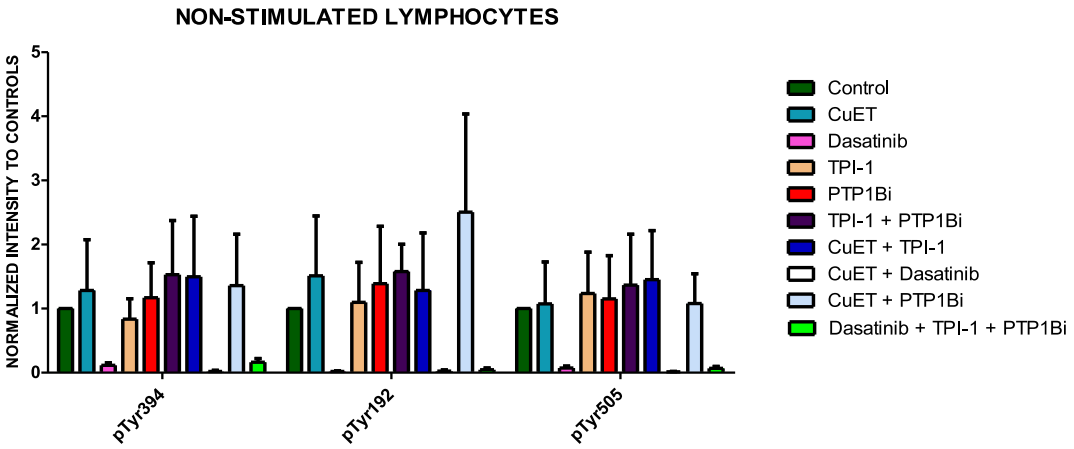

Figure 23. Alterations in Lck phosphorylation profiles in non-stimulated T-lymphocytes following pharmacological interventions. *The bar graph illustrates the relative changes in phosphorylation levels at three specific Lck tyrosine residues: pTyr394, pTyr192, and pTyr505. Immunoblot band intensities for each site were quantified, internally normalized to a housekeeping protein (GAPDH), and subsequently expressed as fold changes relative to the untreated control group (set to 1). The legend indicates the respective single and combinatorial treatments applied, including CuET, Dasatinib, TPI-1, and PTP1Bi. Error bars indicate variability across biological replicates; 9 assays were performed. This figure was made using GraphPad Prism 9.*

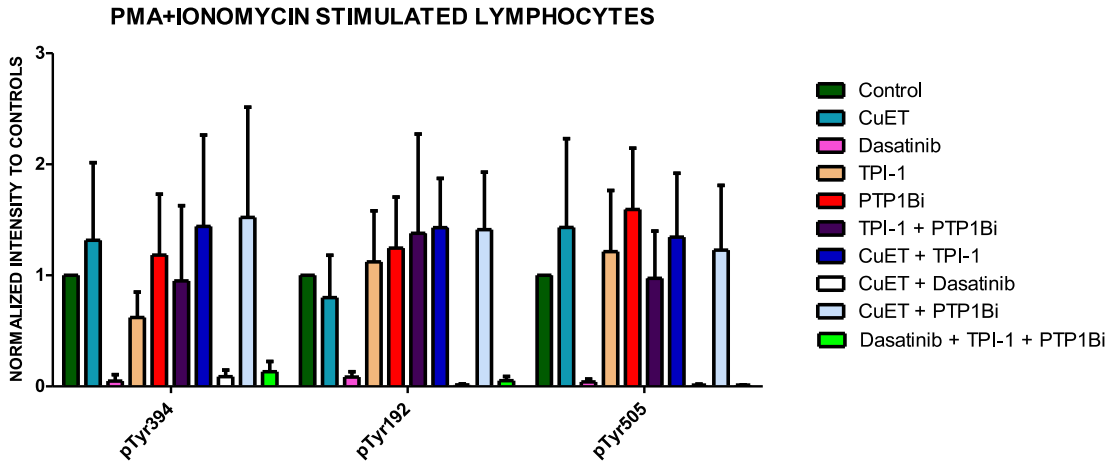

Figure 24. Alterations in Lck phosphorylation profiles in PMA/i-stimulated T-lymphocytes following pharmacological interventions. *The bar graph illustrates the relative changes in phosphorylation levels at three specific Lck tyrosine residues: pTyr394, pTyr192, and pTyr505. Immunoblot band intensities for each site were quantified, internally normalized to a housekeeping protein (GAPDH), and subsequently expressed as fold changes relative to the untreated control group (set to 1). The legend indicates the respective single and combinatorial treatments applied, including CuET, Dasatinib, TPI-1, and PTP1Bi. Error bars indicate variability across biological replicates; 9 assays were performed. This figure was made using GraphPad Prism 9.*

4.3 Cytotoxic effects across multiple cell lines

The cytotoxicity of the compounds, both individually and in combination, was evaluated across a diverse panel of cell lines. The responses varied considerably depending on the cell lineage and genetic background, as summarized in Table 2.

While the A549 and K562 cell lines exhibited no significant changes in viability across any treatments (see Figure 25 and Figure 26 on page 46), significant cytotoxic effects were observed in the lymphoid and colorectal lineages (see Figures 27-30 on pages 47 and 48). Notably, Dasatinib induced a significant decrease in cytotoxicity in MOLT-4 (see Figure 28 on page 47) and HCT116 p53-/- cells (see Figure 30 on page 48), whereas treatments containing CuET and TPI-1 generally resulted in increased cytotoxicity across MOLT-4, Jurkat, and HCT116 cell lines.

***Table 2**. Cytotoxicity of pharmacological treatments across various cell lines.*

Cell Line	Result	Significant Treatments
A549	No significant changes	None
K562	No significant changes	None
MOLT-4	Increased cytotoxicity	CuET, TPI-1
	Decreased cytotoxicity	Dasatinib
Jurkat	Increased cytotoxicity	Dasatinib + TPI-1, CuET, TPI-1, CuET + TPI-1
HCT116 WT	Increased cytotoxicity	TPI-1, CuET + TPI-1, Dasatinib + TPI-1
HCT116 p53 -/-	Increased cytotoxicity	CuET, Dasatinib + TPI-1, TPI-1, CuET + TPI-1
	Decreased cytotoxicity	Dasatinib

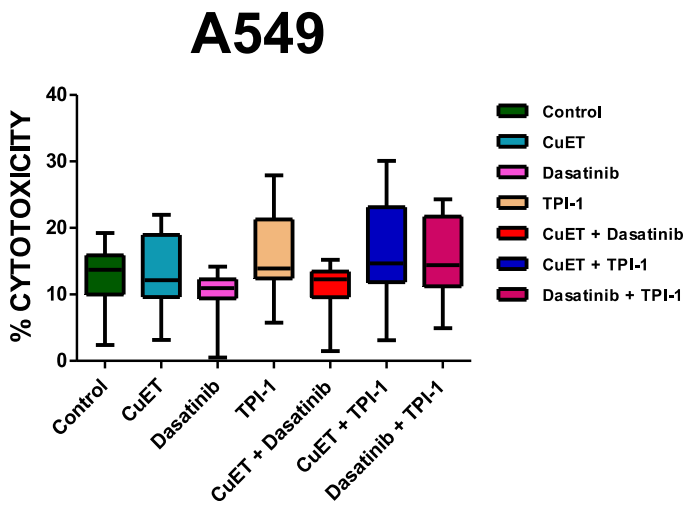

Figure 25. Cytotoxic activity of stimulated lymphocytes against the A549 cell line under various treatment conditions. *The effector-to-target ratio was 5:1, and no statistical significance was observed. The number of assays was 3. One-way ANOVA along with Bonferroni correction was performed. This figure was made using GraphPad Prism 9.*

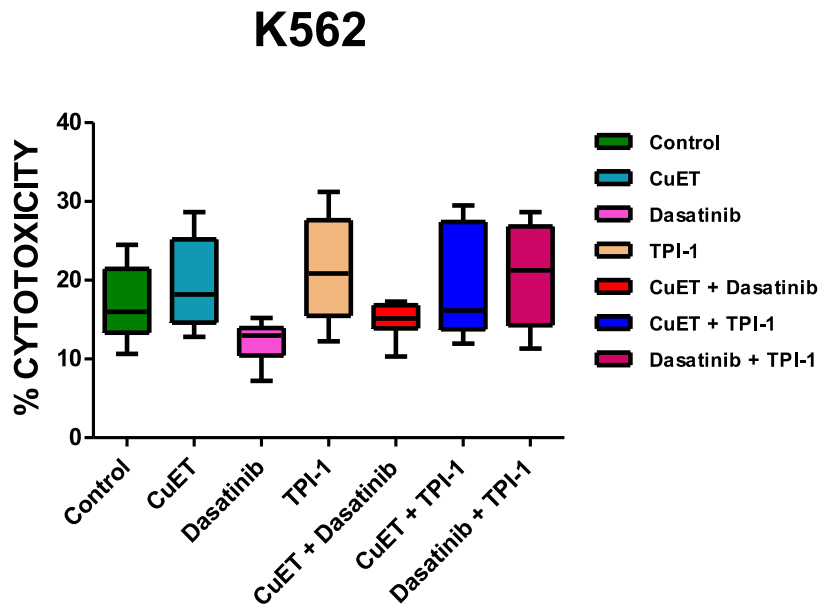

Figure 26. Cytotoxic activity of stimulated lymphocytes against the K562 cell line under various treatment conditions. *The effector-to-target ratio was 5:1, and no statistical significance was observed. The number of assays was 3. One-way ANOVA, along with Bonferroni correction, was performed. This figure was made using GraphPad Prism 9.*

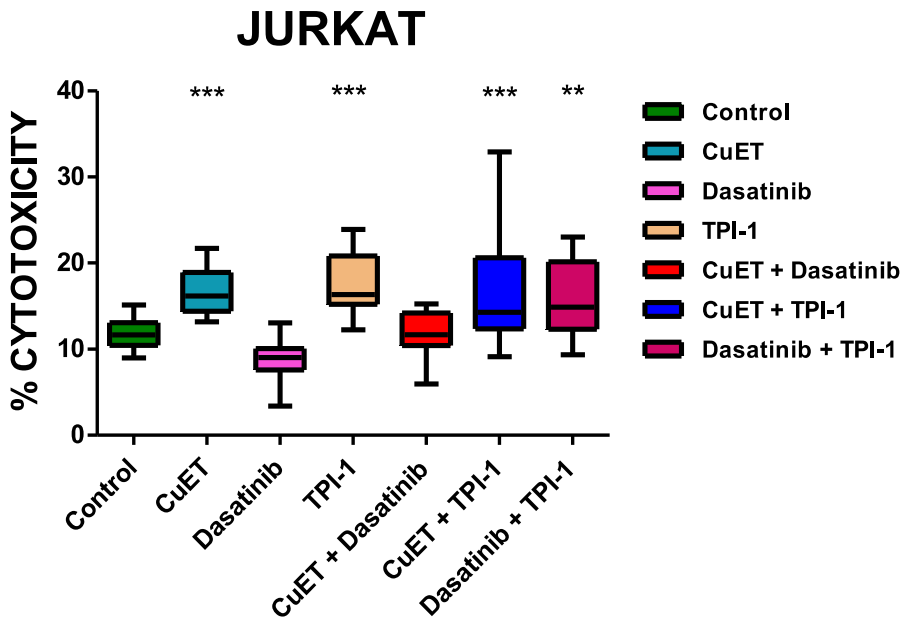

Figure 27. Cytotoxic activity of stimulated lymphocytes against the Jurkat cell line under various treatment conditions. *The effector-to-target ratio was 5:1. Statistical significance compared to the control group is indicated by asterisks above specific boxes (** represents p<0,001, *** represents p<0,0001, number of assays was 3). One-way ANOVA, along with Bonferroni correction, was performed. This figure was made using GraphPad Prism 9.*

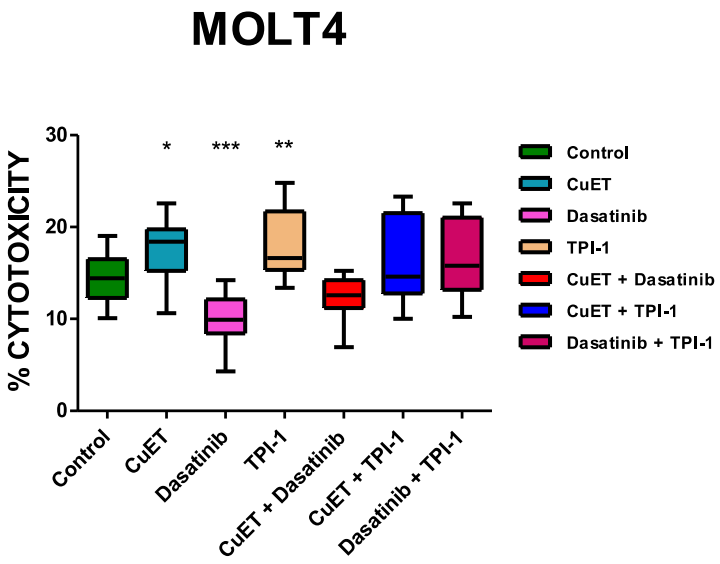

Figure 28. Cytotoxic activity of stimulated lymphocytes against the MOLT-4 cell line under various treatment conditions. *The effector-to-target ratio was 5:1. Statistical significance compared to the control group is indicated by asterisks above specific boxes (* represents p<0,05, ** represents p<0,001, *** represents p<0,0001; number of assays was 3). One-way ANOVA, along with Bonferroni correction, was performed. This figure was made using GraphPad Prism 9.*

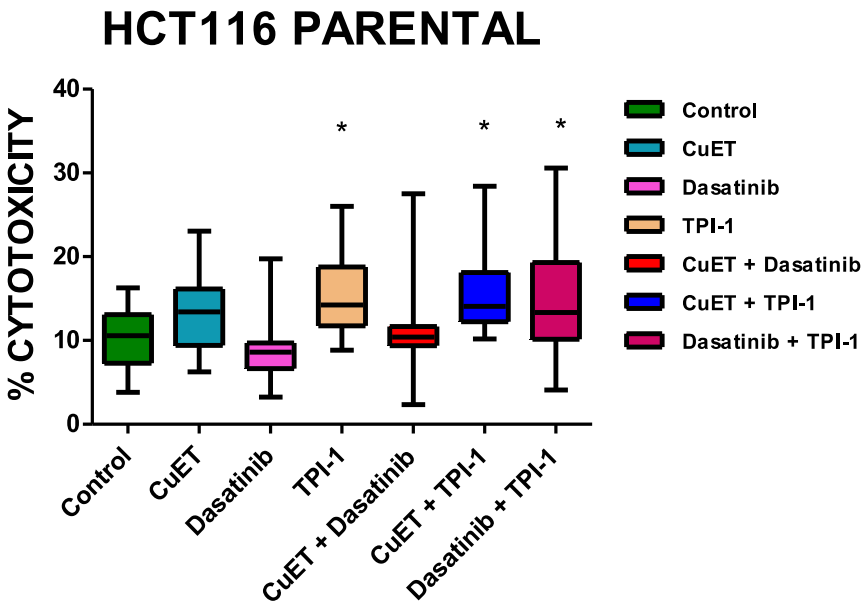

Figure 29. Cytotoxic activity of stimulated lymphocytes against the HCT116 parental cell line under various treatment conditions. *The effector-to-target ratio was 5:1. Statistical significance compared to the control group is indicated by asterisks above specific boxes (* represents p<0,05; number of assays was 3). One-way ANOVA, along with Bonferroni correction, was performed. This figure was made using GraphPad Prism 9.*

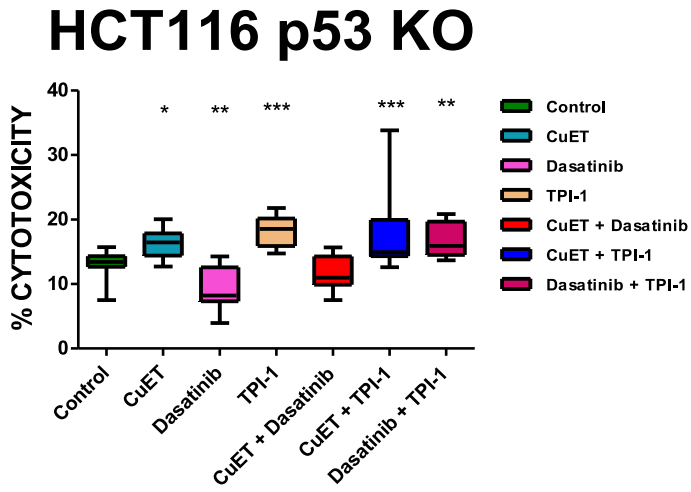

Figure 30. Cytotoxic activity of stimulated lymphocytes against the HCT116 cell line with knocked-out p53 under various treatment conditions. *The effector-to-target ratio was 5:1. Statistical significance compared to the control group is indicated by asterisks above specific boxes (* represents p<0,05, ** represents p<0,001, *** represents p<0,0001; number of assays was 3). One-way ANOVA, along with Bonferroni correction, was performed. This figure was made using GraphPad Prism 9.*

5 DISCUSSION

The present thesis systematically evaluated the pharmacological modulation of the immune checkpoint molecules PD-1 and PD-L1 in primary human T-lymphocytes, alongside the effects of these interventions on Lck phosphorylation and cytotoxic activity against 2D cancer cell cultures. By utilizing distinct stimulation protocols (PMA/ionomycin and PHA) and a panel of targeted agents, including Dasatinib (a Src-family kinase inhibitor), CuET, TPI-1 (an SHP-1 and SHP-2 inhibitor), and PTP1Bi (a PTP1B inhibitor). The discussions encompass intricate, context-dependent regulatory mechanisms that govern the expression of immune checkpoints. The findings may have significant implications for the optimization of combinatorial immunotherapies and for understanding T-cell exhaustion pathways.

5.1 Context-dependent modulation of PD-1 and PD-L1

A primary finding of this study is the highly divergent effects of pharmacological inhibitors, depending on the cellular activation state and the specific mitogenic stimulus applied. PMA/ionomycin induces intracellular activation of the cell. PMA is a known activator of PKC, and ionomycin is a calcium ionophore that enhances PMA's effect on PKC activation.

In the unstimulated PMA/ionomycin cohort (Donors 1–4), PD-L1 was significantly upregulated by CuET, Dasatinib, TPI-1, PTP1Bi, and their combinations. As described in the theoretical part, robust stimulation with PMA/ionomycin bypasses the proximal T-cell receptor (TCR) complex to directly activate protein kinase C (PKC) and increase intracellular calcium. It rapidly drives T-lymphocytes towards exhaustion, leading to a phenotypically altered, unresponsive population. As expected, PMA/I-stimulated cells were less responsive than resting cells (statistically significant differences were less pronounced). However, there was a paradoxical downregulation of PD-L1 in PMA/I-stimulated cells treated with Dasatinib, TPI-1, and the Dasatinib + TPI-1 + PTP1Bi combination. This dynamic shift suggests that basal PD-L1 regulation relies on homeostatic phosphatase and kinase activities that are fundamentally rewired during acute PKC/calcium-mediated activation (R. Zhang et al., 2025). This observed decrease in an exhaustion marker suggests that a partial rescue of exhausted T- lymphocytes occurred under those conditions.

Conversely, in the PHA cohort (Donors 5–8), which stimulates cells via cross-linking of the TCR/CD3 complex, single-positive PD-L1 expression remained entirely unaltered

across all conditions. This discrepancy underscores that PD-L1 expression on T-lymphocytes is highly sensitive to the specific intracellular signaling cascades engaged during activation. Recent literature indicates that TCR-directed stimulation (akin to PHA) versus downstream second-messenger activation (PMA/ionomycin) differentially recruits transcription factors such as NF-κB and AP-1, which directly bind the CD274 (PD-L1) promoter (Green et al., 2012; J. H. Lee et al., 2023). These transcription factors, directly or indirectly, may affect the kinetics of PD-1 and PD-L1 expression.

5.2 PD-1/PD-L1 co-expression and its implications for T-cell exhaustion

While single-positive PD-1 expression was largely unaffected in the PMA/ionomycin cohort, the co-expression of PD-1 and PD-L1 (double-positive cells) was significantly upregulated following stimulation in the presence of Dasatinib, TPI-1, PTP1Bi, and their combinations. In the PHA cohort, the triple combination of Dasatinib + TPI-1 + PTP1Bi also induced a significant upregulation of this double-positive population.

The emergence of a PD-1+/PD-L1+ T-cell population is increasingly recognized as a hallmark of severe T-cell exhaustion and terminal differentiation in chronic infection and tumor microenvironments (Hofmeyer et al., 2011; Jiang et al., 2019). The forced uncoupling of proximal TCR signaling (via Dasatinib) combined with the blockade of negative regulatory phosphatases (via TPI-1 and PTP1Bi) appears to drive T-cells into a hyperdysfunctional or exhausted-like phenotype upon activation (Wu et al., 2026). This observation aligns closely with recent paradigm-shifting discoveries regarding the metabolic and lipidomic landscape of exhausted T-cells. Notably, Medina et al. (2026) demonstrated that exhausted, PD-1+ CD8+ T-cells externalize phosphatidylserine (PS) to the outer plasma membrane, functioning as a non-classical, extrinsic inhibitory molecule. In their chronic lymphocytic choriomeningitis virus (LCMV) model, viable antigen-specific CD8+ T-cells maintained high levels of exposed PS, thereby constraining dendritic cell immunostimulatory capacity. Given that my pharmacological combinations (particularly Dasatinib + TPI-1 + PTP1Bi) rapidly induced a PD-1+/PD-L1+ exhausted-like phenotype, it is plausible that these cells concurrently undergo lipidomic remodeling, including PS externalization. Future studies must evaluate whether the double-positive populations generated by these targeted treatments also exhibit elevated surface PS, as targeting PS in tandem with PD-L1 has been shown to synergistically restore CD8+ T-cell responses and improve viral/tumor control (Medina et al., 2026). The results are in accordance with the proposed mechanism.

5.3 The role of Lck phosphorylation in immune checkpoint regulation

The Western blot analyses provided some yet limited insights into the upstream signaling events regulating these surface phenotypes. Cellular stimulation successfully induced PD-1 expression concurrently with Lck phosphorylation at key regulatory residues (Tyr394, Tyr192, and Tyr505). The semi-quantitative analysis did not reach statistical significance, most likely due to high inter-donor variability, a small sample size (9 donors), and the relatively high error rate of this quantification method, which masked more subtle changes. Qualitative observations confirmed that Dasatinib consistently abrogated Lck phosphorylation at all sites.

Dasatinib is a potent inhibitor of Src-family kinases, including Lck, which is essential for initiating TCR signaling (Schade et al., 2008). The abrogation of Lck phosphorylation by Dasatinib, paired with its ability to upregulate PD-1/PD-L1 co-expression when combined with phosphatase inhibitors (TPI-1/PTP1Bi), suggests a compensatory feedback loop. When proximal TCR signaling is blunted, but downstream negative feedback loops (SHP-1, PTP1B) are simultaneously removed, the T-cell may default to an exhaustion-associated transcriptional program characterized by high expression of coinhibitory receptors (Wu et al., 2026).

5.4 Cytotoxic effects of pharmacological treatments

In addition to immunomodulatory effects, the cytotoxic efficacy of T-lymphocytes treated by pharmacological agents was tested across a panel of cancer cell lines (A549, K562, MOLT-4, Jurkat, HCT116 WT, and HCT116 p53-/-). The results, summarised in Table 2 on page 46, revealed several unexpected deviations from my initial hypotheses, highlighting the complex, cell-type-specific nature of these targeted therapies. The observed differences may result from variability in cell types and, consequently, variations in receptor expression on the cell surface. This variability may ultimately influence the cellular response.

For the solid tumor line A549 (lung carcinoma, resistant to spontaneous killing, described by Tièche et al. (2018)) and the leukemia line K562 (susceptible to spontaneous killing), no significant changes in cytotoxicity were observed across treatments. Conversely, the T-cell leukemia lines (MOLT-4 and Jurkat) and the colorectal carcinoma lines (HCT116 parental and p53-/-) yielded statistically significant results. It can be proposed that CuET, TPI-1, and CuET + TPI-1 treatments would increase cytotoxicity because, as mentioned in the theoretical part, CuET activates T-lymphocytes, and TPI-1

inhibits the inhibitory signals from SHP-1 and SHP-2. Consequently, Dasatinib, along with any combinatory treatments containing it, would decrease cytotoxicity by swiftly abrogating Lck function. CuET and TPI-1 alone and/or in combination increased cell death in MOLT-4, Jurkat, and HCT116 p53-/- cells. However, combinatorial treatments, specifically Dasatinib + TPI-1 (D+T), unexpectedly increased cytotoxicity in Jurkat and both HCT116 lines, suggesting that SHP-1/SHP-2 inhibiton trumped the effects of Dasatinib.

5.5 Synthesis of immunomodulatory and cytotoxic effects

The intersection of my T-lymphocyte checkpoint data and the tumor cytotoxicity data presents a fascinating clinical conundrum. On one hand, combinations like Dasatinib + TPI-1 (D+T) exhibit potent, unexpected direct cytotoxicity against specific leukemic (Jurkat) and solid tumor (HCT116) lines. On the other hand, flow cytometry data demonstrate that the combination (Dasatinib + TPI-1) drives primary human T-cells toward a PD-1+/PD-L1+ double-positive state upon stimulation, indicative of severe immune exhaustion. This co-expression can be an effect in those cells that the treatment could not rescue. In addition, the cell cycle may be crucial to the effect of the inhibitors, since cell cycle-dependent kinases may be affected by the treatment, as reported by Tsang et al. (2012).

5.6 Clinical implications and therapeutic perspectives

The clinical implications of these findings are significant, particularly concerning combination immunotherapy. Dasatinib is extensively utilized in the treatment of chronic myeloid leukemia (CML), and its immunomodulatory off-target effects are currently the focus of rigorous investigation. The data indicate that while Dasatinib alone can suppress proximal T-cell activation (diminished Lck phosphorylation), its combination with other targeted agents (such as SHP-1/PTP1B inhibitors) during active cellular stimulation can paradoxically enrich for a PD-1+/PD-L1+ population. This dual-action profile suggests that while these combinations might successfully debulk a tumor directly, they could simultaneously paralyze the patient's endogenous anti-tumor T-cell response. If these double-positive T-cells also externalize phosphatidylserine as described by Medina et al. (2026), the resulting immunosuppressive microenvironment would severely limit long-term therapeutic efficacy. Therefore, translating these combinations to the clinic would strictly require co-administration of immune checkpoint inhibitors (such as anti-PD-1/PD-L1 or anti-PS antibodies) to rescue T-cells from therapy-induced exhaustion while

allowing the direct cytotoxic effects of D+T or C+T to eliminate tumor cells. As Medina et al. (2026) highlighted, treating exhausted T-cells with a PS-targeting antibody (mch1N11) allowed PD-1+ TCF1+ stem-like CD8+ T-cells to downregulate quiescence-associated genes and proliferate. Therefore, a multimodal approach combining targeted kinase inhibitors such as Dasatinib with both classical checkpoint inhibitors (anti-PD-1/PD-L1) and novel metabolic checkpoint inhibitors (anti-PS) may be required to fully unleash T-cell effector functions and prevent therapy-induced exhaustion. Other mechanisms proposed by Wu (2026) are plausible and warrant further study.

5.7 Limitations and future directions

Several limitations of the current study must be acknowledged. First, the sample size was limited to primary cells from nine, eight, or three donors, divided into two distinct stimulation cohorts. This restricted our statistical power, particularly in the semi-quantitative Western blot analyses of Lck phosphorylation. Second, the *in vitro* nature of the mitogenic stimulation (PMA/ionomycin and PHA) does not fully replicate the complex, antigen-specific TCR engagement occurring within a physiological tumor microenvironment or during chronic viral infection.

Future research should expand to larger patient cohorts and utilize antigen-specific stimulation models to validate these findings. Furthermore, integrating lipidomic profiling to assess phosphatidylserine externalization in the generated PD-1+/PD-L1+ T-cells will be crucial. Determining whether the pharmacological induction of PD-L1 and PD-1 correlates directly with PS exposure will help map the intersection between surface protein checkpoints and lipid metabolic checkpoints (Medina et al., 2026).

6 CONCLUSIONS

This thesis investigated modulation of immune checkpoint molecules PD-1 and PD-L1, Lck phosphorylation, and cytotoxicity in human T-lymphocytes. The effects of kinase and phosphatase inhibitors like Dasatinib, TPI-1, and PTP1Bi were investigated under various mitogenic conditions, PMA/ionomycin and PHA, highlighting the intricate regulatory mechanisms influencing T-cell activation and exhaustion.

Research indicates that immune checkpoint modulation during T-cell activation is influenced by intracellular signaling. Inhibiting T-cell receptor (TCR) signaling with Dasatinib, along with blocking negative regulatory phosphatases (TPI-1 and PTP1Bi), alters checkpoint expression under PMA/ionomycin stimulation. This results in reduced PD-L1 expression and an increase in PD-1+/PD-L1+ T-cells, indicating T-cell exhaustion. Western blot analyses confirm that stimulation raises PD-1 expression and Lck phosphorylation, while Dasatinib inhibits Lck activity.

T-cell-mediated cytotoxicity against 2D cancer cell cultures varied by cell line, presenting clinical challenges. Combinations like Dasatinib and TPI-1 showed strong cytotoxicity against specific leukemic (Jurkat) and solid tumor (HCT116) lines but risk T-cell exhaustion, potentially weakening the overall anti-tumor immune response despite reducing tumor burden.

The clinical translation of these findings requires a nuanced approach, balancing systemic administration of targeted kinase and phosphatase inhibitors to minimize off-target effects. To enhance efficacy and prevent immune paralysis, agents like Dasatinib and TPI-1 may need to be combined with immune checkpoint inhibitors, such as anti-PD-1/PD-L1. Future studies should investigate the lipidomic and metabolic changes in PD-1+/PD-L1+ populations to improve immunotherapy combinations, combat T-cell exhaustion, and restore anti-tumor immunity.

7 REFERENCES

Acuto, O., & Michel, F. (2003). CD28-mediated co-stimulation: a quantitative support for TCR signalling. Nature reviews. *Immunology*, 3(12), 939–951. https://doi.org/10.1038/nri1248

Agata, Y., Kawasaki, A., Nishimura, H., Ishida, Y., Tsubat, T., Yagita, H., & Honjo, T. (1996). Expression of the PD-1 antigen on the surface of stimulated mouse T and B lymphocytes. *International Immunology*, *8*(5), 765–772. https://doi.org/10.1093/intimm/8.5.765

Aguado, E., Martínez-Florensa, M., & Aparicio, P. (2006). Activation of T lymphocytes and the role of the adapter LAT. *Transplant Immunology*, *17*(1), 23–26. https://doi.org/10.1016/j.trim.2006.09.013

Ahn, E., Araki, K., Hashimoto, M., Li, W., Riley, J. L., Cheung, J., Sharpe, A. H., Freeman, G. J., Irving, B. A., & Ahmed, R. (2018). Role of PD-1 during effector CD8 T cell differentiation. *Proceedings of the National Academy of Sciences*, *115*(18), 4749–4754. https://doi.org/10.1073/pnas.1718217115

Arnaud, J., Huchenq, A., Vernhes, M. C., Caspar-Bauguil, S., Lenfant, F., Sancho, J., Terhorst, C., & Rubin, B. (1997). The interchain disulfide bond between TCR alpha beta heterodimers on human T cells is not required for TCR-CD3 membrane expression and signal transduction. *International immunology*, 9(4), 615–626. https://doi.org/10.1093/intimm/9.4.615

Arnaud, M., Crouin, C., Deon, C., Loyaux, D., & Bertoglio, J. (2004). Phosphorylation of Grb2-Associated Binder 2 on Serine 623 by ERK MAPK Regulates Its Association with the Phosphatase SHP-2 and Decreases STAT5 Activation. *The Journal of Immunology*, *173*(6), 3962–3971. https://doi.org/10.4049/jimmunol.173.6.3962

Artyomov, M. N., Lis, M., Devadas, S., Davis, M. M., & Chakraborty, A. K. (2010). CD4 and CD8 binding to MHC molecules primarily acts to enhance Lck delivery. *Proceedings of the National Academy of Sciences*, *107*(39), 16916–16921. https://doi.org/10.1073/pnas.1010568107

Athie-Morales, V., Smits, H. H., Cantrell, D. A., & Hilkens, C. M. U. (2004). Sustained IL-12 signaling is required for TH1 development. *The Journal of Immunology*, *172*(1), 61–69. https://doi.org/10.4049/jimmunol.172.1.61

Baecher-Allan, C., Brown, J. A., Freeman, G. J., & Hafler, D. A. (2003). CD4 + CD25 + Regulatory Cells from Human Peripheral Blood Express Very High Levels of CD25 Ex Vivo. *Novartis Foundation Symposium*, *252*, 67–91. https://doi.org/10.1002/0470871628.ch6

Bao, K., & Reinhardt, R. L. (2015). The differential expression of IL-4 and IL-13 and its impact on type-2 immunity. *Cytokine*, 75(1), 25–37. https://doi.org/10.1016/j.cyto.2015.05.008

Bardhan, K., Patsoukis, N., Sari, D., Anagnostou, T., Chatterjee, P., Freeman, G. J., Li, L., & Boussiotis, V. A. (2015). PD-1 inhibits TCR proximal signaling by sequestering SHP-2 phosphatase and facilitating CSK-Mediated inhibitory phosphorylation of LCK. *Blood*, *126*(23), 283. https://doi.org/10.1182/blood.v126.23.283.283

Baumgartner, C. K., Ebrahimi-Nik, H., Iracheta-Vellve, A., Hamel, K. M., Olander, K. E., Davis, T. G. R., McGuire, K. A., Halvorsen, G. T., Avila, O. I., Patel, C. H., Kim, S. Y., Kammula, A. V., Muscato, A. J., Halliwill, K., Geda, P., Klinge, K. L., Xiong, Z., Duggan, R., Mu, L., . . . Manguso, R. T. (2023). The PTPN2/PTPN1 inhibitor ABBV-CLS-484 unleashes potent anti-tumour immunity. *Nature*, 622(7984), 850–862. https://doi.org/10.1038/s41586-023-06575-7

Bengsch, B., Johnson, A. L., Kurachi, M., Odorizzi, P. M., Pauken, K. E., Attanasio, J., Stelekati, E., McLane, L. M., Paley, M. A., Delgoffe, G. M., & Wherry, E. J. (2016). Bioenergetic insufficiencies due to metabolic alterations regulated by the inhibitory receptor PD-1 are an early driver of CD8 + T cell exhaustion. *Immunity*, *45*(2), 358–373. https://doi.org/10.1016/j.immuni.2016.07.008

Bennett, A. M., Tang, T. L., Sugimoto, S., Walsh, C. T., & Neel, B. G. (1994). Protein-tyrosine-phosphatase SHPTP2 couples platelet-derived growth factor receptor beta to Ras. *Proceedings of the National Academy of Sciences*, *91*(15), 7335–7339. https://doi.org/10.1073/pnas.91.15.7335

Bio-Rad Laboratories. (2020). Image Lab Software (Version 6.1.0) [Computer software]. https://www.bio-rad.com/en-us/product/image-lab-software

BioRender. (2024). BioRender [Web application]. https://biorender.com

Blackburn, S. D., Shin, H., Haining, W. N., Zou, T., Workman, C. J., Polley, A., Betts, M. R., Freeman, G. J., Vignali, D. a. A., & Wherry, E. J. (2008). Coregulation of CD8+ T cell exhaustion by multiple inhibitory receptors during chronic viral infection. *Nature Immunology*, *10*(1), 29–37. https://doi.org/10.1038/ni.1679

Bommhardt, U., Schraven, B., & Simeoni, L. (2019). Beyond TCR signaling: Emerging functions of LCK in cancer and immunotherapy. *International Journal of Molecular Sciences*, 20(14), 3500. https://doi.org/10.3390/ijms20143500

Bozso, S. J., Kang, J. J. H., & Nagendran, J. (2020). The role of competing mechanisms on Lck regulation. *Immunologic Research*, *68*(5), 289–295. https://doi.org/10.1007/s12026-020-09148-2

Bretscher, P. A. (1999). A two-step, two-signal model for the primary activation of precursor helper T cells. *Proceedings of the National Academy of Sciences*, *96*(1), 185–190. https://doi.org/10.1073/pnas.96.1.185

Bretscher, P., & Cohn, M. (1970). A theory of Self-Nonself discrimination. *Science*, *169*(3950), 1042–1049. https://doi.org/10.1126/science.169.3950.1042

Buchbinder, E. I., & Desai, A. (2015). CTLA-4 and PD-1 pathways. *American Journal of Clinical Oncology*, *39*(1), 98–106. https://doi.org/10.1097/coc.0000000000000239

Burchat, A., Borhani, D. W., Calderwood, D. J., Hirst, G. C., Li, B., & Stachlewitz, R. F. (2005). Discovery of A-770041, a src-family selective orally active lck inhibitor that prevents organ allograft rejection. *Bioorganic & Medicinal Chemistry Letters*, *16*(1), 118–122. https://doi.org/10.1016/j.bmcl.2005.09.039

Burleson, G. R., Burleson, S. C., & Burleson, F. G. (2015). Pulmonary immunology of infectious disease. In *Elsevier eBooks* (pp. 581–600). https://doi.org/10.1016/b978-0-12-404577-4.00030-8

Butterworth, S., Overduin, M., & Barr, A. J. (2014). Targeting protein tyrosine phosphatase SHP2 for therapeutic intervention. *Future Medicinal Chemistry*, *6*(12), 1423–1437. https://doi.org/10.4155/fmc.14.88

Carson, G. R., Kuestner, R. E., Ahmed, A., Pettey, C. L., & Concino, M. F. (1991). Six chains of the human T cell antigen receptor.CD3 complex are necessary and sufficient for processing the receptor heterodimer to the cell surface. *Journal of Biological Chemistry*, *266*(12), 7883–7887. https://doi.org/10.1016/s0021-9258(20)89532-5

Cortés, K. C., Osuch, S., Perlejewski, K., Radkowski, M., Janiak, M., Berak, H., Rauch, A., Fehr, J. S., Hoffmann, M., Günthard, H. F., & Metzner, K. J. (2023). T-Cell exhaustion in HIV-1/Hepatitis C virus coinfection is reduced after successful treatment of chronic hepatitis C. *Open Forum Infectious Diseases*, *10*(11), ofad514. https://doi.org/10.1093/ofid/ofad514

Courtney, A. H., Amacher, J. F., Kadlecek, T. A., Mollenauer, M. N., Au-Yeung, B. B., Kuriyan, J., & Weiss, A. (2017). A Phosphosite within the SH2 Domain of Lck Regulates Its Activation by CD45. *Molecular Cell*, *67*(3), 498-511.e6. https://doi.org/10.1016/j.molcel.2017.06.024

Curtsinger, J. M., Lins, D. C., & Mescher, M. F. (2003). Signal 3 Determines Tolerance versus Full Activation of Naive CD8 T Cells. *The Journal of Experimental Medicine*, *197*(9), 1141–1151. https://doi.org/10.1084/jem.20021910

Dance, M., Montagner, A., Salles, J., Yart, A., & Raynal, P. (2007). The molecular functions of Shp2 in the Ras/Mitogen-activated protein kinase (ERK1/2) pathway. *Cellular Signalling*, *20*(3), 453–459. https://doi.org/10.1016/j.cellsig.2007.10.002

Darian, E., Guvench, O., Yu, B., Qu, C., & MacKerell, A. D. (2011). Structural mechanism associated with domain opening in gain-of-function mutations in SHP2 phosphatase. *Proteins Structure Function and Bioinformatics*, *79*(5), 1573–1588. https://doi.org/10.1002/prot.22984

Davis, S. J., & Van Der Merwe, P. A. (2006). The kinetic-segregation model: TCR triggering and beyond. *Nature Immunology*, *7*(8), 803–809. https://doi.org/10.1038/ni1369

De Sanctis, J., Garmendia, J., Duchová, H., Valentini, V., Puskasu, A., Kubíčková, A., & Hajdúch, M. (2024). LCK Function and modulation: Immune cytotoxic response and tumor treatment More than a simple event. *Cancers*, *16*(15), 2630. https://doi.org/10.3390/cancers16152630

Dong, H., Zhu, G., Tamada, K., & Chen, L. (1999). B7-H1, a third member of the B7 family, co-stimulates T-cell proliferation and interleukin-10 secretion. *Nature Medicine*, *5*(12), 1365–1369. https://doi.org/10.1038/70932

Dosset, M., & Zanetti, M. (2022). Disulfiram's journey from rubber vulcanization to T-cell activation. *The EMBO Journal*, *41*(16), e111862. https://doi.org/10.15252/embj.2022111862

Dumut, D. C., Hajduch, M., Zacharias, A. M., Duan, Q., Frydrych, I., Rozankova, Z., Popper, M., Garic, D., Paun, R. A., Centorame, A., Shah, J., Mistrik, M., Dzubak, P., De Sanctis, J. B., & Radzioch, D. (2025). Diethyldithiocarbamate-copper complex ignites the tumor microenvironment through NKG2D-NKG2DL axis. *Frontiers in Immunology*, *16*, 1491450. https://doi.org/10.3389/fimmu.2025.1491450

Duraiswamy, J., Ibegbu, C. C., Masopust, D., Miller, J. D., Araki, K., Doho, G. H., Tata, P., Gupta, S., Zilliox, M. J., Nakaya, H. I., Pulendran, B., Haining, W. N., Freeman, G. J., & Ahmed, R. (2011). Phenotype, function, and gene expression profiles of programmed death-1HI CD8 T cells in healthy human adults. *The Journal of Immunology*, *186*(7), 4200–4212. https://doi.org/10.4049/jimmunol.1001783

Elkamhawy, A., Ali, E. M. H., & Lee, K. (2021). New horizons in drug discovery of lymphocyte-specific protein tyrosine kinase (Lck) inhibitors: a decade review (2011–2021) focussing on structure–activity relationship (SAR) and docking insights. *Journal of Enzyme Inhibition and Medicinal Chemistry*, *36*(1), 1572–1600. https://doi.org/10.1080/14756366.2021.1937143

Fedele, C., Ran, H., Diskin, B., Wei, W., Jen, J., Geer, M. J., Araki, K., Ozerdem, U., Simeone, D. M., Miller, G., Neel, B. G., & Tang, K. H. (2018). SHP2 inhibition prevents adaptive resistance to MEK inhibitors in multiple cancer models. *Cancer Discovery*, *8*(10), 1237–1249. https://doi.org/10.1158/2159-8290.cd-18-0444

Fernández-Aguilar, L. M., Vico-Barranco, I., Arbulo-Echevarria, M. M., & Aguado, E. (2023). A story of Kinases and adaptors: The role of LCK, ZAP-70 and LAT in switch Panel governing T-Cell development and activation. *Biology*, *12*(9), 1163. https://doi.org/10.3390/biology12091163

Fernández-Aguilar, L. M., Vico-Barranco, I., Arbulo-Echevarria, M. M., & Aguado, E. (2023b). A story of Kinases and adaptors: The role of LCK, ZAP-70 and LAT in switch Panel governing T-Cell development and activation. *Biology*, *12*(9), 1163. https://doi.org/10.3390/biology12091163

Forde, P. M., Spicer, J., Lu, S., Provencio, M., Mitsudomi, T., Awad, M. M., Felip, E., Broderick, S. R., Brahmer, J. R., Swanson, S. J., Kerr, K., Wang, C., Ciuleanu, T., Saylors, G. B., Tanaka, F., Ito, H., Chen, K., Liberman, M., Vokes, E. E., . . . Girard, N. (2022). Neoadjuvant Nivolumab plus Chemotherapy in Resectable Lung Cancer. *New England Journal of Medicine*, *386*(21), 1973–1985. https://doi.org/10.1056/nejmoa2202170

Francisco, L. M., Sage, P. T., & Sharpe, A. H. (2010). The PD-1 pathway in tolerance and autoimmunity. *Immunological Reviews*, *236*(1), 219–242. https://doi.org/10.1111/j.1600-065x.2010.00923.x

Francisco, L. M., Sage, P. T., & Sharpe, A. H. (2010). The PD-1 pathway in tolerance and autoimmunity. *Immunological Reviews*, *236*(1), 219–242. https://doi.org/10.1111/j.1600-065x.2010.00923.x

Freeman, G. J., Long, A. J., Iwai, Y., Bourque, K., Chernova, T., Nishimura, H., Fitz, L. J., Malenkovich, N., Okazaki, T., Byrne, M. C., Horton, H. F., Fouser, L., Carter, L., Ling, V., Bowman, M. R., Carreno, B. M., Collins, M., Wood, C. R., & Honjo, T. (2000). Engagement of the PD-1 immunoinhibitory receptor by a novel B7 family member leads to negative regulation of lymphocyte activation. *The Journal of Experimental Medicine*, *192*(7), 1027–1034. https://doi.org/10.1084/jem.192.7.1027

Freeman, G. J., Wherry, E. J., Ahmed, R., & Sharpe, A. H. (2006). Reinvigorating exhausted HIV-specific T cells via PD-1–PD-1 ligand blockade. *The Journal of Experimental Medicine*, *203*(10), 2223–2227. https://doi.org/10.1084/jem.20061800

Gao, R., Li, X., Gao, H., Zhao, K., Liu, X., Liu, J., Wang, Q., Zhu, Y., Chen, H., Xiang, S., Zhan, Y., Yin, R., Yu, M., Ning, H., Yang, X., & Li, C. (2022). Protein phosphatase 2A catalytic subunit β suppresses PMA/ionomycin-induced T-cell activation by negatively regulating PI3K/Akt signaling. *FEBS Journal*, *289*(15), 4518–4535. https://doi.org/10.1111/febs.16370

Ge, Q., Holler, P. D., Mahajan, V. S., Nuygen, T., Eisen, H. N., & Chen, J. (2006). Development of CD4+T cells expressing a nominally MHC class I-restricted T cell receptor by two different mechanisms. *Proceedings of the National Academy of Sciences*, *103*(6), 1822–1827. https://doi.org/10.1073/pnas.0510561103

Goral, S. (2011). The three-signal hypothesis of lymphocyte activation/targets for immunosuppression. *Dialysis & Transplantation*, *40*(1), 14–16. https://doi.org/10.1002/dat.20527

Grammarly. (2024). Grammarly [Web application]. https://www.grammarly.com

GraphPad Software. (2022). GraphPad Prism (Version 9.5.0) [Computer software]. https://www.graphpad.com

Green, M. R., Rodig, S., Juszczynski, P., Ouyang, J., Sinha, P., O'Donnell, E., Neuberg, D., & Shipp, M. A. (2012). Constitutive AP-1 activity and EBV infection induce PD-L1 in hodgkin lymphomas and posttransplant lymphoproliferative disorders: Implications for targeted therapy. *Clinical Cancer Research*, *18*(6), 1611–1618. https://doi.org/10.1158/1078-0432.ccr-11-1942

Hamid, O., Robert, C., Daud, A., Hodi, F. S., Hwu, W., Kefford, R., Wolchok, J. D., Hersey, P., Joseph, R. W., Weber, J. S., Dronca, R., Gangadhar, T. C., Patnaik, A., Zarour, H., Joshua, A. M., Gergich, K., Elassaiss-Schaap, J., Algazi, A., Mateus, C., . . . Ribas, A. (2013). Safety and Tumor Responses with Lambrolizumab (Anti–PD-1) in Melanoma. *New England Journal of Medicine*, *369*(2), 134–144. https://doi.org/10.1056/nejmoa1305133

Haque, S. J., Harbor, P., Tabrizi, M., Yi, T., & Williams, B. R. (1998). Protein-tyrosine phosphatase SHP-1 is a negative regulator of IL-4- and IL-13-dependent signal transduction. *Journal of Biological Chemistry*, *273*(51), 33893–33896. https://doi.org/10.1074/jbc.273.51.33893

Hashimoto, M., Kamphorst, A. O., Im, S. J., Kissick, H. T., Pillai, R. N., Ramalingam, S. S., Araki, K., & Ahmed, R. (2018). CD8 T cell exhaustion in Chronic Infection and Cancer: Opportunities for interventions. *Annual Review of Medicine*, *69*(1), 301–318. https://doi.org/10.1146/annurev-med-012017-043208

Haynes, N. M., Allen, C. D. C., Lesley, R., Ansel, K. M., Killeen, N., & Cyster, J. G. (2007). Role of CXCR5 and CCR7 in follicular TH cell positioning and appearance of a programmed

cell death Gene-1High Germinal Center-Associated subpopulation. *The Journal of Immunology*, *179*(8), 5099–5108. https://doi.org/10.4049/jimmunol.179.8.5099

Hendriks, W. J. a. J., Van Cruchten, R. T. P., & Pulido, R. (2023). Hereditable variants of classical protein tyrosine phosphatase genes: Will they prove innocent or guilty? *Frontiers in Cell and Developmental Biology*, *10*, 1051311. https://doi.org/10.3389/fcell.2022.1051311

Hofmeyer, K. A., Jeon, H., & Zang, X. (2011). The PD-1/PD-L1 (B7-H1) pathway in Chronic Infection-Induced Cytotoxic T lymphocyte exhaustion. *BioMed Research International*, *2011*(1), 451694. https://doi.org/10.1155/2011/451694

Holtmeier, W., & Kabelitz, D. (2005). gammadelta T cells link innate and adaptive immune responses. Chemical immunology and allergy, 86, 151–183. https://doi.org/10.1159/000086659

Hui, E., Cheung, J., Zhu, J., Su, X., Taylor, M. J., Wallweber, H. A., Sasmal, D. K., Huang, J., Kim, J. M., Mellman, I., & Vale, R. D. (2017). T cell costimulatory receptor CD28 is a primary target for PD-1–mediated inhibition. *Science*, *355*(6332), 1428–1433. https://doi.org/10.1126/science.aaf1292

Chan, A. C., Irving, B. A., Fraser, J. D., & Weiss, A. (1991). The zeta chain is associated with a tyrosine kinase and upon T-cell antigen receptor stimulation associates with ZAP-70, a 70-kDa tyrosine phosphoprotein. *Proceedings of the National Academy of Sciences*, *88*(20), 9166–9170. https://doi.org/10.1073/pnas.88.20.9166

Chan, A. C., Irving, B. A., Fraser, J. D., & Weiss, A. (1991). The zeta chain is associated with a tyrosine kinase and upon T-cell antigen receptor stimulation associates with ZAP-70, a 70-kDa tyrosine phosphoprotein. Proceedings of the National Academy of Sciences, 88(20), 9166–9170. https://doi.org/10.1073/pnas.88.20.9166

Chang, C., Qiu, J., O'Sullivan, D., Buck, M. D., Noguchi, T., Curtis, J. D., Chen, Q., Gindin, M., Gubin, M. M., Van Der Windt, G. J., Tonc, E., Schreiber, R. D., Pearce, E. J., & Pearce, E. L. (2015). Metabolic competition in the tumor microenvironment is a driver of cancer progression. *Cell*, *162*(6), 1229–1241. https://doi.org/10.1016/j.cell.2015.08.016

Chen, Y. P., LaMarche, M. J., Chan, H. M., Fekkes, P., Garcia-Fortanet, J., Acker, M. G., Antonakos, B., Chen, C. H., Chen, Z., Cooke, V. G., Dobson, J. R., Deng, Z., Fei, F., Firestone, B., Fodor, M., Fridrich, C., Gao, H., Grunenfelder, D., Hao, H., . . . Fortin, P. D. (2016). Allosteric inhibition of SHP2 phosphatase inhibits cancers driven by receptor tyrosine kinases. *Nature*, *535*(7610), 148–152. https://doi.org/10.1038/nature18621

Inderberg, E. M., Mensali, N., Oksvold, M. P., Fallang, L., Fåne, A., Skorstad, G., Stenvik, G., Progida, C., Bakke, O., Kvalheim, G., Myklebust, J. H., & Wälchli, S. (2017). Human c-SRC kinase (CSK) overexpression makes T cells dummy. *Cancer Immunology Immunotherapy*, *67*(4), 525–536. https://doi.org/10.1007/s00262-017-2105-9

Janeway, C. A. (2001). How the immune system protects the host from infection. *Microbes and Infection*, *3*(13), 1167–1171. https://doi.org/10.1016/s1286-4579(01)01477-0

Jarvis, L. A., Toering, S. J., Simon, M. A., Krasnow, M. A., & Smith-Bolton, R. K. (2006). Sprouty proteins are in vivo targets of Corkscrew/SHP-2 tyrosine phosphatases. *Development*, *133*(6), 1133–1142. https://doi.org/10.1242/dev.02255

Jiang, X., Wang, J., Deng, X., Xiong, F., Ge, J., Xiang, B., Wu, X., Ma, J., Zhou, M., Li, X., Li, Y., Li, G., Xiong, W., Guo, C., & Zeng, Z. (2019). Role of the tumor microenvironment in PD-L1/PD-1-mediated tumor immune escape. *Molecular Cancer*, *18*(1), 10. https://doi.org/10.1186/s12943-018-0928-4

Johnson, M., Langdon, R., Ellison, D., Spira, A., Amin, H., Castine, M., Daniel, D., Larson, T., Sohoni, S., Chen, Y., Hayes, J., Yang, L., Masciari, S., Wang, X., & Toya, S. (2022). EP08.02-111 RMC-4630, a SHP2 Inhibitor, in Combination with Sotorasib for Advanced

KRASG12C NSCLC After Failure of Prior Standard Therapies: A Phase 2 Trial. *Journal of Thoracic Oncology*, *17*(9), S454–S455. https://doi.org/10.1016/j.jtho.2022.07.794

Kaech, S. M., & Cui, W. (2012). Transcriptional control of effector and memory CD8+ T cell differentiation. *Nature Reviews. Immunology*, *12*(11), 749–761. https://doi.org/10.1038/nri3307

Kan, A. K. C., Tang, W. T., & Li, P. H. (2024). Helper T cell subsets: Development, function and clinical role in hypersensitivity reactions in the modern perspective. *Heliyon*, *10*(9), e30553. https://doi.org/10.1016/j.heliyon.2024.e30553

Kästle, M., Merten, C., Hartig, R., Kaehne, T., Liaunardy-Jopeace, A., Woessner, N. M., Schamel, W. W., James, J., Minguet, S., Simeoni, L., & Schraven, B. (2020). Tyrosine 192 within the SH2 domain of the Src-protein tyrosine kinase p56Lck regulates T-cell activation independently of Lck/CD45 interactions. *Cell Communication and Signaling*, *18*(1), 183. https://doi.org/10.1186/s12964-020-00673-z

Kästle, M., Merten, C., Hartig, R., Kaehne, T., Liaunardy-Jopeace, A., Woessner, N. M., Schamel, W. W., James, J., Minguet, S., Simeoni, L., & Schraven, B. (2020Cour). Tyrosine 192 within the SH2 domain of the Src-protein tyrosine kinase p56Lck regulates T-cell activation independently of Lck/CD45 interactions. Cell Communication and Signaling, 18(1), 183. https://doi.org/10.1186/s12964-020-00673-z

Keam, S. J. (2022). Tremelimumab: First approval. Drugs, 83(1), 93–102. https://doi.org/10.1007/s40265-022-01827-8

Keir, M. E., Butte, M. J., Freeman, G. J., & Sharpe, A. H. (2008). PD-1 and its ligands in tolerance and immunity. *Annual Review of Immunology*, *26*(1), 677–704. https://doi.org/10.1146/annurev.immunol.26.021607.090331

Kim, P. W., Sun, Z. J., Blacklow, S. C., Wagner, G., & Eck, M. J. (2003). A zinc clasp structure tethers LCK to T cell coreceptors CD4 and CD8. *Science*, *301*(5640), 1725–1728. https://doi.org/10.1126/science.1085643

Kim, P. W., Sun, Z. J., Blacklow, S. C., Wagner, G., & Eck, M. J. (2003b). A zinc clasp structure tethers LCK to T cell coreceptors CD4 and CD8. *Science*, *301*(5640), 1725–1728. https://doi.org/10.1126/science.1085643

Kim, S. K., & Cho, S. W. (2022). The evasion mechanisms of cancer immunity and drug intervention in the tumor microenvironment. *Frontiers in Pharmacology*, *13*, 868695. https://doi.org/10.3389/fphar.2022.868695

Kinter, A. L., Godbout, E. J., McNally, J. P., Sereti, I., Roby, G. A., O'Shea, M. A., & Fauci, A. S. (2008). The common Γ-Chain cytokines IL-2, IL-7, IL-15, and IL-21 induce the expression of programmed death-1 and its ligands. *The Journal of Immunology*, *181*(10), 6738–6746. https://doi.org/10.4049/jimmunol.181.10.6738

Kiratikanon, S., Chattipakorn, S. C., Chattipakorn, N., & Kumfu, S. (2022). The regulatory effects of PTPN6 on inflammatory process: Reports from mice to men. *Archives of Biochemistry and Biophysics*, *721*, 109189. https://doi.org/10.1016/j.abb.2022.109189

Kumari, N., Brahma, M., & Maruthi, M. (2023). Targeting immune checkpoints for cancer therapy. In *Elsevier eBooks* (pp. 95–134). https://doi.org/10.1016/b978-0-443-16034-9.00012-5

Kundu, S., Fan, K., Cao, M., Lindner, D. J., Zhao, Z. J., Borden, E., & Yi, T. (2010). Novel SHP-1 Inhibitors Tyrosine Phosphatase Inhibitor-1 and Analogs with Preclinical Anti-Tumor Activities as Tolerated Oral Agents. *The Journal of Immunology*, *184*(11), 6529–6536. https://doi.org/10.4049/jimmunol.0903562

Kurochkina, N., & Guha, U. (2012). SH3 domains: modules of protein–protein interactions. *Biophysical Reviews*, *5*(1), 29–39. https://doi.org/10.1007/s12551-012-0081-z

LaMarche, M. J., Acker, M., Argintaru, A., Bauer, D., Boisclair, J., Chan, H., Chen, C. H., Chen, Y., Chen, Z., Deng, Z., Dore, M., Dunstan, D., Fan, J., Fekkes, P., Firestone, B., Fodor, M.,

Garcia-Fortanet, J., Fortin, P. D., Fridrich, C., . . . Zhu, S. (2020). Identification of TNO155, an allosteric SHP2 inhibitor for the treatment of cancer. *Journal of Medicinal Chemistry*, *63*(22), 13578–13594. https://doi.org/10.1021/acs.jmedchem.0c01170

LaRochelle, J. R., Fodor, M., Vemulapalli, V., Mohseni, M., Wang, P., Stams, T., LaMarche, M. J., Chopra, R., Acker, M. G., & Blacklow, S. C. (2018). Structural reorganization of SHP2 by oncogenic mutations and implications for oncoprotein resistance to allosteric inhibition. *Nature Communications*, *9*(1), 4508. https://doi.org/10.1038/s41467-018-06823-9

Latchman, Y., Wood, C. R., Chernova, T., Chaudhary, D., Borde, M., Chernova, I., Iwai, Y., Long, A. J., Brown, J. A., Nunes, R., Greenfield, E. A., Bourque, K., Boussiotis, V. A., Carter, L. L., Carreno, B. M., Malenkovich, N., Nishimura, H., Okazaki, T., Honjo, T., . . . Freeman, G. J. (2001). PD-L2 is a second ligand for PD-1 and inhibits T cell activation. *Nature Immunology*, *2*(3), 261–268. https://doi.org/10.1038/85330

Lee, H., Cho, M., & Choi, J. (2020). Bystander CD4+ T cells: crossroads between innate and adaptive immunity. *Experimental & Molecular Medicine*, *52*(8), 1255–1263. https://doi.org/10.1038/s12276-020-00486-7

Li, F., Roy, S., Niculcea, J., Gould, K., Adams, E. J., Van Der Merwe, P. A., & Choudhuri, K. (2024). Ligand-induced segregation from large cell-surface phosphatases is a critical step in γδ TCR triggering. *Cell Reports*, *43*(9), 114761. https://doi.org/10.1016/j.celrep.2024.114761

Li, L., Guo, X., Shi, X., Li, C., Wu, W., Yan, C., Wang, H., Li, H., & Xu, C. (2017). Ionic CD3−Lck interaction regulates the initiation of T-cell receptor signaling. *Proceedings of the National Academy of Sciences*, *114*(29), E5891–E5899. https://doi.org/10.1073/pnas.1701990114

Li, X. C., Rothstein, D. M., & Sayegh, M. H. (2009). Costimulatory pathways in transplantation: challenges and new developments. *Immunological Reviews*, *229*(1), 271–293. https://doi.org/10.1111/j.1600-065x.2009.00781.x

Lipson, E. J., & Drake, C. G. (2011). Ipilimumab: an Anti-CTLA-4 antibody for metastatic melanoma. *Clinical Cancer Research*, *17*(22), 6958–6962. https://doi.org/10.1158/1078-0432.ccr-11-1595

Luo, Y., Li, J., Zong, Y., Sun, M., Zheng, W., Zhu, J., Liu, L., & Liu, B. (2022). Discovery of the SHP2 allosteric inhibitor 2-((3R,4R)-4-amino-3-methyl-2-oxa-8-azaspiro[4.5]decan-8-yl)-5-(2,3-dichlorophenyl)-3-methylpyrrolo[2,1-f][1,2,4] triazin-4(3H)-one. *Journal of Enzyme Inhibition and Medicinal Chemistry*, *38*(1), 398–404. https://doi.org/10.1080/14756366.2022.2151594

Malissen, B., Aguado, E., & Malissen, M. (2005). Role of the LAT adaptor in T-Cell development and TH2 differentiation. *Advances in Immunology*, *87*, 1–25. https://doi.org/10.1016/s0065-2776(05)87001-4

Malissen, B., Grégoire, C., Malissen, M., & Roncagalli, R. (2014). Integrative biology of T cell activation. *Nature Immunology*, *15*(9), 790–797. https://doi.org/10.1038/ni.2959

Marasco, M., Berteotti, A., Weyershaeuser, J., Thorausch, N., Sikorska, J., Krausze, J., Brandt, H. J., Kirkpatrick, J., Rios, P., Schamel, W. W., Köhn, M., & Carlomagno, T. (2020). Molecular mechanism of SHP2 activation by PD-1 stimulation. *Science Advances*, *6*(5), eaay4458. https://doi.org/10.1126/sciadv.aay4458

Maroun, C. R., Naujokas, M. A., Holgado-Madruga, M., Wong, A. J., & Park, M. (2000). The Tyrosine Phosphatase SHP-2 Is Required for Sustained Activation of Extracellular Signal-Regulated Kinase and Epithelial Morphogenesis Downstream from the Met Receptor Tyrosine Kinase. *Molecular and Cellular Biology*, *20*(22), 8513–8525. https://doi.org/10.1128/mcb.20.22.8513-8525.2000

Medina, C. B., Sobierajska, E., Gong, M., McManus, D. T., Thapa, M., Lee, J., Im, S. J., Toombs, J. E., Mitchell, J. M., Wang, Y., Carlisle, J. W., Freeman, G. J., Master, V. A., Ramalingam, S. S., Kissick, H. T., Li, S., Brekken, R. A., & Ahmed, R. (2026). Exposed

phosphatidylserine is an inhibitory molecule in T cell exhaustion. *Nature*. https://doi.org/10.1038/s41586-026-10266-4

Motzer, R. J., Rini, B. I., McDermott, D. F., Redman, B. G., Kuzel, T. M., Harrison, M. R., Vaishampayan, U. N., Drabkin, H. A., George, S., Logan, T. F., Margolin, K. A., Plimack, E. R., Lambert, A. M., Waxman, I. M., & Hammers, H. J. (2014). Nivolumab for metastatic renal cell carcinoma: results of a randomized phase II trial. *Journal of Clinical Oncology*, *33*(13), 1430–1437. https://doi.org/10.1200/jco.2014.59.0703

Movafagh, A., Heydary, H., Mortazavi-Tabatabaei, S. A., & Azargashb, E. (2011). The Significance Application of Indigenous Phytohemagglutinin (PHA) Mitogen on Metaphase and Cell Culture Procedure. *Iranian journal of pharmaceutical research : IJPR*, *10*(4), 895–903.

Neel, B. G., Gu, H., & Pao, L. (2003). The 'Shp'ing news: SH2 domain-containing tyrosine phosphatases in cell signaling. *Trends in Biochemical Sciences*, *28*(6), 284–293. https://doi.org/10.1016/s0968-0004(03)00091-4

Oestreich, K. J., Yoon, H., Ahmed, R., & Boss, J. M. (2008). NFATc1 Regulates PD-1 Expression upon T Cell Activation. *The Journal of Immunology*, *181*(7), 4832–4839. https://doi.org/10.4049/jimmunol.181.7.4832

Palacios, E. H., & Weiss, A. (2004). Function of the Src-family kinases, Lck and Fyn, in T-cell development and activation. *Oncogene*, *23*(48), 7990–8000. https://doi.org/10.1038/sj.onc.1208074

Panchamoorthy, G., Fukazawa, T., Stolz, L., Payne, G., Reedquist, K., Shoelson, S., Songyang, Z., Cantley, L., Walsh, C., & Band, H. (1994). Physical and Functional Interactions between SH2 and SH3 Domains of the Src Family Protein Tyrosine Kinase p59 fyn. *Molecular and Cellular Biology*, *14*(9), 6372–6385. https://doi.org/10.1128/mcb.14.9.6372-6385.1994

Panchamoorthy, G., Fukazawa, T., Stolz, L., Payne, G., Reedquist, K., Shoelson, S., Songyang, Z., Cantley, L., Walsh, C., & Band, H. (1994b). Physical and Functional Interactions between SH2 and SH3 Domains of the Src Family Protein Tyrosine Kinase p59 fyn. *Molecular and Cellular Biology*, *14*(9), 6372–6385. https://doi.org/10.1128/mcb.14.9.6372-6385.1994

Parkin, J., & Cohen, B. (2001). An overview of the immune system. *The Lancet*, *357*(9270), 1777–1789. https://doi.org/10.1016/s0140-6736(00)04904-7

Patsoukis, N., Bardhan, K., Chatterjee, P., Sari, D., Liu, B., Bell, L. N., Karoly, E. D., Freeman, G. J., Petkova, V., Seth, P., Li, L., & Boussiotis, V. A. (2015). PD-1 alters T-cell metabolic reprogramming by inhibiting glycolysis and promoting lipolysis and fatty acid oxidation. *Nature Communications*, *6*(1), 6692. https://doi.org/10.1038/ncomms7692

Patsoukis, N., Duke-Cohan, J. S., Chaudhri, A., Aksoylar, H., Wang, Q., Berg, A., Freeman, G. J., & Boussiotis, V. A. (2020). Interaction of SHP-2 SH2 domains with PD-1 ITSM induces PD-1 dimerization and SHP-2 activation. *Communications Biology*, *3*(1), 128. https://doi.org/10.1038/s42003-020-0845-0

Pauken, K. E., & Wherry, E. J. (2015). Overcoming T cell exhaustion in infection and cancer. Trends in Immunology, 36(4), 265–276. https://doi.org/10.1016/j.it.2015.02.008

Pauken, K. E., Sammons, M. A., Odorizzi, P. M., Manne, S., Godec, J., Khan, O., Drake, A. M., Chen, Z., Sen, D. R., Kurachi, M., Barnitz, R. A., Bartman, C., Bengsch, B., Huang, A. C., Schenkel, J. M., Vahedi, G., Haining, W. N., Berger, S. L., & Wherry, E. J. (2016). Epigenetic stability of exhausted T cells limits durability of reinvigoration by PD-1 blockade. *Science*, *354*(6316), 1160–1165. https://doi.org/10.1126/science.aaf2807

Pennock, N. D., White, J. T., Cross, E. W., Cheney, E. E., Tamburini, B. A., & Kedl, R. M. (2013). T cell responses: naïve to memory and everything in between. *AJP Advances in Physiology Education*, *37*(4), 273–283. https://doi.org/10.1152/advan.00066.2013

Pierotti, C. L., & Köhn, M. (2026). Regulation and activity of the phosphatase SHP2: SH2 domains, dephosphorylation activity, and beyond. *Biochemical Society Transactions*, *54*(1), 15–24. https://doi.org/10.1042/bst20253102

Poole, R. M. (2014). Pembrolizumab: First global approval. *Drugs*, *74*(16), 1973–1981. https://doi.org/10.1007/s40265-014-0314-5

Powell, M. D., Read, K. A., Sreekumar, B. K., Jones, D. M., & Oestreich, K. J. (2019). IL-12 signaling drives the differentiation and function of a TH1-derived TFH1-like cell population. *Scientific Reports*, *9*(1), 13991. https://doi.org/10.1038/s41598-019-50614-1

Qu, Z., Dong, J., & Zhang, Z. (2023). Protein tyrosine phosphatases as emerging targets for cancer immunotherapy. *British Journal of Pharmacology*, *183*(6), 1233–1249. https://doi.org/10.1111/bph.16304

Ran, H., Tsutsumi, R., Araki, T., & Neel, B. G. (2016). Sticking It to Cancer with Molecular Glue for SHP2. *Cancer Cell*, *30*(2), 194–196. https://doi.org/10.1016/j.ccell.2016.07.010

Raskov, H., Orhan, A., Christensen, J. P., & Gögenur, I. (2020). Cytotoxic CD8+ T cells in cancer and cancer immunotherapy. *British Journal of Cancer*, *124*(2), 359–367. https://doi.org/10.1038/s41416-020-01048-4

Riella, L., Paterson, A., Sharpe, A., & Chandraker, A. (2012). Role of the PD-1 pathway in the immune response. *American Journal of Transplantation*, *12*(10), 2575–2587. https://doi.org/10.1111/j.1600-6143.2012.04224.x

Rossy, J., Williamson, D. J., & Gaus, K. (2012). How does the kinase Lck phosphorylate the T cell receptor? Spatial organization as a regulatory mechanism. *Frontiers in Immunology*, *3*, 167. https://doi.org/10.3389/fimmu.2012.00167

Rowshanravan, B., Halliday, N., & Sansom, D. M. (2017). CTLA-4: a moving target in immunotherapy. *Blood, 131*(1), 58–67. https://doi.org/10.1182/blood-2017-06-741033

Rowshanravan, B., Halliday, N., & Sansom, D. M. (2017b). CTLA-4: a moving target in immunotherapy. *Blood*, *131*(1), 58–67. https://doi.org/10.1182/blood-2017-06-741033

Sakaguchi, S., Yamaguchi, T., Nomura, T., & Ono, M. (2008). Regulatory T cells and immune tolerance. *Cell*, *133*(5), 775–787. https://doi.org/10.1016/j.cell.2008.05.009

Sandner, S. E., Clarkson, M. R., Salama, A. D., Sanchez-Fueyo, A., Domenig, C., Habicht, A., Najafian, N., Yagita, H., Azuma, M., Turka, L. A., & Sayegh, M. H. (2005). Role of the programmed Death-1 pathway in regulation of alloimmune responses in vivo. *The Journal of Immunology*, *174*(6), 3408–3415. https://doi.org/10.4049/jimmunol.174.6.3408

Santana, M. A., & Esquivel-Guadarrama, F. (2006). Cell biology of T cell activation and differentiation. *International Review of Cytology*, *250*, 217–274. https://doi.org/10.1016/s0074-7696(06)50006-3

Shah, K., Al-Haidari, A., Sun, J., & Kazi, J. U. (2021). T cell receptor (TCR) signaling in health and disease. *Signal Transduction and Targeted Therapy*, *6*(1), 412. https://doi.org/10.1038/s41392-021-00823-w

Schade, A. E., Schieven, G. L., Townsend, R., Jankowska, A. M., Susulic, V., Zhang, R., Szpurka, H., & Maciejewski, J. P. (2007). Dasatinib, a small-molecule protein tyrosine kinase inhibitor, inhibits T-cell activation and proliferation. *Blood*, *111*(3), 1366–1377. https://doi.org/10.1182/blood-2007-04-084814

Schildberg, F. A., Klein, S. R., Freeman, G. J., & Sharpe, A. H. (2016). Coinhibitory pathways in the B7-CD28 Ligand-Receptor family. *Immunity*, *44*(5), 955–972. https://doi.org/10.1016/j.immuni.2016.05.002

Schildberg, F. A., Klein, S. R., Freeman, G. J., & Sharpe, A. H. (2016). Coinhibitory pathways in the B7-CD28 Ligand-Receptor family. *Immunity*, 44(5), 955–972. https://doi.org/10.1016/j.immuni.2016.05.002

Srinivasan, S., Zhu, C., & McShan, A. C. (2024). Structure, function, and immunomodulation of the CD8 co-receptor. *Frontiers in Immunology*, *15*, 1412513. https://doi.org/10.3389/fimmu.2024.1412513

Stachlewitz, R. F., Hart, M. A., Bettencourt, B., Kebede, T., Schwartz, A., Ratnofsky, S. E., Calderwood, D. J., Waegell, W. O., & Hirst, G. C. (2005). A-770041, a novel and selective Small-Molecule inhibitor of LCK, prevents heart allograft rejection. *Journal of Pharmacology and Experimental Therapeutics*, *315*(1), 36–41. https://doi.org/10.1124/jpet.105.089169

Stachlewitz, R. F., Hart, M. A., Bettencourt, B., Kebede, T., Schwartz, A., Ratnofsky, S. E., Calderwood, D. J., Waegell, W. O., & Hirst, G. C. (2005b). A-770041, a novel and selective Small-Molecule inhibitor of LCK, prevents heart allograft rejection. *Journal of Pharmacology and Experimental Therapeutics*, *315*(1), 36–41. https://doi.org/10.1124/jpet.105.089169

Staron, M. M., Gray, S. M., Marshall, H. D., Parish, I. A., Chen, J. H., Perry, C. J., Cui, G., Li, M. O., & Kaech, S. M. (2014). The Transcription Factor FoxO1 Sustains Expression of the Inhibitory Receptor PD-1 and Survival of Antiviral CD8+ T Cells during Chronic Infection. *Immunity*, *41*(5), 802–814. https://doi.org/10.1016/j.immuni.2014.10.013

Straus, D. (1992). Genetic evidence for the involvement of the lck tyrosine kinase in signal transduction through the T cell antigen receptor. *Cell*, *70*(4), 585–593. https://doi.org/10.1016/0092-8674(92)90428-f

Tamir, I., Porto, J. M. D., & Cambier, J. C. (2000). Cytoplasmic protein tyrosine phosphatases SHP-1 and SHP-2: regulators of B cell signal transduction. *Current Opinion in Immunology*, *12*(3), 307–315. https://doi.org/10.1016/s0952-7915(00)00092-3

Tartaglia, M., Gelb, B. D., & Zenker, M. (2011). Noonan syndrome and clinically related disorders. *Best Practice & Research Clinical Endocrinology & Metabolism*, *25*(1), 161–179. https://doi.org/10.1016/j.beem.2010.09.002

Taube, J. M., Klein, A., Brahmer, J. R., Xu, H., Pan, X., Kim, J. H., Chen, L., Pardoll, D. M., Topalian, S. L., & Anders, R. A. (2014). Association of PD-1, PD-1 Ligands, and Other Features of the Tumor Immune Microenvironment with Response to Anti–PD-1 Therapy. *Clinical Cancer Research*, *20*(19), 5064–5074. https://doi.org/10.1158/1078-0432.ccr-13-3271

Tawbi, H. A., Schadendorf, D., Lipson, E. J., Ascierto, P. A., Matamala, L., Gutiérrez, E. C., Rutkowski, P., Gogas, H. J., Lao, C. D., De Menezes, J. J., Dalle, S., Arance, A., Grob, J., Srivastava, S., Abaskharoun, M., Hamilton, M., Keidel, S., Simonsen, K. L., Sobiesk, A. M., . . . Long, G. V. (2022). Relatlimab and Nivolumab versus Nivolumab in Untreated Advanced Melanoma. *New England Journal of Medicine*, *386*(1), 24–34. https://doi.org/10.1056/nejmoa2109970

Tièche, C. C., Gao, Y., Bührer, E. D., Hobi, N., Berezowska, S. A., Wyler, K., Froment, L., Weis, S., Peng, R., Bruggmann, R., Schär, P., Amrein, M. A., Hall, S. R. R., Dorn, P., Kocher, G., Riether, C., Ochsenbein, A., Schmid, R. A., & Marti, T. M. (2018). Tumor initiation capacity and therapy resistance are differential features of EMT-Related subpopulations in the NSCLC cell line A549. *Neoplasia*, *21*(2), 185–196. https://doi.org/10.1016/j.neo.2018.09.008

Tonks, N. K. (2006). Protein tyrosine phosphatases: from genes, to function, to disease. *Nature Reviews Molecular Cell Biology*, *7*(11), 833–846. https://doi.org/10.1038/nrm2039

Topalian, S. L., Hodi, F. S., Brahmer, J. R., Gettinger, S. N., Smith, D. C., McDermott, D. F., Powderly, J. D., Carvajal, R. D., Sosman, J. A., Atkins, M. B., Leming, P. D., Spigel, D. R., Antonia, S. J., Horn, L., Drake, C. G., Pardoll, D. M., Chen, L., Sharfman, W. H., Anders, R. A., . . . Sznol, M. (2012). Safety, activity, and immune correlates of Anti–PD-1 antibody in cancer. *New England Journal of Medicine*, *366*(26), 2443–2454. https://doi.org/10.1056/nejmoa1200690

Tsang, Y. H., Han, X., Man, W. Y., Lee, N., & Poon, R. Y. C. (2012). Novel functions of the phosphatase SHP2 in the DNA replication and damage checkpoints. *PLoS ONE*, *7*(11), e49943. https://doi.org/10.1371/journal.pone.0049943

Tseng, S., Otsuji, M., Gorski, K., Huang, X., Slansky, J. E., Pai, S. I., Shalabi, A., Shin, T., Pardoll, D. M., & Tsuchiya, H. (2001). B7-Dc, a New Dendritic Cell Molecule with Potent Costimulatory Properties for T Cells. *The Journal of Experimental Medicine*, *193*(7), 839–846. https://doi.org/10.1084/jem.193.7.839

Tumeh, P. C., Harview, C. L., Yearley, J. H., Shintaku, I. P., Taylor, E. J. M., Robert, L., Chmielowski, B., Spasic, M., Henry, G., Ciobanu, V., West, A. N., Carmona, M., Kivork, C., Seja, E., Cherry, G., Gutierrez, A. J., Grogan, T. R., Mateus, C., Tomasic, G., . . . Ribas, A. (2014). PD-1 blockade induces responses by inhibiting adaptive immune resistance. *Nature*, *515*(7528), 568–571. https://doi.org/10.1038/nature13954

Van Boxel, G. I., Holmes, S., Fugger, L., & Jones, E. Y. (2010). An Alternative Conformation of the T-Cell Receptor α Constant Region. *Journal of Molecular Biology*, *400*(4), 828–837. https://doi.org/10.1016/j.jmb.2010.05.053

Van Laethem, F., Tikhonova, A. N., Pobezinsky, L. A., Tai, X., Kimura, M. Y., Saout, C. L., Guinter, T. I., Adams, A., Sharrow, S. O., Bernhardt, G., Feigenbaum, L., & Singer, A. (2013). Lck Availability during Thymic Selection Determines the Recognition Specificity of the T Cell Repertoire. *Cell*, *154*(6), 1326–1341. https://doi.org/10.1016/j.cell.2013.08.009

Vigano, S., Bobisse, S., Coukos, G., Perreau, M., & Harari, A. (2020). Cancer and HIV-1 infection: Patterns of chronic antigen exposure. *Frontiers in Immunology*, *11*, 1350. https://doi.org/10.3389/fimmu.2020.01350

Vyas, J. M., Van Der Veen, A. G., & Ploegh, H. L. (2008). The known unknowns of antigen processing and presentation. *Nature Reviews. Immunology*, *8*(8), 607–618. https://doi.org/10.1038/nri2368

Wakelee, H., Liberman, M., Kato, T., Tsuboi, M., Lee, S., Gao, S., Chen, K., Dooms, C., Majem, M., Eigendorff, E., Martinengo, G. L., Bylicki, O., Rodríguez-Abreu, D., Chaft, J. E., Novello, S., Yang, J., Keller, S. M., Samkari, A., & Spicer, J. D. (2023). Perioperative Pembrolizumab for Early-Stage Non–Small-Cell lung cancer. *New England Journal of Medicine*, *389*(6), 491–503. https://doi.org/10.1056/nejmoa2302983

Walunas, T. L., Lenschow, D. J., Bakker, C. Y., Linsley, P. S., Freeman, G. J., Green, J. M., Thompson, C. B., & Bluestone, J. A. (1994). CTLA-4 can function as a negative regulator of T cell activation. *Immunity*, *1*(5), 405–413. https://doi.org/10.1016/1074-7613(94)90071-x

Wang, Q., Zhu, T., Miao, N., Qu, Y., Wang, Z., Chao, Y., Wang, J., Wu, W., Xu, X., Xu, C., Xia, L., & Wang, F. (2022). Disulfiram bolsters T-cell anti-tumor immunity through direct activation of LCK-mediated TCR signaling. *The EMBO Journal*, *41*(16), e110636. https://doi.org/10.15252/embj.2022110636

Watson, H. A., Wehenkel, S., Matthews, J., & Ager, A. (2016). SHP-1: the next checkpoint target for cancer immunotherapy? *Biochemical Society Transactions*, *44*(2), 356–362. https://doi.org/10.1042/bst20150251

Wherry, E. J. (2011). T cell exhaustion. *Nature Immunology*, *12*(6), 492–499. https://doi.org/10.1038/ni.2035

Wherry, E. J., Ha, S., Kaech, S. M., Haining, W. N., Sarkar, S., Kalia, V., Subramaniam, S., Blattman, J. N., Barber, D. L., & Ahmed, R. (2007). Molecular Signature of CD8+ T Cell Exhaustion during Chronic Viral Infection. *Immunity*, *27*(5), 824. https://doi.org/10.1016/j.immuni.2007.11.006

Wu, Y., Wu, Y., Gao, Z., Yu, W., Zhang, L., & Zhou, F. (2026). Revitalizing T cells: breakthroughs and challenges in overcoming T cell exhaustion. *Signal Transduction and Targeted Therapy*, *11*(1), 2. https://doi.org/10.1038/s41392-025-02327-3

Yamazaki, T., Akiba, H., Iwai, H., Matsuda, H., Aoki, M., Tanno, Y., Shin, T., Tsuchiya, H., Pardoll, D. M., Okumura, K., Azuma, M., & Yagita, H. (2002). Expression of programmed death 1 ligands by murine T cells and APC. *The Journal of Immunology*, *169*(10), 5538–5545. https://doi.org/10.4049/jimmunol.169.10.5538

Yang, W., Klaman, L. D., Chen, B., Araki, T., Harada, H., Thomas, S. M., George, E. L., & Neel, B. G. (2006). An SHP2/SFK/RAS/ERK signaling pathway controls trophoblast stem cell survival. *Developmental Cell*, *10*(3), 317–327. https://doi.org/10.1016/j.devcel.2006.01.002

Ye, B., Liu, X., Li, X., Kong, H., Tian, L., & Chen, Y. (2015). T-cell exhaustion in chronic hepatitis B infection: current knowledge and clinical significance. *Cell Death and Disease*, *6*(3), e1694. https://doi.org/10.1038/cddis.2015.42

Yokosuka, T., Takamatsu, M., Kobayashi-Imanishi, W., Hashimoto-Tane, A., Azuma, M., & Saito, T. (2012). Programmed cell death 1 forms negative costimulatory microclusters that directly inhibit T cell receptor signaling by recruiting phosphatase SHP2. *The Journal of Experimental Medicine*, *209*(6), 1201–1217. https://doi.org/10.1084/jem.20112741

Youngblood, B., Noto, A., Porichis, F., Akondy, R. S., Ndhlovu, Z. M., Austin, J. W., Bordi, R., Procopio, F. A., Miura, T., Allen, T. M., Sidney, J., Sette, A., Walker, B. D., Ahmed, R., Boss, J. M., Sékaly, R., & Kaufmann, D. E. (2013). Cutting edge: Prolonged exposure to HIV reinforces a poised epigenetic program for PD-1 expression in Virus-Specific CD8 T cells. *The Journal of Immunology*, *191*(2), 540–544. https://doi.org/10.4049/jimmunol.1203161

Youngblood, B., Oestreich, K. J., Ha, S., Duraiswamy, J., Akondy, R. S., West, E. E., Wei, Z., Lu, P., Austin, J. W., Riley, J. L., Boss, J. M., & Ahmed, R. (2011). Chronic Virus Infection Enforces Demethylation of the Locus that Encodes PD-1 in Antigen-Specific CD8+ T Cells. *Immunity*, *35*(3), 400–412. https://doi.org/10.1016/j.immuni.2011.06.015

Zeng, Z., Wei, F., & Ren, X. (2020). Exhausted T cells and epigenetic status. *Cancer Biology and Medicine*, *17*(4), 923–936. https://doi.org/10.20892/j.issn.2095-3941.2020.0338

Zhang, R., Liao, W., Chen, X., Wang, J., Li, J., Chen, G., Wu, W., Wang, X., Zhang, Y., Chen, Z., Zhu, X., Lin, Z., Zhu, Y., Ma, L., & Yu, H. (2025). PKCα regulates the secretion of PDL1-carrying small extracellular vesicles in a p53-dependent manner. *Cell Death and Disease*, *16*(1), 19. https://doi.org/10.1038/s41419-025-07341-5

Zhang, S., Zong, Y., Chen, L., Li, Q., Li, Z., & Meng, R. (2023). The immunomodulatory function and antitumor effect of disulfiram: paving the way for novel cancer therapeutics. *Discover Oncology*, *14*(1), 103. https://doi.org/10.1007/s12672-023-00729-9

Zhao, Y., Niu, C., & Cui, J. (2018). Gamma-delta (γδ) T cells: friend or foe in cancer development? *Journal of Translational Medicine*, *16*(1), 3. https://doi.org/10.1186/s12967-017-1378-2

Zinselmeyer, B. H., Heydari, S., Sacristán, C., Nayak, D., Cammer, M., Herz, J., Cheng, X., Davis, S. J., Dustin, M. L., & McGavern, D. B. (2013). PD-1 promotes immune exhaustion by inducing antiviral T cell motility paralysis. *The Journal of Experimental Medicine*, *210*(4), 757–774. https://doi.org/10.1084/jem.20121416

8 LIST OF ABBREVIATIONS

Abbreviation	Explanation
AICD	Activation-induced cell death
APC / APCs	Antigen-Presenting Cell(s)
BCR	B-cell receptor
C domain	Constant immunoglobulin-like domain
C-SH2	C-terminal SH2 domain
CD (e.g., CD3)	Cluster of Differentiation
Csk	C-terminal Src kinase.
CTLA-4	Cytotoxic T-lymphocyte-associated protein 4
CuET	bis(diethyldithiocarbamate)copper complex
DMEM	Dulbecco's Modified Eagle Medium
FoxO1	Forkhead box O1
HBV	Hepatitis B
HCV	Hepatitis C
HIV	Human Immunodeficiency Virus
ICIs	Immune Checkpoint Inhibitors
IFN-γ	Interferon-gamma
Ig	Immunoglobulin
IL (e.g., IL-2)	Interleukin.
ITAMs	Immunoreceptor Tyrosine-based Activation Motifs.
ITIM / ITIMs	Immunoreceptor tyrosine-based inhibitory motif(s)
ITk	Interleukin-2-inducible T-cell kinase.
ITSM	Immunoreceptor tyrosine-based switch motif
LAT	Linker for Activation of T-cells.
Lck	Lymphocyte-specific protein tyrosine kinase.
MAPK	Mitogen-Activated Protein Kinase
MFI	Mean fluorescence intensity
MHC	Major Histocompatibility Complex
N-SH2	N-terminal SH2 domain
NF-κB	Nuclear factor kappa B
NFAT	Nuclear factor of activated T-cells (e.g., NFATc1)
NK	Natural killer (cells)
NKT	Natural killer T-cells
NPL4	Nuclear Protein Localization protein 4
NSCLC	Non-small cell lung cancer
p53-/-	p53 knock-out.
PBMC	Peripheral blood mononuclear cell

PBS	Phosphate-buffered saline:.
PD-1	Programmed cell death protein 1.
PD-L1 / PD-L2	Programmed death-ligands 1 and 2
PGC-1α	Peroxisome proliferator-activated receptor γ coactivator 1α
PHA	Phytohemagglutinin
PI	Propidium iodide
PKC	Protein Kinase C
PLCγ1	Phospholipase Cγ1
PMA	Phorbol 12-myristate 13-acetate
pMHC	Peptide-Major Histocompatibility Complex
PTKs	Protein tyrosine kinases
PTP	Protein tyrosine phosphatase
PTP1B	Protein Tyrosine Phosphatase 1B
PTP1Bi	PTP1B inhibitor
RAG1 / RAG2	Recombinases
SH1, SH2, SH3, SH4	Src Homology domains (1, 2, 3, 4)
SH2	Src homology 2 domain
SHP-1	Src homology 2 domain-containing phosphatase 1
SHP-2	Src homology 2 domain-containing phosphatase 2
SHPs	Src homology 2 domain-containing phosphatases
SLP-76	SH2 domain-containing Leukocyte Protein of 76 kDa
Spry	Sprouty (proteins)
Tc	Cytotoxic T-cell
TCR	T-cell receptor
TFH	T follicular helper cells
Th	Helper T-cell
TK	Tyrosine kinase
TLRs	Toll-like receptors
TNF-α	Tumor necrosis factor alpha
TPI-1	An experimental compound/inhibitor used in combination treatments.
Treg / Tregs	Regulatory T-cell(s)
UD	Unique Domain: A specific N-terminal structural domain of Lck that facilitates interaction with CD4/CD8 co-receptors.
V domain	Variable immunoglobulin-like domain
ZAP-70	Zeta-chain-associated protein kinase 70

9 SUPPLEMENTARY DATA

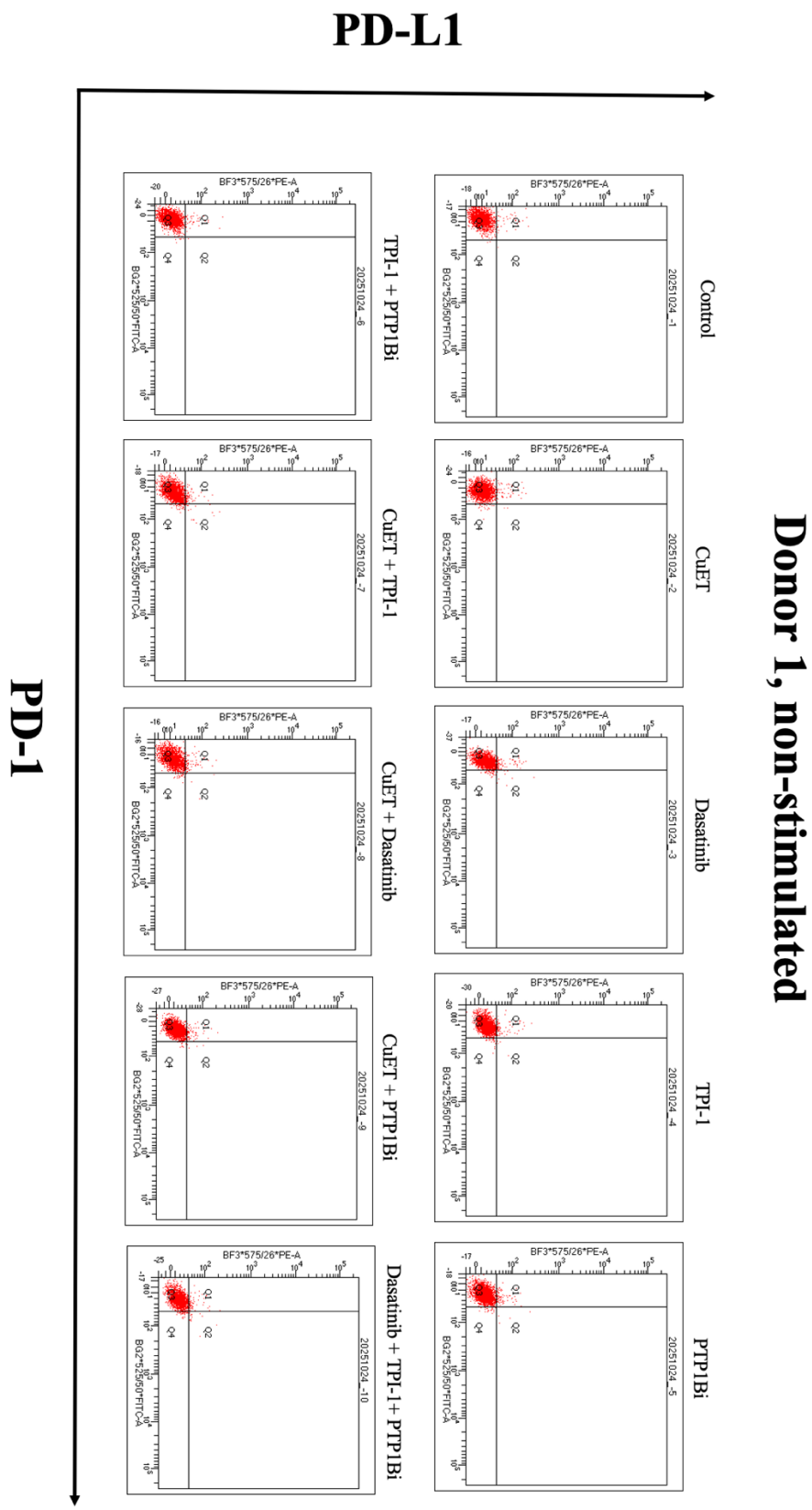

Supplementary Figure 1. Flow cytometry histograms illustrating the distribution of cells expressing PD-L1 and/or PD-1 during individual conditions of a non-stimulated donor 1.

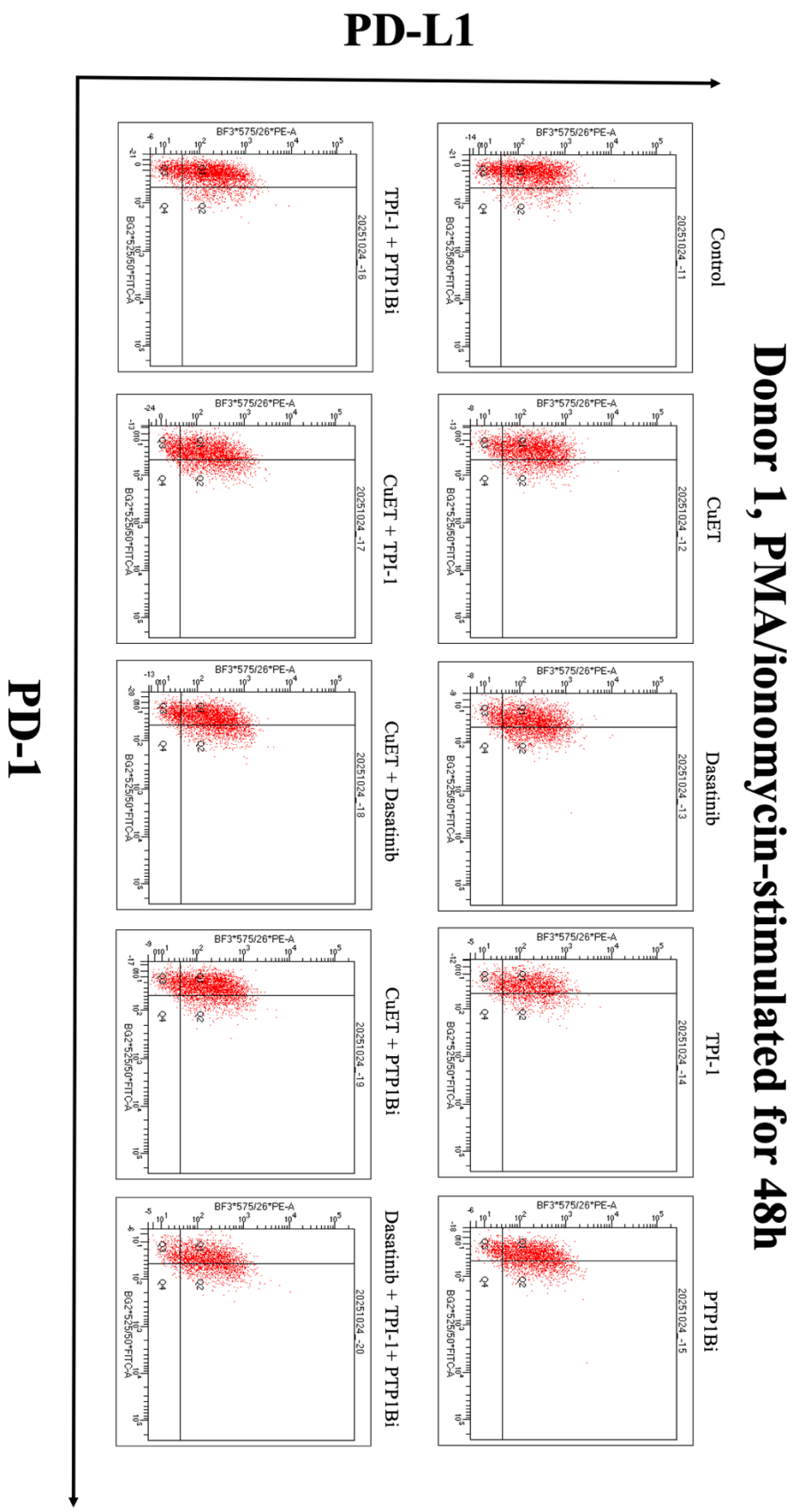

Supplementary Figure 2. Flow cytometry histograms illustrating the distribution of cells expressing PD-L1 and/or PD-1 during individual conditions of a PMA/ionomycin-stimulated (48h) donor 1.

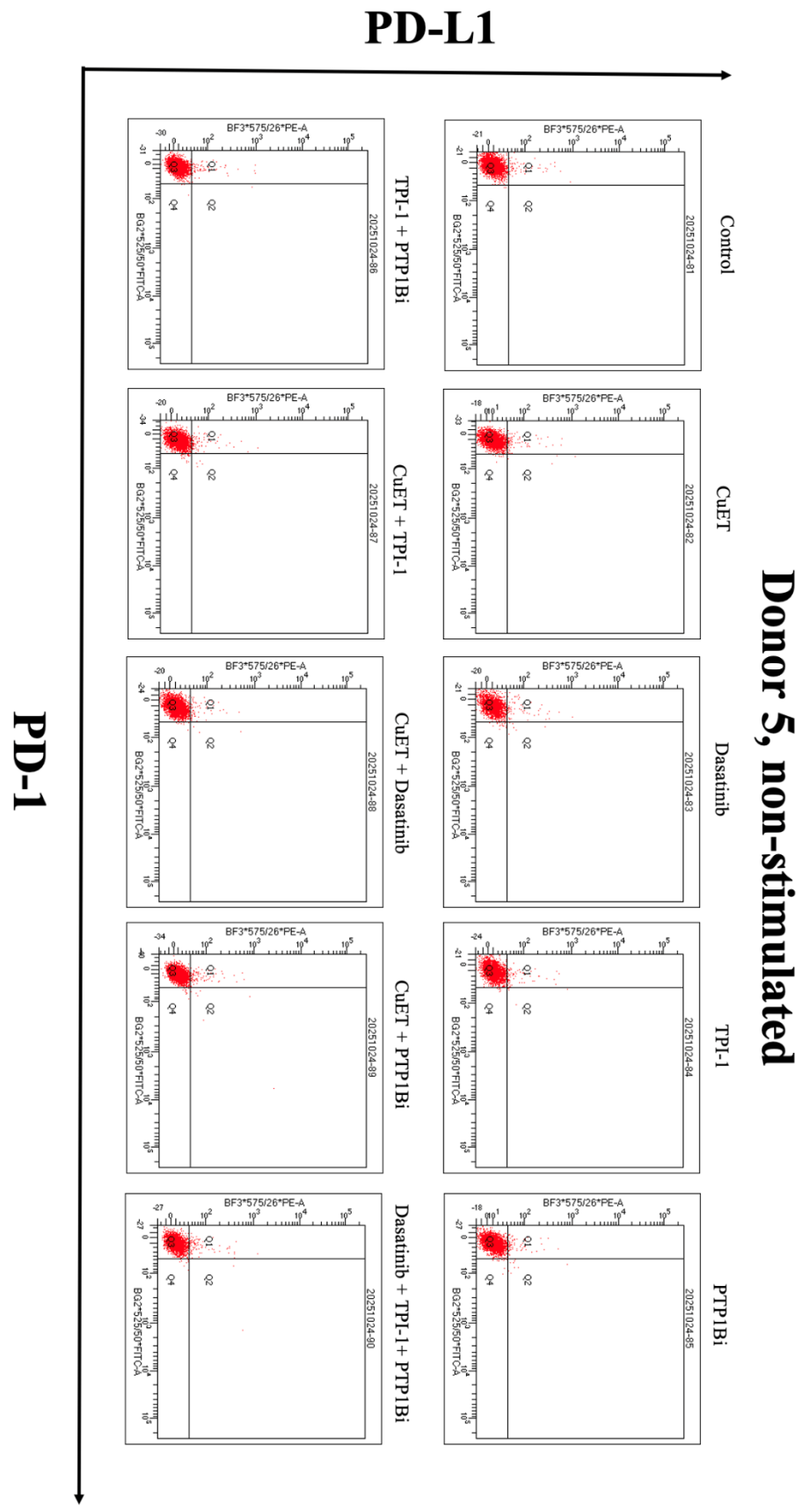

Supplementary Figure 3. Flow cytometry histograms illustrating the distribution of cells expressing PD-L1 and/or PD-1 during individual conditions of a non-stimulated donor 5.

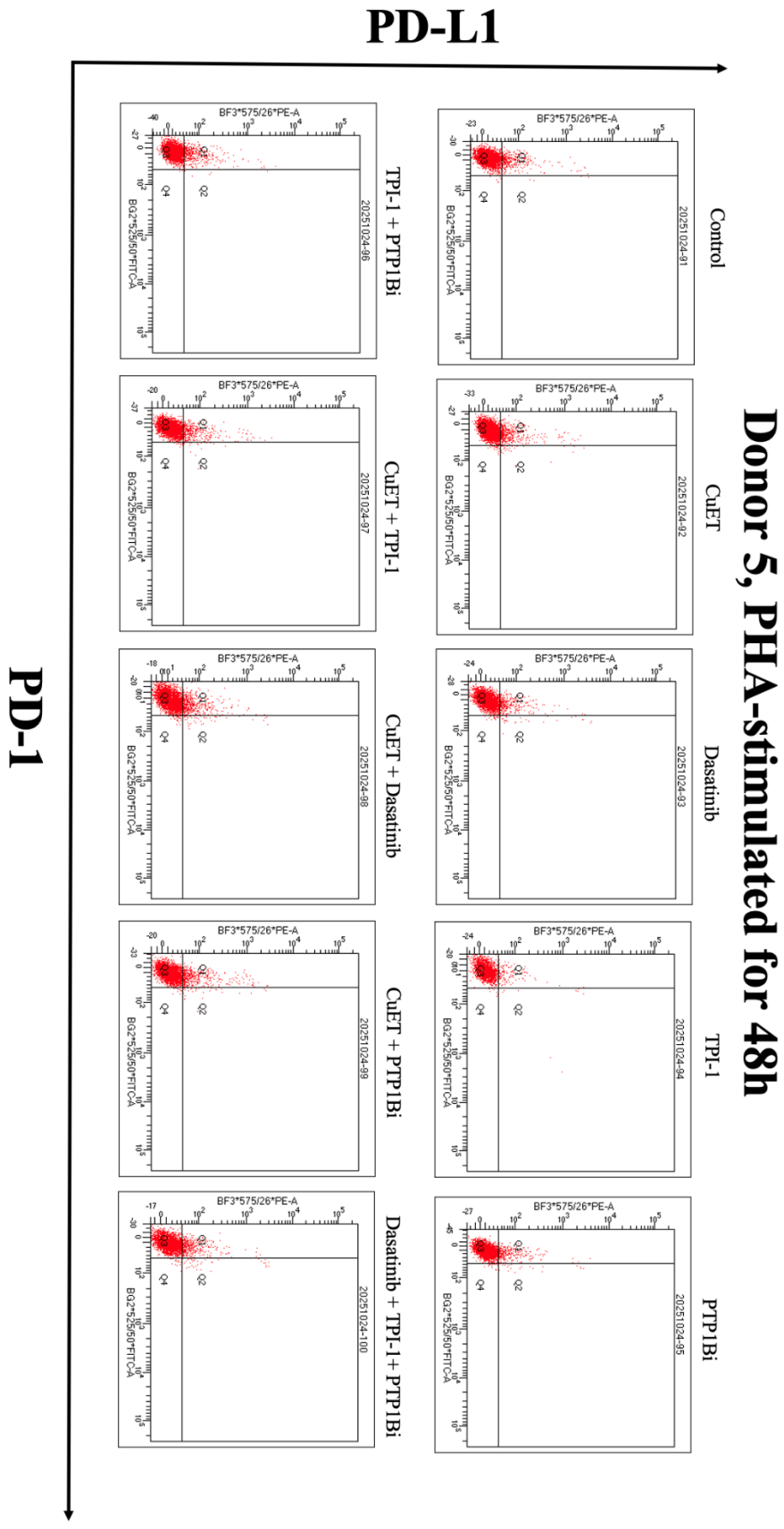

Supplementary Figure 4. Flow cytometry histograms illustrating the distribution of cells expressing PD-L1 and/or PD-1 during individual conditions of a PHA -stimulated (48h) donor 5.